# Influence of Endocannabinoids on the Function of the Pituitary Gland with Focus on Folliculo-Stellate, Corticotroph, and Lactotroph Cell Lines

**Dissertation**

**zur Erlangung des Doktorgrades**

**der Naturwissenschaften**

**vorgelegt beim Fachbereich Biochemie, Chemie und Pharmazie (14)**

**der Johann Wolfgang Goethe - Universität**

**in Frankfurt am Main**

**von**

**Irena Ivanova**

**aus B. Slatina, Bulgarien**

**Frankfurt 2015**

**D30**

vom Fachbereich Biochemie, Chemie und Pharmazie (14)

der Johann Wolfgang Goethe – Universität als Dissertation angenommen.

Dekan: Prof. Dr. rer. nat. M. Karas

Gutachter: Prof. Dr. med. H.-W. Korf

Prof. Dr. rer. nat. M. Schubert-Zsilavecz

Datum der Disputation: 26.05.2015

# Contents

# List of figures

# Abbreviations

## A

AA arachidonic acid

(m) Ab (monoclonal) antibody

ABC(1) ATP-binding cassette (type 1)

AC adenyl cyclase

ACh acetylcholine

ACTH adrenocorticotropin

AEA anandamide

2-AG 2-arachidonylglycerol

Anx A1 annexin A1

Arc arcuate nucleus

aPV periventricular nucleus

ATP adenosine triphosphate

AVP arginine vasopressin

## C

C corticotroph

Ca $Ca^{2+}$ calcium cations

$[Ca^{2+}]_i$ intracellular Ca concentration

cAMP cyclic adenosine monophosphate

$CB_1$ cannabinoid receptor type 1

cGMP cyclic guanosine monophosphate

CINC cytokine-induced neutrophil chemoattractant, IL-8

CNS central nervous system

CREB cyclic AMP-responding element-binding protein

CRH corticotropin

## D

DA dopamine

DAB 3,3'-diaminobenzidine

DAGL diacylglycerol lipase

DAPI 4',6-diamidino-2-phenylindole

Dex dexamethasone

DG diacyl glycerol

DNA deoxyribonucleic acid

## E

E 17 ß –E 2, estradiol

EC endocannabinoids

ECS endocannabinoid system

ER E receptor

rER rough endoplasmic retikulum

sER smooth endoplasmic retikulum

## F

FAAH fatty acid amide hydrolase

Fpr(-rs1) formyl peptide receptor (related sequence 1)

FS folliculo-stellate cells

FSH follicule stimulating hormone

## G

GC glucocorticoids

Gi,s,q,o – G-protein-coupled receptor with an inhibitory, stimulatory, , or other

GH growth hormone

GnRH gonadotropin releasing hormone

GR GC receptor

GRE GC receptor binding response elements

GTP guanosine triphosphate

## H

HPA hypothalamo-pituitary axis

Huvecs human umbilical vein endothelial cells

## I

IB immunoblot

ICC immunocytochemistry

IHC immunohistochemistry

IL(-1beta,-6) interleukin

IP3 inositol trisphosphate

ISH *in situ* hybridization

## K

kDA kilodalton (an unified atomic mass unit for proteins)

## L

L lactotroph

LH luteinizing hormone

LHA lateral hypothalamic area

L-NAME Nω-Nitro-L-arginine methyl ester

LPS lipopolysaccharides

## M

MAGL monoacylglycerol lipase

MAP(K) mitogen-activated protein kinase

MBH medial basal hypothalamus

ME median eminence

mRNA messenger ribonucleic acid

## N

NF-κβ nuclear factor kappa-light-chain-enhancer of activated B cells

NO nitric oxide

## O

OC optic chiasm

OT oxytocin

## P

PAG periaqueductal grey

PCR polymerase chain reaction

PD pars distalis

PHDA periventricular hypophyseal dopaminergic neurons

PI pars intermedia

PIP2 phosphatidylinositol 4,5-bisphosphate

PKA protein kinase A

PLA2 phospholipase A2

PLC phospholipase C

PLD phospholipase D

PN pars nervosa

POA preoptic area

POMC pro-opiomelanocortin

PRL prolactin

PT pars tuberalis

PVN paraventricular nucleus

## R

RNA ribonucleic acid

## S

SCN suprachiasmatic nucleus

SNARE soluble NSF attachment protein receptor, plays an essential role in vesicle fusion and thus exocytosis

SON supraoptic nucleus

## T

TIDA tuberoinfundibular dopaminergic neurons

THDA tuberohypophysial dopaminergic neurons

TRH thyrotropin (thyroid releasing hormone)

TSH thyroliberin (thyroid stimulating hormone)

## V

VMH ventromedial hypothalamic nucleus

VIP vasoactive intestinal peptide

VPAC1 VIP/PACAP receptor type 1

V3 third ventricle

## W

WIN WIN 55.212-2 mesylate

## Z

ZT zeitgeber

# Abstract

The endocannabinoids (EC), their synthetizing and metabolizing enzymes, and the cannabinoid (CB) receptors comprise the endocannabinoid system (ECS) that has been detected by Yasuo et al. (2010) in rodent and human brain areas essential for circadian rhythmic control and hormone secretion. The EC are secreted in the pars tuberalis formation (PT) of the pituitary gland and unfold their effect as ligands on cannabinoid receptors type 1 ($CB_1$) in the pars distalis (PD). The $CB_1$ is mostly expressed on folliculo-stellate (fs) cells of the PD. The fs cells execute regulative and supportive functions to adjacent hormone-producing cells (Allaerts and Venkelecom, 2005; Mitsuishi et al., 2013). The lipid and calcium binding protein Annexin A1 (Anx A1) and the cell membrane permeable compound nitric oxide (NO) have been detected in the fs cells (Woods et al., 1990; Devnath and Inoue, 2008). There are published findings indicating strong influence of Anx A1 and NO on hormone production (Taylor et al. 1993; Venkelecom et al, 1997). The hypothesis of this study is that the EC influence hormonal secretion by acting upon $CB_1$ receptors on fs cells and thus activating or inhibiting Anx A1 and NO that directly affect adjacent glandular cells.

Prevalently cell models were used to carry out the experimental work. The TtT/GF and Tpit/F1 cell lines represent the fs cells, the AtT20/D16v stand for the ACTH-producing corticotroph (C) cells, and GH4C1 for the PRL-producing lactotroph (L) cells. Whenever comparison with an integrity model was possible tissue from C3H mice was used. Chemoluminescent and photometrical detection, enzyme-linked immunosorbent assay (ELISA), fluorescence-activated cell sorting (FACS), immunoblot (IB), immunocyto- and immunohisto-chemical analysis (ICC, IHC), *in situ* hybridization (ISH), and (q) PCR methods were used as assaying tools to investigate $CB_1$, Anx A1, the Anx A1 receptor - Fpr-rs1, NO, ACTH, and PRL.

$CB_1$ was detected on the fs, C, and L cell models. The presence of fatty acid amide hydrolase (FAAH, an EC degrading enzyme) was confirmed in the fs

cells. Incubations of the fs cells with $CB_1$ agonists (2-AG, AEA, WIN) and antagonist (otenabant) were performed and resulting increase of Anx A1, and inhibition of NO were detected. Anx A1 binding sites, known as formyl peptide like receptor – related sequence 1 (Fpr-rs1) were identified on the C and L cells. The hormone-producing cells were treated with a 2-AG, Anx A1, and NO and the resulting changes in the levels of ACTH and PRL were detected. Anx A1 acted stimulatory on ACTH in the C AtT20/D16v cell and inhibitory on PRL in the L GH4C1 cell. NO inhibited both ACTH and PRL release. Additional analysis of the levels of expression of mRNA for Anx A1 and Fpr-rs1 in murine PD tissue demonstrated that while the expression of the first was not influenced by time, the expression of the latter was activated during the subjective day.

The here presented study shows that EC influence the ACTH release stimulatory through activating Anx A1 and inhibiting NO. As for PRL, the EC unfold an inhibition through activating Anx A1, and stimulation through inhibiting NO. A clear regulatory linkeage between the EC and ACTH and PRL control is revealed, involving the fs cells with possible time-dependence.

# Hypothesis

The hypothesis in this work is that Annexin A1 (Anx A1) and nitric oxide (NO) are the tools with which the folliculo-stellate (fs) cells influence the adjacent glandular cells.

The fs cells, mostly present in the pars distalis (PD) of the pituitary gland execute regulative and supportive functions to the hormone-producing cells (in this study, particularly, cells that produce adrenocorticotropin (ACTH) and prolactin (PRL). Since their very discovery, hypotheses have been proposed about their regulative interactions with other cell populations.

Anx A1 has been detected in the fs cells of the PD (and to lesser degree in pars intermedia, PI and pars nervosa, PN) (Woods et al., 1990). Anx A1 is even proposed as a marker protein of the fs cells, just as specific as S-100ß (Cocchia and Miami, 1980; Allaerts and Vankelecom, 2005). This protein is closely coupled to the ACTH regulation circuit and is directly up-regulated by glucocorticoids (GC) (Flower and Blackwell, 1979). Buckingham et al. (2006) have demonstrated that Anx A1 inhibits CRH-induced ACTH release. Experiments with pituitary gland slices and lactotroph (L) cells suggest its inhibitory effect on PRL as well (Taylor et al., 1993; Morris et al., 2002).

NO clearly interferes with hormone release by interacting with the exocytotic process. It has been shown that fs cells produce NO (Vankelecom et al., 1997). There must be some intricate mechanisms involved since also hormonal - corticotroph (C) and L cells do produce NO.

The endocannabinoids (EC) are regulated in a circadian, possibly also in a circannual manner, and are closely related to mechanisms involving hormone production, such as wakening and reproduction. The EC are evidently connected to ACTH and PRL regulation as shown by Morgan (2000) and Yasuo and Korf (2011).

The proposed mechanism displayed in Fig. 1, is that EC synthetized in the pars tuberalis (PT) inhibit the production of Anx A1 and NO from the fs cells and Anx A1 and NO, further inhibit the release of ACTH from the C and PRL from the L cells. Summed up, a disinhibition of ACTH and PRL production by the EC is hypothetized.

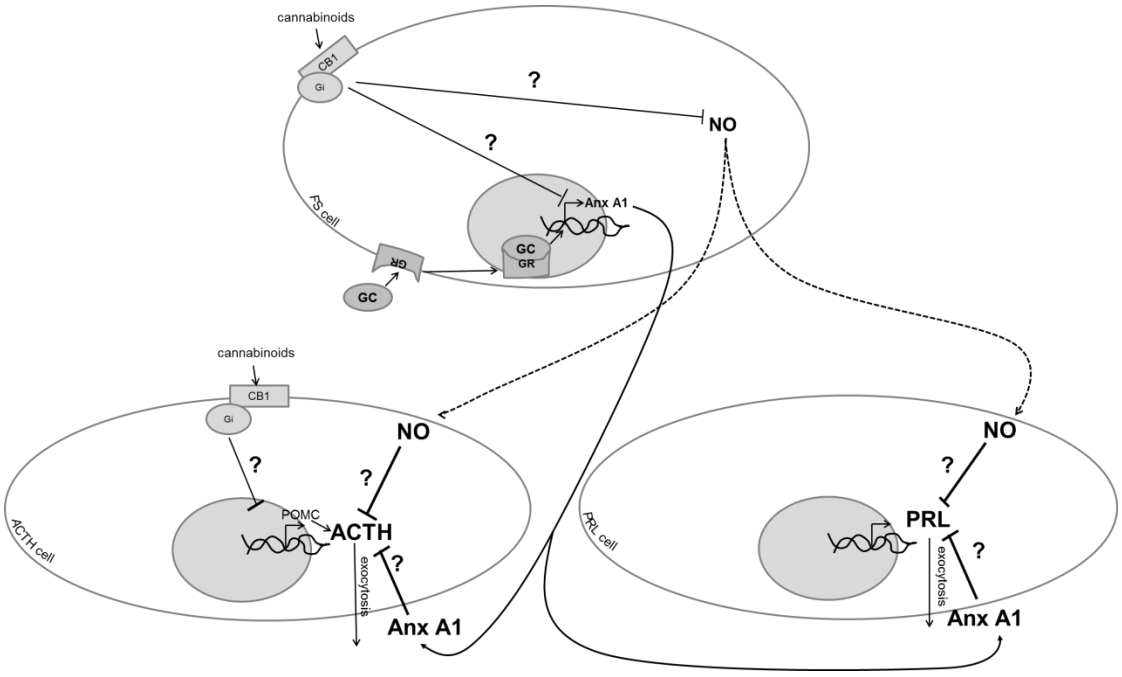


Fig. 1: Proposed mechanism is that endocannabinoids inhibit the production of Anx A1 and NO from the fs cells and Anx A1 and NO, on their side, inhibit the release of ACTH and PRL from hormonal cells. ACTH adrenocorticotropin; Anx A1 annexin A1; $CB_1$ cannabinoid receptor type 1; FS folliculo-stellate cells; GC glucocorticoids; GR GC receptor; NO nitric oxide; POMC pro-opiomelanocortin; PRL prolactin.

The aim of this study was to investigate the influence of EC on fs, C, and L cells. With the assumed existence of an intricate intercellular, regulative mechanism involving Anx A1 and NO as messengers, the focus fell on their impact on ACTH and PRL release.

# Introduction

## 1 The hypothalamic-pituitary axis

### 1.1 Anatomy of the murine hypothalamus

The hypothalamus is part of the diencephalon. It lies ventrally and rostrally to the thalamus (Fig. 2) and commands the sympathetic and parasympathetic nervous system. Furthermore it coordinates the autonomic with the endocrine system and acts itself as an endocrine organ.

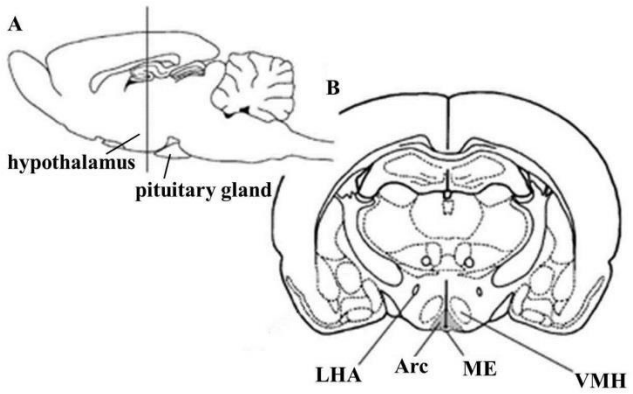


Fig. 2: (A) Sagittal view of the hypothalamus and the pituitary gland in the mouse brain. (B) Coronal section at a level shown by a vertical line in (A). Arc, arcuate nucleus; LHA, lateral hypothalamic area; ME, median eminence; VMH, ventromedial nucleus of the hypothalamus. (Modified from Kishi and Elmquist, 2005.)

At its ventral side the hypothalamus is connected to the pituitary gland via the pituitary stalk. Rostral to the pituitary stalk lies the optic chiasm (OC).

### 1.2 Anatomical location of the third ventricle

The third ventricle (ventriculus tertius) lies between the two parts of the thalamus and connects to the lateral and fourth ventricle as part of the brain cavity system.

Laterally it is limited by the bilateral parts of the thalamus, and dorsally by the tela choroidea. The ventral side of the third ventricle is formed by the infundibulum, the OC, the median eminence (ME) and the tuber cinereum. Occipitally, the third ventricle lies adjacent to recessus pinealis and suprapinealis, rostrally to the recessus infundibularis and supraopticus.

## 1.3 Anatomy of the pituitary gland

### Gross anatomy of the murine pituitary gland

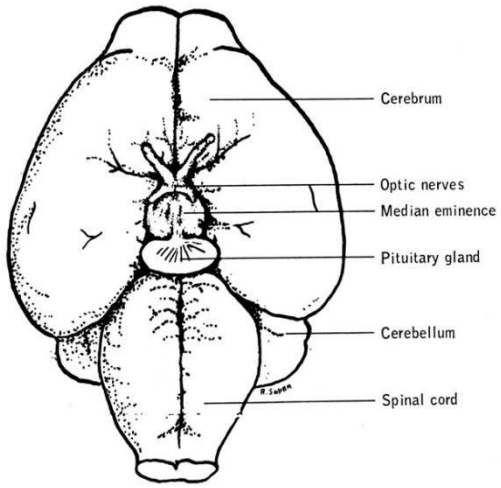


Fig. 3: Drawing of the ventral aspect of the brain to demonstrate the location of the pituitary gland.
(From Green et al., 1966.)

The pituitary gland (hypophysis cerebri) in the mouse rests on the dorsal surface of the basisphenoid bone of the skull and is attached to the floor of the brain by a fragile stalk (Fig. 3).

The gland is slightly flattened dorsoventrally and has an elongated oval shape with its long axis perpendicular to that of the head. The ventral surface is well-vascularized and homogeneous and can be separated into distinct regions. The pituitary gland is divided into anterior, intermediate, and posterior lobes. The anterior lobe contains pars tuberalis (PT) and pars anterior, also known as pars distalis (PD). PT surrounds the pituitary stalk, also called infundibulum. PD is the well-vascularized remainder of the anterior lobe. The posterior lobe is also known as neural lobe or pars neurosa (PN). PN is derived embryologically from the floor of the third ventricle of the brain. Bordering the PN is the narrow layer of the intermediate lobe that is also known as pars intermedia (PI).

The pituitary gland is consistently heavier in female rodents than in male counterparts. The average weight of the pituitary gland of the adult female mouse exceeds that of the male of the same age and strain by 0.5 to 1.5 mg.

**Microscopic anatomy of the murine pituitary gland**

The PN is made up of endings of neurons (magnocellular neurosecretory neurons in the supraoptic (SON) and paraventricular nuclei (PVN) in the hypothalamus), glial cells, ependymal cells, and connective tissue supporting capillaries and sinusoids. The lining cells of the sinusoids show phagocytic activity and are possibly fs cells.

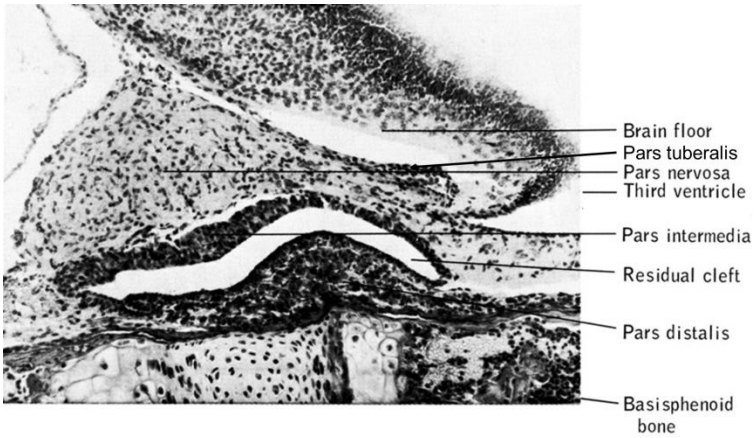


Fig. 4: Sagittal section through the pituitary gland of a newborn mouse (x 100). (From Green et al., 1966.)

The cells of the PI are arranged in groups separated by fibrous connective tissue strands with scarce vascular elements. Most of the cells have oval nuclei and are polygonal with non-granular basophilic cytoplasm rich in melanocyte-stimulating hormone (MSH), β-endorphin and adrenocorticotrope hormone (ACTH). A few chromophobic stellate cells with long processes are interspersed.

The PI and PD are separated by the residual cleft, lined throughout by low cuboidal epithelium. The cells in the PD are arranged in branching cords separated by sinusoids and are of a chromophobic or chromophilic cytological type. Chromophobic cells with spacious nuclei surrounded by small amounts of non-granular cytoplasm make up about 50% of the population, the rest being chromophilic of the acidophilic or basophilic type (Halmi and Gude, 1954).

The fs cells (see 3.1) are chromophobic and make up to 5-10% of the whole cell population. They are small star-like shaped cells with ovoid nucleus and long cytoplasmatic processes intertwining between endocrine cells, and are dispersed throughout the whole pituitary gland. They are morphologically similar to dendritic cells and positive for the dendritic cell marker protein S-100 (Cocchia and Miami, 1980).

The most common chromophilic cell is acidophil, a small round or oval cell with a centrally located nucleus and eosinophilic cytoplasm, which makes up about 40% of the whole number of cells in the PD. L cells (see 3.3) make up to 20% of the acidophilic population and are dispersed in the anterior lobe (Mitchner et al., 1998). The smallest group, making up less than 11%, are basophilic cells. The basophiles, that represent C cells (see 3.2), are small, ovoid cells with short processes (Childs et al., 1987). They count for up to 10% of the cells in a normal pituitary gland and are dispersed in PI, PD and PT. Their distribution is denser in the central portions of the anterior lobe, and they are more numerous in male rodents than in females (GuéRineau et al., 1991; Marchetti et al., 1987).

Some endocrine cells in the pituitary are connected by gap junctions (Fletcher et al., 1975). L cells are prevalent in being connected by gap junctions as compared to somatotrophes, gonadotrophes and thyrotrophes (Meda et al., 1993).

## 1.4 Hormonal regulation

**Hypothalamic-pituitary axis**

As the anterior lobe of the pituitary gland lacks its own nerve supply, the control is regulated by factors produced by the neurosecretory neurons of the hypothalamus. These are hypophysiotropic hormones stimulating or inhibiting the release of hormones from the pituitary gland (Fig. 5).

The neurosecretory system of the hypothalamus comprises the magnocellular[1] and parvocellular[2] part. The magnocellular part includes neurons in the paraventricular nucleus (PVN) and supraoptic nucleus (SON) that synthesize oxytocin (OT) and arginine vasopressin (AVP) that are transported by the hypothalamic-pituitary axis (HPA) through the ME and released from axonal terminals into the PN.

[1] Magnocellular – *magnus* big, *cellula* cell
[2] Parvocellular – *parvus* small, *cellula* cell

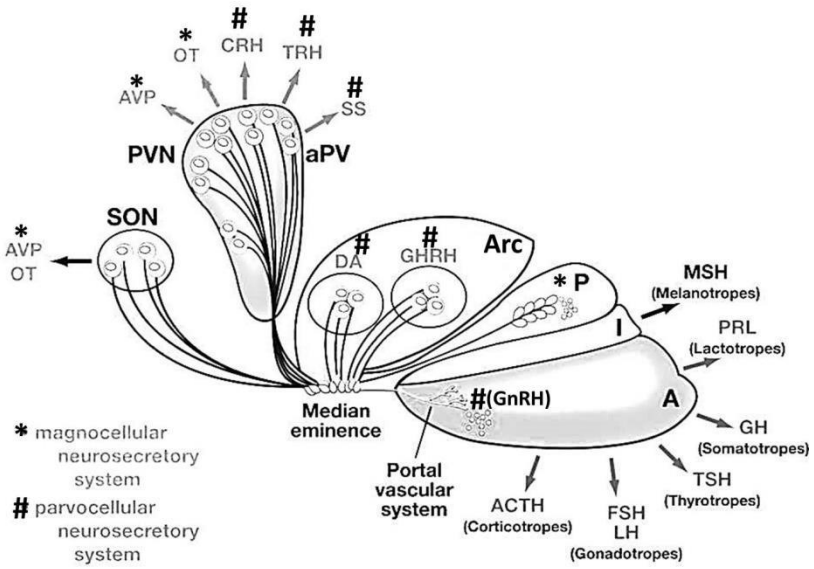


Fig. 5: The hypothalamic-pituitary axis. Areas: SON, supraoptic nucleus; PVN, paraventricular nucleus; aPV, periventricular nucleus; Arc, arcuate nucleus; P, posterior lobe; I, intermediate lobe; A, anterior lobe. Factors: AVP, arginine vasopressin; OT, oxytocin; CRH, corticotropin releasing hormone; TRH, thyrotropin releasing hormone; SS, somatostatin; DA, dopamine; GHRH, growth hormone releasing hormone; GnRH, gonadotropin releasing hormone; MSH, melanocyte-stimulating hormone; PRL, prolactin; GH, growth hormone; TSH, thyrotropin inhibiting hormone; FSH, follicle-stimulating hormone; LH, luteinizing hormone; ACTH, adrenocorticotropic hormone. (Modified from Dasen and Rosenfeld, 2001.)

Synthesis and secretion of follicle-stimulating hormone (FSH) and luteinizing hormone (LH) from gonadotroph cells in the PD are regulated by gonadotropin releasing hormone (GnRH) produced by the parvocellular neurons of the preoptic area (POA) and released into the portal vascular system. Corticotropin releasing hormone (CRH) and thyrotropin releasing hormone (TRH) are synthesized by neurons in the PVN. CRH affects the release of ACTH and MSH from C cells in the PD. TRH affects the release of thyroid-stimulating hormone (TSH) from the thyrotrophic cells. Growth hormone releasing hormone (GHRH) and dopamine (DA) are synthesized by neurons of the arcuate nucleus (Arc) and the adjacent ventromedial nucleus (VMH) of the hypothalamus and affect the release of growth hormone (GH) from somatotrophs and prolactin (PRL) from L cells in the PD, respectively. Somatostatin (SS) is mainly synthesized by neurons in anterior periventricular nucleus (aPV) of the hypothalamus. The parvocellular neurons project to the ME where they release hormones that are transported to the anterior pituitary lobe by the portal vascular system.

The function of OT is uterotonic, it stimulates milk-ejection, facilitates reproduction and brood care, controls body fluid and cardiovascular hoemostasis (reviewed by Gimpl and Fahrenholz, 2001). AVP regulates extracellular fluid volume and acts as a

vasoconstrictor (reviewed by den Ouden and Meinders, 2005). FSH regulates development, growth, pubertal maturation, and reproductive processes, while LH triggers ovulation and development of the corpus luteum in females, and stimulates Leydig cell production of testosterone in males (reviewed by Howles, 2000). MSH regulates the synthesis, concentration and distribution of pigment granules (melanin)[3]. TSH causes the thyroid gland to produce triiodothyronine (T3) and thyroxine (T4), thus controling metabolism (Yamamura et al., 2006). GH stimulates protein synthesis and increases fat breakdown to provide the energy necessary for tissue growth. It also antagonizes the action of insulin[4]. SS regulates insulin and glucagon, hence affects cell proliferation (Gyr et al., 1987).

**ACTH regulation**

ACTH was isolated in 1943 and synthesized in 1963 (Simpson et al., 1943; Pickering et al., 1963). It stimulates glucocorticoid (GC) synthesis and secretion from the zona fasciculata in the adrenal cortex. GC in turn negatively influence the secretion of ACTH (Cone and Mountjoy, 1993; Mountjoy et al., 1992; Smith and Vale, 2006).

GC exercise different functions via their corresponding receptors (Munck et al., 1984; Munck 2005). Their main function is the redistribution of energy resources in order to restore homeostasis (Herman and Seroogy, 2006; Jacobson, 2005). They stimulate gluconeogenesis and thus promote lipolysis and protein catabolism (Mastorakos and Pavlatou, 2005). GCs also stimulate the appetite by acting on certain brain areas (McEwen, 2000).

CRH and AVP are secreted in a circadian manner (Chrousos and Gold, 1992). The amplitude of release in rodents increases in the early evening, which leads to an increase in ACTH and GC release. This process is interrupted in rodents by light, feeding and stress (Geracioti et al., 1992; Hiroshige and Wada-Okada, 1973).

[3] Source – Encyclopædia Britannica, http://www.britannica.com/EBchecked/topic/373748/melanocyte-stimulating-hormone-MSH
[4] http://www.britannica.com/EBchecked/topic/247255/growth-hormone-GH

Rhythms in GC secretion and serum concentration are well known and are some of the first cues indicating SCN as the brain clock. SCN lesions led to loss of corticosterone rhythm (Moore and Eichler, 1972). Humans, nonhuman primates and rodents display circadian changes in GC secretion (Weitzman et al., 1971; Moore and Eichler, 1972; Gallagher et al., 1973; Dubey et al., 1983; Van Cauter and Refetoff, 1985; Czeisler and Klerman, 1999). The corticoid secretion begins to rise before waking in nocturnal and diurnal species and peaks during the day in diurnal, and during the night in nocturnal species (Adler et al., 1983; Albers et al., 1985; Ottenweller et al., 1987). The adrenal gland itself also manifests rhythms in clock-gene expression, influencing the rhythmic responsiveness to pituitary ACTH (Ungar and Halberg, 1962; Dunn et al., 1972; Buijs et al., 1997; Bittman et al., 2003; Kalsbeek et al., 2003; K. Oishi et al., 2003; Guo et al., 2006; Oster et al., 2006; Fahrenkrug et al., 2008).

Highest plasma levels of corticosterone in the rat are found short before the dark period begins (scotoperiod) (Márquez et al., 2005). Highest plasma cortisol is found short after awakening and the lowest in the evening (Armario, 2006). Therefore GC seem to embody the function of a mediator for the activity period.

The GC feedback inhibition in the brain takes place through two types of glucocorticoid receptors (GR): type I is activated by basal GC concentration while type II is activated by basal and elevated GC concentration. The PVN expresses a high density of the GR type I. The hippocampus expresses both types of the receptor and GC infusion in those areas reduces HPA axis activity (Smith and Vale, 2006).

**PRL regulation**

PRL was identified by Riddle et al. in 1933. Studies with fish, birds and rabbits revealed the importance of this hormone for brood care (Blüm and Fiedler, 1965; Lehrman and Brody, 1961; Zarrow et al., 1961). It influences lactation, water and electrolyte balance, growth, development, immunoregulation, stress response, anxiety induced behavior suppression, and regulates OT neurons, suppresses fertility, stimulates appetite, food intake, myelination in the central nervous system (CNS) and neurogeneration in the olfactory bulb (Freeman et al., 2000; Grattan et al., 2008; Bole-Feysot et al., 2013; Pfaff et al.,2009).

PRL available in the CNS is transported via special carrier proteins to its target areas, the most important of which is the hypothalamus (Walsh et al., 1987). Knowledge on PRL secretion control was provided by Hokfelt and Fuxe (1972), who discovered its link with the DA synthesis, Ben-Jonathan et al. (1977), who showed that PRL is inhibited by DA and by Gudelsky and Porter (1979), who confirmed that PRL promotes DA secretion into the pituitary portal vessels.

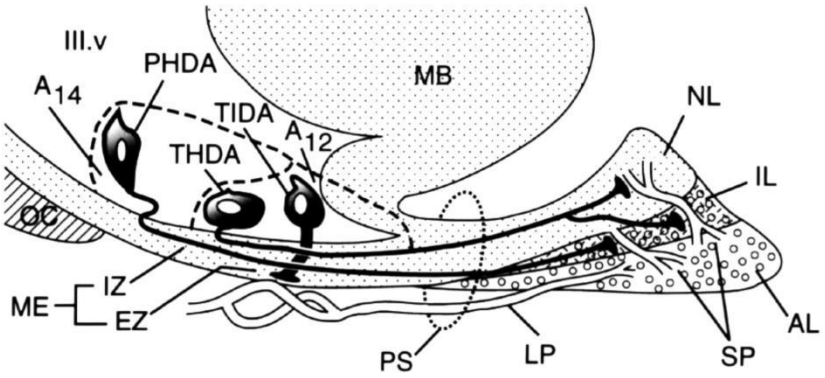


Fig. 6: Dopaminergic neurons project from hypothalamic structures to regions of the pituitary gland reaching PRL-producing cells. TIDA neurons project from the dorsomedial Arc to the external zone of the ME. DA is then transported to the anterior pituitary lobe, where it acts on type 2 DA receptors. THDA neurons project from the rostral Arc to the intermediate lobe and posterior lobe. PHDA neurons project from the aPV to the intermediate lobe. DA from the THDA and PHDA neurons is transported through the short vessels from the posterior lobe to the anterior lobe. A12, Arc; A14, aPV; AL, anterior lobe; IL, intermediate lobe; LP, long portal veins; MB, mediobasal area; ME, median eminence; EZ, external layer; IZ, internal layer; NL, neural lobe; OC, optic chiasm; PHDA, periventricular tuberohypophyseal dopaminergic; PS, pituitary stalk; SP, short portal veins; TIDA, tuberoinfundibular dopaminergic; THDA, tuberohypophyseal dopaminergic. (From Lerant et al., 1996.)

PRL is controlled mainly by the inhibitory DA produced by three groups of hypothalamic neurons (Fig. 6). The tuberoinfundibular dopaminergic (TIDA), tuberohypophyseal dopaminergic (THDA) and periventricular tuberohypophyseal dopaminergic neurons (PHDA) are involved in inhibiting PRL (Freeman et al., 2000) and are all under the control of SCN projections (Horvath, 1997). Rhythmic PRL release results from timed TIDA and PHDA neural activity, but not THDA (Sellix and Freeman, 2003; Sellix et al., 2004).

Lesions in the PVN and PN impair suckling induced PRL (Kiss et al., 1986; Murai and Ben-Jonathan, 1987; Bodnár et al., 2004) meaning that a highly effective PRL releasing factor should have its origin in the PVN and involves the PN. So far, there is a lot of controversy regarding TRH, TSH, AVP, OT and salsolinol as potential releasing factors for PRL (Greef et al., 1987; Rondeel et al., 1988; Thomas et al., 1988; Nagy et al., 1991; Samson et al., 1986; Johnston and Negro-Vilar, 1988; Tóth et al., 2001).

Salsolinol is a DA derivative found in PN and involved in stress and suckling induced PRL secretion and thus most promising PRL releasing factor (Bodnár et al., 2004).

In humans PRL has a diurnal rhythm with highest plasma concentration at night and lowest in the waking hours (Freeman et al., 2000). In rats, PRL follows a circadian pattern that is lost after SCN lesions (Bethea et al., 1979; Mai et al., 1994). Circandianly controlled PRL peaks occur additional to the baseline along with the LH proestrus surge in rats and mice (Blake, 1976; Bethea and Neill, 1980).

## 1.5 Portal vascular system of HPA and ME

A structure in which neurosecretory factors are secreted into blood vessels is referred to as a neurohemal organ. The axonal terminals of the hypothalamo-ME tract terminate in the outer layer of the ME, where secreted releasing and inhibiting hormones produced by the hypothalamic neurons are able to diffuse into the adjacent portal vessels.

Popa and Fielding first noted that the capillary network below the human hypothalamus is connected through portal vessels to the PD (Popa, 1930). In 1947, Green and Harris proposed that the hypothalamus may regulate pituitary functions by means of humoral factors carried in the portal vessels.

The physiological importance of the ME is based on the fact that it is an integrative part of the pituitary portal system connecting the hypothalamus with the anterior lobe of the pituitary gland. It is the ME where the hypothalamic releasing and inhibitory hormones collect before entering the portal system.

The ME lies ventrocaudal to the hypothalamus at the base of the third ventricle (Fig. 2). A small swelling on the tuber cinereum posterior to the infundibulum may extend rostrally as far anterior as the OC, while merging caudally with the PN. In its microstructure the ME is divided into internal and external layers. The internal layer is further differentiated into ependymal and fiber layers. The fiber layer is traversed by axons of the HPA (see 1.4.1). The primary capillary plexus of the portal vessels in large part is located between the ME and the PT. The ME itself is devoid of a blood brain barrier and is part of the circumventricular organs.

# 2 Rhythms

## 2.1 Circadian rhythms

The Earth rotating around its axis determines the period length of circadian[5] rhythms – about 24h. Organisms are capable of generating self-sustained "free-running" (endogenous) circadian rhythms. The circadian system is well conserved during evolution from unicellular to multicellular organisms. It influences a variety of behavioural and autonomic functions and can be synchronized to environmental cues which are called "zeitgebers", such as the change between day and night (Korf and von Gall, 2013).

In the course of phylogenetic development, circadian organization has evolved in almost all living organisms to anticipate the rhythmic day-night change (Dunlap, 1999;Dvornyk et al., 2003; Johnson et al., 1998).

In multicellular organisms the circadian system comprises a "central" circadian rhythm generator ("master clock") and multiple subsidiary clocks in the periphery (slave oscillators, peripheral clocks) (Fig. 7). Both, the central circadian rhythm generator and the slave oscillators contain molecular clockworks including clock genes and their protein products that interact with each other in transcriptional and translational feedback loops.

The master clock is located in a distinct region of the brain, the bilaterally arranged suprachiasmatic nuclei (SCN) of the hypothalamus. They integrate the light impulse information from the retino-hypothalamic tract (RHT) and translate it into neuronal, neuroendocrine and hormonal factors targeting the peripheral clocks. SCN neurons belonging to the circadian system contain a molecular clockwork involving autoregulatory transcriptional and translational feedback loops of clock genes and rhythmic output signals of a circadian period length (Okamura et al., 2002;Reppert and Weaver, 2002), Fig. 7.

[5] *Circa* – about, *dian* – day.

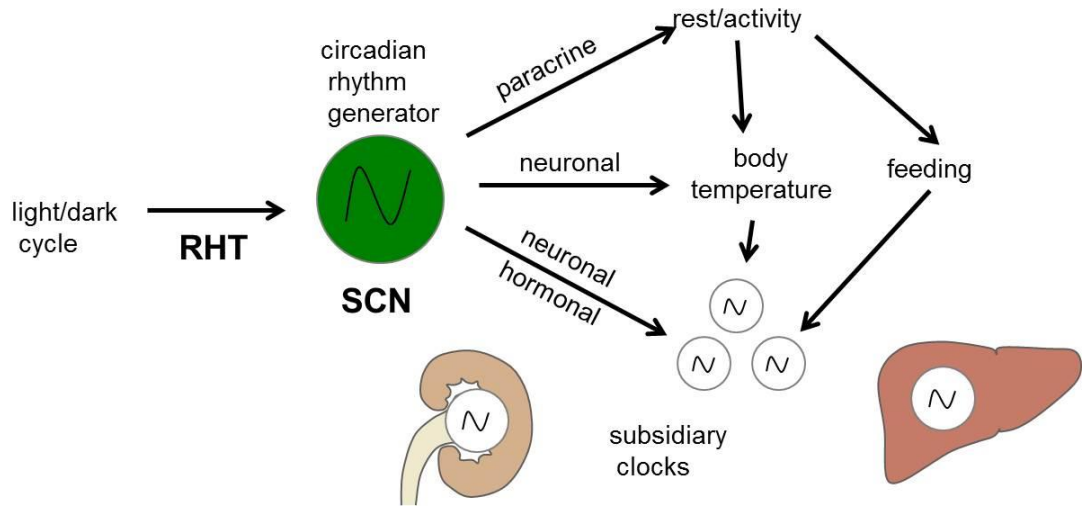


Fig. 7: Structure of the timing system with SCN as a pacemaker, syncronising the subsidiary clocks in the brain and periphery. (From Korf and von Gall, 2013.)

One clockwork cycle includes the transcriptional activators CLOCK/NPAS2 and BMAL1, which have a helix-loop-helix DNA binding domain and two Per-Arnt-Sim protein interaction domains that form heterodimers, which bind the E-box (like) enhancer elements from the promoter region of clock *Per1*, *Per2, Cry1*, *Cry2* and of "clock-controlled" genes (Fig. 8). The protein products of the *Per* and *Cry* genes, on the other hand, constitute repressor complexes with further proteins – casein kinase 1ε and δ. The repressor complex is transported to the nucleus where it binds to promoter regions and inhibits its own transcription, mediated by CLOCK/NPAS2 and BMAL1. The cycle ends with hyperphosphorylation, ubiquitination and proteoasomal degradation of the complexes. The main negative feedback loop is modulated by further feedback loops, involving the orphan nuclear receptors REV-ERBα and RORα, which control the expression of *Bmal1* (Korf and Stehle, 2002; Reppert and Weaver, 2002; von Gall et al., 2003).

The master clock can generate a self-sustained rhythm, whereas the peripheral clocks lose their rhythmicity after several cycles. To prevent a desynchronization, the peripheral clocks need to be coordinated by multiple direct and indirect output pathways of the central rhythm generator. Synchronization is not possible by a single "entrainment" signal, but requires a combination of factors, which differ among the different tissues and organs. In addition, peripheral clocks can be directly entrained by various external (environmental) stimuli (Takahashi, 2004).

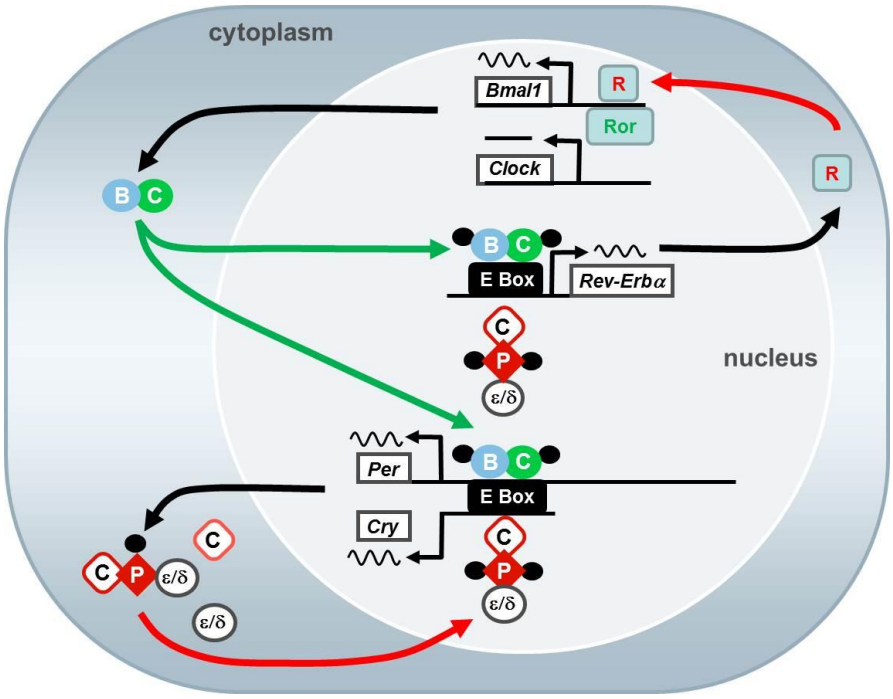


Fig. 8: The clock mechanism comprises interactive positive (green) and negative (red) feedback loops. CLOCK (C, oval) and BMAL1 (B, oval) form heterodimers and activate transcription of the Per, Cry and Rev-Erbα genes through E-box elements. As the levels of PER proteins increase (P, red rhombus), they complex with CRY proteins (C, rhombus) and CKIε/CKIδ (ε/δ, circle), and are phosphorylated (p). In the nucleus, the CRY–PER–CKIε/CKIδ complexes associate with CLOCK–BMAL1 heterodimers to shut down transcription while the heterodimer remains bound to DNA. For the positive feedback loop, increasing REV-ERBα levels (R, box) act through Rev-Erb/ROR response elements in the Bmal1 promoter to repress (-) Bmal1 transcription. CRY-mediated inhibition of CLOCK–BMAL1-mediated transcription de-represses (activates) Bmal1 transcription, because REV-ERBα-mediated repression is inhibited. (From Reppert and Weaver, 2002.)

Mammals possess an intricate circadian system, sustained by evolutionary advances, such as constant body temperature. Some of the functions that are directly influenced by the endogenous rhythm are locomotor activity, sleep-wake cycle, control of body temperature, food intake and metabolism (Elliott 1976). The cell cycle is affected as well (Korf and von Gall, 2013).

The most important neuroendocrine tool of the circadian system is melatonin, which is produced at night in the pineal gland under the control of the SCN. Melatonin, a chronobiotic, acts upon specific receptors, feeds back to the SCN and modulates several autonomic functions (Arendt and Skene, 2005).

GC are secreted by day from the adrenal gland cortex. They activate GR that are widely distributed in the body and thus transmit the circadian timing signal (Chrousos and Gold, 1992).

The feeding-fasting cycles which under normal conditions are in phase with the rest-activity rhythms are controlled by the peripheral clocks in the liver, kidney, pancreas

and heart. In these organs, the expression profiles of many circadian genes are influenced by the timing of food intake. This entrainment may be mediated by hormones secreted upon feeding or fasting e.g., cholecystokinine, ghrelin or leptin, by food metabolites, e.g., glucose, cholesterol, fatty acids, by postprandial temperature elevations and by the intracellular redox state ratio. The molecular clockwork in peripheral tissues controls circadian rhythms in metabolic and physiologic cell-/organ-function. The importance of molecular clocks is underlined by microarray studies showing that up to 20% of the genes expressed in peripheral organs (liver, muscle, adipose tissue) are rhythmic suggesting that a considerable portion of the transcriptome is controlled by the circadian system. The rhythmically expressed genes encode proteins and enzymes involved in biosynthetic and metabolic processes such as lipid metabolism, glycolysis and gluconeogenesis, oxidative phosphorylation and detoxification pathways. Notably, in many of these pathways the rate-limiting enzymes are under circadian control. These data indicate a close interrelationship between the circadian system and energy metabolism (Arendt et al., 1985; Takahashi, 2004; Korf and von Gall, 2013).

## 2.2 Circannual rhythms

A biological rhythm with an endogenous period close to a year is called a circannual rhythm. Circannual rhythms are self-sustainable and entrainable.They influence seasonal changes in body weight, food consumption, and the occurrence of hibernation.

In 1896 Dubois first suggested that the mentioned processes are timed. It was then Rowan in 1926 who investigated the annual photoperiodism in migrating birds and some fish species. The first term for those rhythms was “circannian” – established by Pengelley and Fischer in 1957, based on their experimental demonstration of an annual rhythm with a golden-mantled ground squirrel (Spermophilus lateralis). They showed that the seasonal alternation of hibernation and active state persisted for two years in constant conditions of temperature and daylength with a period close to 300 days. The fact that the period length does not overlap with the duration of a year hints to the endogenous character of the rhythm of the animal. Later on, Gwinner (2010) studied song birds raised in captivity, to find that their nocturnal restlessness reflects the natural duration of migration and that they would find their wintering quarter in Africa (the direction of migration with respect to annual cycle changes) without ever being there.

Summed up –physiological alternations lead to a certain adaptive behavioural pattern (breeding, migration) and were caused by slow seasonal changes (daylength).

Lincoln and his group showed that the gonadal function of Soay sheep depends on the photoperiod. His suggestion was that the SCN and pineal gland regulate the gonadal function by a melatonin signal sent to the pituitary gland. Moreover, when the neural path connecting the SCN and pineal with the pituitary gland was interrupted, the circannual oscillation of PRL secretion from the pituitary persisted in constant cycles under constant long days, suggesting an eventual role of the pituitary gland as a pacemaker for the circannual rhythm (Hazlerigg et al., 2004; Lincoln et al., 2006).

# 3 Experimental models

## 3.1 FS cells

The fs cells represent a heterogeneous cell population first described in 1953 by Rinehart and Farquhar. They were named "folliculo-stellate" by Evelyne Vila-Porcile in 1972 because of their appearance and follicule forming ability and studied only after 1980 when a protein marker S-100β of them was discovered (Cocchia and Miami, 1980).

They are small star-like shaped cells with ovoid nucleus and long cytoplasmatic processes intertwining between endocrine cells and forming an elaborate three-dimensional anatomical network in which the endocrine cells are embedded. They have been ascribed various roles and functions such as being stem cells, having phagocytotic activity, regulating supportive, nutritive, regulative and communicative activities between the hypothalamus and hormone producing glandular cell populations in the pituitary gland (Morris and Christian, 2011; Vankelecom, 2012; Mitsuishi et al., 2013).

They produce a number of factors that modulate pituitary hormone release by paracrine or juxtacrine mechanisms: basic fibroblast growth factor (bFGF), vascular endothelial growth factor (VEGF), follistatin, cytokines such as leukemia inhibitory factor (LIF ), interleukin 6 ( IL-6), macrophage migration inhibitory factor (MIF ) (Allaerts and Vankelecom, 2005). Nitric oxide (NO) has also been detected in FS cells - Ceccatelli (1993) detected nNOS in rat pituitary FS cells, and Vankelecom et al. (1997) detected iNOS.

**The fs TtT/GF cell line**

Kinji Inoue has developed the fs TtT/GF cell line in 1992 using TtTb cell line that has been induced by radiothyroidectomy and causing tumor growth in an euthyroid mouse (Inoue et al., 1992; Ito et al., 1984).

Inoue et al. (1999) found that the TtT/GF cells express GFAP (glial fibrillary acidic protein), S-100 and respond strongly to PACAP. Gloddek et al. (1999) showed that bFGF, VEGF, PACAP, and GR are expressed in the TtT/GF cell line. The expression of cytokines has been studied by Allaerts and Vankelecom (2005).

**The fs Tpit/F1 cell line**

Kinji Inoue has developed a second fs Tpit/F1 cell line in 2000 from the anterior pituitary cells of a large T antigen transgenic mouse. He and Devnath showed that the cells express nNOS, S-100, GFAP, bFGF, VEGF, IL-6, glutamine synthase (GS), and pituitary restricted transcription factor (Ptx1) (Devnath and Inoue, 2008).

## 3.2 C cells

The C cells are small, ovoid cells with short processes (Childs et al., 1987). The C cells express pro-opiomelanocortin (POMC) that is a precursor molecule of ACTH, MSH, and β-endorphin and hence secrete the latter mentioned peptides. The main stimulus of secretion is CRH, along with vasoactive intestinal peptide (VIP), OT, EGF and angiotensin II. The C cells in Syrian hamster express the $CB_1$ receptor (Yasuo et al., 2010).

**The C AtT20/D16v cell line**

Furth et al. developed in 1953 ACTH secreting tumors, out of which the AtT20/D1 cell line was developed, to be followed by AtT20/D16v and further AtT20/D16:16 (Tashjian, 1979; Woods et al., 1992). AtT20/D1 grow in suspension culture, while AtT20/D16v are adherent with slight suspension preference, and AtT20/D16:16 are strictly adherent.

AtT20/D16v were confirmed to produce POMC (Phillips and Tashjian, 1982). AtT20/D1 and AtT20/D16v express the GR (Svec and Rudis, 1981; Kitchener et al.

2004). AtT20/D16v express nNOS (Qian et al., 1999), eNOS, and iNOS (Ohta et al., 1993).

## 3.3 L cells

The L cells are dispersed in PD and PI and express intracellular estrogen receptors (ER) (Mitchner et al., 1998). Additionally, estradiol, TRH, VIP, IL-6, and CIN induce rapid, non-genomic and slow, genomic PRL release from the L cells (Morris et al., 2002).

**The L GH4C1 cell line**

The establishment of three strains of epithelial cells, among which GH4C1, from a transplantable rat pituitary tumor (MtT/W5) was performed by Tashjian et al. (1968; 1979).

GH4C1 express PRL in prevalence to GH (Tashjian et al., 1968) and manifest ER (Reese and Katzenellenbogen, 1992). GH4C1 express nNOS (GH3 (Qian et al., 1998), eNOS, and iNOS (Qian et al., 1999). $CB_1$ but not $CB_2$ was determined by Ho and Zhao in 1996 on GH4C1 cells.

## 3.4 Mus musculus

The mouse (Mus musculus) presents a suitable model for studying and investigating biological functions in man due to its close phylogenetic relation(ship) to man. The general processes such as oogenesis, spermatogenesis, fertilization, organ development are comparable. The quick generation turnover with life span of two to three years, gestation about twenty days resulting in a brood of five to twelve animals that are already six to eight weeks after birth sexually mature, shortens experimental time immensely. Small size, cheap and easy maintenance are great benefits worth mentioning. Moreover, there is a great deal of literature based on the rodent, and more specifically on mouse models.

The strains available are thoroughly genetically characterized. Despite the obvious physical differences, the murine genome is entirely sequenced and is up to 80% identical with the human one (Mouse Genome Sequencing Consortium, 2002). Human and murine genomes are thus described as synthenic and orthologically close. All methods used for genetic manipulation and *in vitro* cultivation of embryos are well

established which allows the selective analysis of specific genes using knock out (gene inactivation), knock in (gene overactivation), and transgenic (insertion of xenogenes) animals.

The inbred strain C3H was developed from L.C. Strong at the Bussey Institute, after crossing of Bagg albino female with a DBA male and used as an animal model comparison. An inbred strain is defined as one derived from more than 20 consecutive sister and brother matings. This directly leads to homozygotosy, which provides on one hand greater level of controllability of the experimental set, but on the other hand further pitfalls as well. For instance C3H mice are blind due to homozygotosy for retinal degeneration 1 mutation, Pde6brd1 (Chang et al., 2002). However, there are more differences between the "real" wild type and the laboratory inbred mouse. One of them is the relatively small genetic pool, leading to small number of genetic polymorphisms that would be usual among a broad mouse population. Another difference is rather interesting – inbred strains have longer chromosomal telomeres. Furthermore, laboratory animals are more susceptible to infections and cancer diseases.

# 4 Annexin A1

## 4.1 Discovery

Flower and Blackwell (1979) count as the discoverers of the protein Annexin A1 (Anx A1). It was found based on its properties as an inhibitor of the phospholipase A2 (PLA2) and thus inhibitor of eicosanoid generation as well.

In the beginning the protein had various names: macrocortin (from peritoneal exudates from GC-treated rats) (Blackwell et al., 1980); renocortin (from rat renal medulla cells) (Russo-Marie and Duval, 1982); lipomodulin (from isolated neutrophils) (Hirata et al., 1980). It was accepted that these three proteins were functionally identical and it was agreed on a uniform name - lipocortin (Di Rosa et al., 1984). In1986 Wallner et al. 1986 cloned the protein and numbered it lipocortin1. In 1990 41 researchers agreed on the

name annexin[6] proposed by Geisow (due to its membrane binding properties) and the numbering system proposed by Pepinsky (Crumpton and Dedman, 1990).

## 4.2 Genetics

The ANXA1 gene is located on chromosome 9 in humans, the exact locus is starting at 75766673 and ending at 75785309 bp from pter with 8 splice variants known so far[7]. The Anxa1 gene in mice is located on chromosome 19, 20373428-20390944 bp with 7 splice variants[2]. The exon-intron organization of ANXA1 genes in vertebrates have been described and are highly conserved, each gene consisting of 13 exons.


Fig. 9: The ANXA1 gene contains 13 exons, of which the first and last are uncoding 5' and 3' sequences (black regions), with the translation initiator codon (AUG) found near the beginning of the second exon (grey regions). (Modified from Rodrigues-Lisoni, 2010.)

The comparison of conserved and variable residues between human Anx A1 protein and annexin protein from different vertebrates shows amino acid identities of 100% (Pan troglodytes), 91% (Canis familliaris), 87% (Mus musculus) and 89% (Rattus norvegicus) (Rodrigues-Lisoni et al., 2006).

The gene regulation is driven by GC through consensus sequences present in the upstream region of TATA box and cyclic AMP-responding element-binding protein (CREB) transcription factor (Fig. 10, Fig. 11; Horlick et al., 1991; Antonicelli et al., 2001). Already in 1986, Wallner et al. recognized the putative GREs (GC response elements) in the Anx A1 gene.

GC enhance Anx A1 expression, lead to its translocation from the cytoplasm to the outer cell membrane surface in a mechanism different from exocytosis. It includes

[6] Annex – from latin (annexare) to bind
[7] Ensembl genetic database - February 2014:
http://www.ensembl.org/Homo_sapiens/Gene/Summary?db=core;g=ENSG00000135046;r=9:75766673-75785309
http://www.ensembl.org/Mus_musculus/Gene/Summary?db=core;g=ENSMUSG00000024659;r=19:20373428-20390944

activation of the GC receptor and subsequent kinase cascade as well as Anx A1 transformation (phosphorylation, glycosilation).

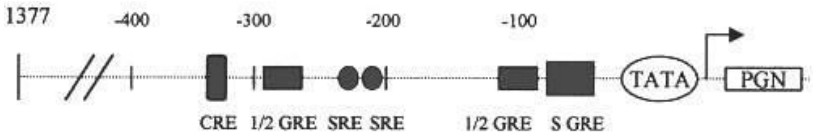


Fig. 10: The Anx A1 promoter sequence in the mouse JEG3 cell. (Modified from Antonicelli et al., 2001.)

Furthermore, ATP-dependent K+ channels are stimulated and ATP-binding cassette transporter (ABC) is recruited to externalize Anx A1 (Philip et al., 1998; Solito et al., 2003; Solito et al., 2006; Chapman et al., 2003).

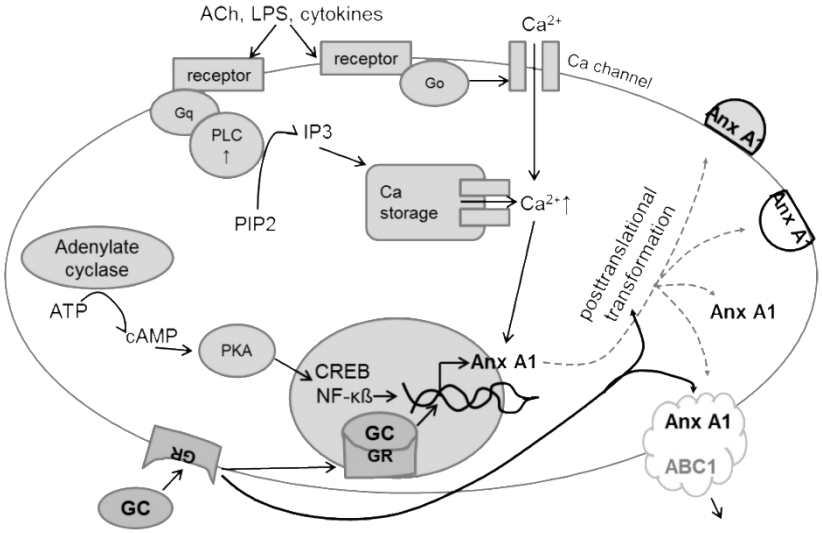


Fig. 11: Regulation of Anx A1 gene expression and subsequent modulation of the protein.

## 4.3 Protein characteristics

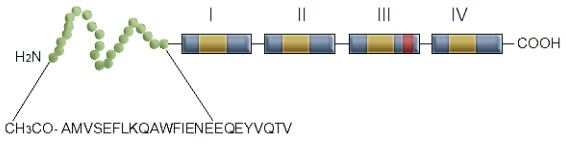


Fig. 12: The Anx A1 protein. N-terminal region with amino acids and four repeats of 70-75 amino acids in C-terminal region. (Modified from Rodrigues-Lisoni, 2010.)

Anx A1 is a member of the annexin suprafamily characterized by a C-terminal homologous domain with 4 to 8 repeats of 70-75 aminoacids, responsible for calcium and phospholipid binding properties (Fig. 12). Due to these properties, Anx A1 can bind membranous structures. The variable N-terminal region is unique for each annexin

member in length and sequence and includes potential sites of phosphorylation, glycosylation and peptidase action (Gerke and Moss, 2002).

The protein sequence is arranged around a hydrophobic core (≥80% of the amino acids), giving the protein a "doughnut" 3D shape in space. Four Ca binding sites have been first postulated by Schlaepfer and Haigler (1987).

There is some controversy regarding the exact molecular size and structure of Anx A1 due to the Anx A1 -activity of peptides of size as low as 1.6 and higher than 200 kDa with most noticeable candidates weighing 15, 24, 33, 37, 39 and 40 kDa. This diversity is explained by the fact that the precursor protein is being cleaved and posttranslationally transformed according to the functions it has to suit. Moreover, different complexes (e.g. with S-100) or dimers have been reported to take place (Blackwell et al., 1980; Vong et al., 2007).

**Posttranslational modification**

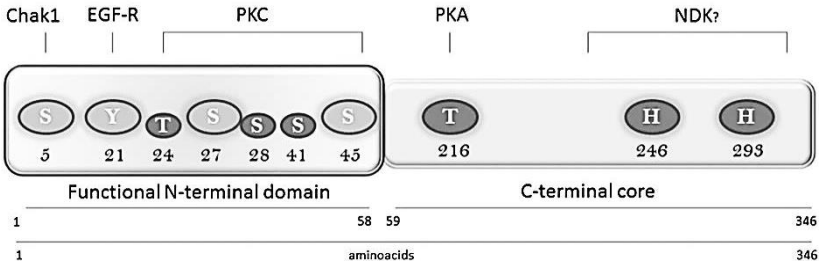


Fig. 13: Phosphorylation sites on the Anx A1 molecule. (Modified from D'Acunto et al., 2013.)

Anx A1 is available in different forms regarding molecular weight, local distribution and functions due to its different variants that result after phosphorylation by the phosphokinase A (PKC), C (PKA), epidermal growth factor (EGF) receptor and transient receptor potential cation channel (TRPM 7) kinases. Phosphorylation on the Ser5 residue results in building a complex with the S-100 protein; phosphorylation on the Ser27 residue results in translocation of the molecule from the cytosol to the membrane. After phosphorylation on the Tyr21, Anx A1 acts inhibitory on the insulin receptor. GC lead to phosphorylation on the Thr216 by PKA and a new class of channel kinases, the TRPM 7 phosphorylate Ser5. TRPM 7 is bifunctional, consisting of a TRP ion channel and a protein kinase domain (D'Acunto et al., 2014).

## 4.4 Function

### Anx A1 inhibits PLA2

PLA2 exists in more than one form and does not obey the classical Michaelis-Menten enzyme kinetics (Chang et al., 1987; Burke and Dennis, 2008; Sun et al., 2014) which complicates PLA2 inhibition assays. It was Hirata et al. (1980) who succeeded in demonstrating PLA2 inhibition by Anx A1 in a cell free system. Further studies of Hirata (1982) showed that Anx A1 reduced the Vmax of the enzyme catalyzed reaction, but not the Km value for the substrate. Later, it could be specified that Anx A1 interacts with the cytosolic form and not the secretory of PLA2 (Croxtall et al., 1996).

### Anx A1 inhibits COX-2

Vakalopoulou et al. suggested in 1991 that Anx A1 binds to mRNA AU-rich at the 3' end and thus prevents its translation. Cyclooxygenase 2 (COX-2) and iNOS mRNA have AU-repeats at their 3' end (Bailey, 1991). Both COX-2 and subsequent prostaglandin 2 (PGE2) increase was blocked by dexamethasone (Dex) in A549 cells, but only PGE2 inhibition was reversed by an anti-Anx A1 Ab (Newman et al., 1994). Since the COX-2 promoter contains GRE sequences it is possible that the enzyme expression is directly regulated by GC (Tazawa et al., 1994). However, Anx A1 prevents prostaglandin and EC synthesis by inhibiting PLA2, that plays an essential role in providing arachidonic acid (AA) as a substrate.

### Anx A1 inhibits iNOS

iNOS gene is GC sensitive (Gilbert and Herschman, 1993), but does not contain GRE elements (Martin et al., 1994). An experiment performed on macrophagial J774 cells demonstrated the inhibitory role of Anx A1 on iNOS expression regulation (Ferlazzo et al., 2003). Moreover, it was earlier shown that lipopolysaccharides (LPS)- induced iNOS expression was reversed by an anti-Anx A1 Ab (Wu et al., 1995). Minghetti et al. (1999) showed as well, that LPS- induced iNOS was inhibited by Dex induced Anx A1.

## 4.5 Localization

Anx A1 is expressed in the tongue, tonsils, cells of the immune system, placenta, epithelium of the lung, renal system, in adypocytes, smooth muscles and cardiomyocytes (BioGPS/ GeneAtlas U133A, Fig. 14).

As for the CNS, Anx A1 is expressed in the pituitary gland, olfactory bulb, hypothalamus (ME, PVN, Arc, and aPV) (Smith et al., 1993). Anx A1 is abundant in ependymal cells, close to CRH/AVP neurons in the PVN (Theogaraj et al., 2005).

Furthermore, Anx A1 has been detected in: the ependyma of rat ( Woods et al., 1990; Smith et al., 1993; McKanna and Zhang, 1997), human (Johnson et al., 1989; Dreier et al., 1998); glial cells in the rat ( McKanna, 1993; McKanna and Zhang, 1997), human (Johnson et al., 1989; Eberhard et al., 1994); in the human hippocampus (Eberhard et al., 1994) and rat cerebellum (Young et al., 1999) (Table 1).

Table 1: Presence of Anx A1 in various cell types in the brain. (Modified from Solito et al., 2008.)

| Anatomical location | Species | Cell type |
|---|---|---|
| **Ependymal cells** | | |
| Lining the ventricular system, including the specialised tanycytes of the third ventricle and the choroid plexus | Rat | |
| | Human | |
| | Mouse | Absent from the hypothalamic median eminence |
| **Glial cells** | | |
| Subependymal layer | Human | Astrocytes (intracellular and diffuse) |
| Unspecified region | Human | ANXA1 (not ANXA2 or ANXA4) in microglia; absent in astrocytes and oligodendrocytes |
| Hippocampus | Human | ANXA1 (with ANXA2 and ANXA4) in subependymal astrocytes |
| Thalamus and throughout the brain | Rat | Restricted to glia (ramified microglia); absent in astrocytes and neurons |
| Throughout the brain, highest in neostriatum | Rat | Present in microglia |
| Hypothalamus, hippocampus | Rat | Scattered non-neuronal cells (glia?) |
| Midbrain | Mouse | Signal detected in a few scattered glial cells |
| **Vascular tissue** | | |
| Hippocampus | Human | Endothelial cells and smooth muscle of the main veins |
| Cerebellum | Rat | Vessels associated with interneurons |
| Vessels throughout the brain | Mouse | Endothelial cells and pericytes |
| **Neurons** | | |
| Hippocampus | Human | Primarily cytoplasmic, with a diffuse and granular pattern |
| Substantia nigra pars compacta | Human | Co-localised with neuromelanin |
| Unspecified region | Human | ANXA1 and ANXA4 (but not ANXA2) |
| Hippocampal dentate gyrus | Rat | Cytoplasmic |
| Cerebellum | Rat | Purkinje cells |
| Substantia nigra pars compacta | Mouse | Distribution resembles that of dopaminergic neurons |

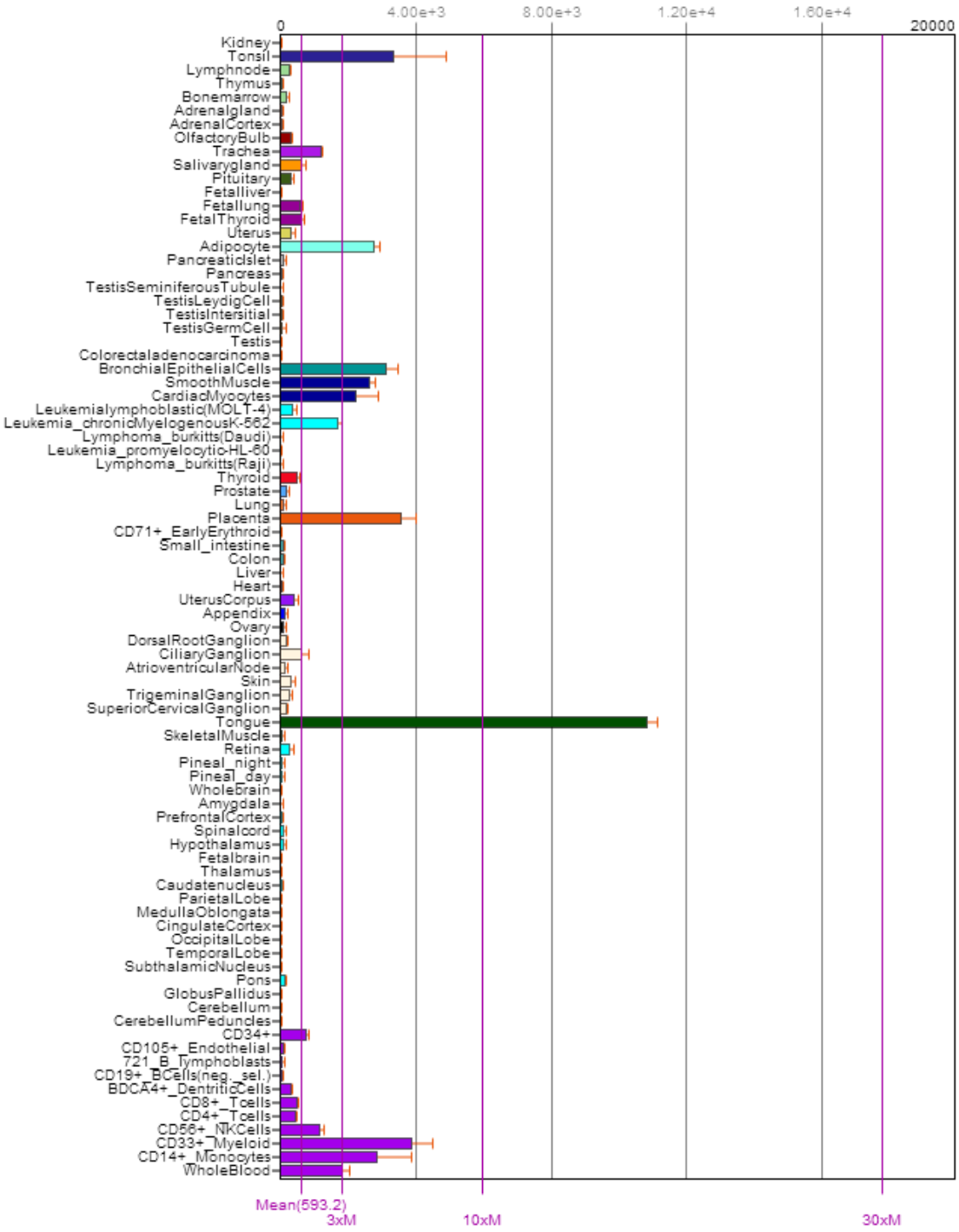


Fig. 14: Anx A1 mRNA tissue distribution after BioGPS/ GeneAtlas U133A.
(Source, accessed April 5, 2014 - http://biogps.org/#goto=genereport&id=301).

## 4.6 Pitfalls in Anx A1 research

Browning et al. in 1989 reported that Anx A1 is present at very high levels in cultured cell lines (*in vitro*) as opposed to an *in vivo* state.

It was Croxtall and Flower (1992), who found that serum in the cell culture media stimulates Anx A1 synthesis which led to the necessity of cultivating the cells serum-free before performing experiments involving measurements of Anx A1 (Philipps et al., 1989).

Since a large amount of Anx A1 is bound in a $Ca^{2+}$ dependent manner on the cell membrane, it can be rinsed only with Ca-free and/ or EDTA solutions prior to further analysis. Skipping collecting the membranous Anx A1 would lead to losing an essential part of the Anx A1 protein and hence to an underestimation of the Anx A1 available in and on the cell.

## 4.7 Anx A1 receptors

Anx A1 acts upon formyl peptide type receptor (FPR). Schiffmann et al. in 1975 provided indications for the existence of a receptor as a high affinity binding site on the surface of neutrophils for N-formylmethionine peptide (fMLF). However, Boulay et al. (1990) introduced it as a novel receptor activated through N-formyl peptides.

In the human, there are three formyl peptide receptors – FPR, FPRL1, and FPRL2, all lying on chromosome 19 (q13.4) (Bao et al., 1992). In the mouse, there are seven formyl peptide receptors coded on chromosome 17 (A3.2) (Gao et al., 1998). The Fpr1 is the murine counterpart for the human FPR; Fpr-rs1[8] and Fpr-rs2 for FPRL1, the latter having lower binding affinity for fMLF; Fpr-rs3,4,5,6, and 7 have no counterparts in the human organism, and no murine orthologue exists for the human FPRL2 (Migeotte et al., 2006; John et al., 2008).

The FPRs are a family of seven transmembrane domain pertussis toxin-insensitive Gi protein-coupled receptors, activating phospholipase C (PLC) and ultimately releasing $Ca^{2+}$ from intracellular stores (Wenzel-Seifert et al., 1999).

[8] Fpr-rs1 – formyl peptide receptor related sequence 1

## Distribution

Fprs are expressed mainly in mammalian phagocytic leukocytes, but distributed in other tissues and cell types as well.

Table 2: Fpr in the human and mouse organism; agonists and tissue distribution. (Modified from John et al., 2008.)

**The human and murine formyl peptide receptor families: selective agonists and tissue distribution**

| Receptor | Agonists | Expression |
|---|---|---|
| Human | | |
| FPR | fMLP and other formyl peptides, WKYMVm peptide, WKYMVM, other hexapeptides, T20(DP178), T21(DP107), gG-2p20, HIV gp41, ANXA1, $ANXA1_{Ac2-12}$, $ANXA1_{Ac2-26}$, $ANXA1_{Ac9-25}$, Cathepsin G | Neutrophils, monocytes/macrophages, dendritic cells, U937 cells, some epithelial cells (especially those with secretory function), some endocrine cells (thyroid follicular cells and adrenal cortical cells), Kupffer cells, smooth muscle cells, endothelial cells, fibroblasts |
| FPRL1/ALX-R | fMLP and other formyl peptides, $LXA_4$ and 15-epi-$LXA_4$, serum amyloid A, MMK1, Quin-C1, NADPH dehydrogenase, Subunit I-derived peptide, T21 (DP107), WKYMVm peptide, WKYMVM, other hexapeptides, temporin, sCKβ8-1, SHAAG, D2D388-274, Upar84–95, amyloid β, PrP106–126, MMK-1, humanin, formylated humanin, PACAP27, LL-37, Hp2–20, N36, F peptide, V3 peptide, ANXA1, $ANXA1_{Ac2-12}$, $ANXA1_{Ac2-26}$ | Neutrophils, monocytes/macrophages, epithelial cells, dendritic cells, B lymphocytes, T cells, microglial cells, astrocytes, fibroblasts, hepatocytes |
| FPRL2 | fMLP and other formyl peptides, ANXA1, $ANXA1_{Ac2-26}$, Hp2–20, WKYMVm peptide, WKYMVM, humanin, F2L | Monocytes/macrophages, dendritic cells, HL-60 cells |
| Mouse | | |
| Fpr1 | fMLP and other formyl peptides, ANXA1, $ANXA1_{Ac2-26}$, Spinorphin, WKYMVm | Neutrophils, mononuclear cells, microglial cells, dendritic cells, hippocampus; hypothalamus, anterior pituitary, adrenal and spleen |
| Fpr-rs1/Fprl1 | fMLP and other formyl peptides, ANXA1, $ANXA1_{Ac2-26}$, HIV-derived peptides, humanin | Neutrophils, microglia, spleen, lung, liver, hippocampus hypothalamus, anterior pituitary, and adrenal |
| Fpr-rs2/Fprl2 | fMLP and other formyl peptides, T20 (DP178), humanin, V3 peptide, MMK1, WKYMVm, CRAMP, F2L, serum amyloid A, amyloid $\beta_{1-42}$ | Neutrophils, microglia, spleen, lung, hippocampus hypothalamus, anterior pituitary, and adrenal |
| Fpr-rs3/Fprl3 | Unknown | Skeletal muscle |
| Fpr-rs4/Fprl4 | Unknown | Unknown |
| Fpr-rs5/Fprl5 | Unknown | May not encode a functional receptor |
| Fpr-rs6/Fprl6 | Unknown | Testis, spleen, skeletal muscle, hypothalamus, and anterior pituitary |
| Fpr-rs7/Fprl7 | Unknown | Heart, liver, spleen, smooth muscle, lung, pancreas, hypothalamus, and pituitary |

## Anx A1 binding sites on pituitary cells

Christian et al. used in 1997 human recombinant Anx A1 to mark the specific binding sites on dispersed pituitary cells and sorted the cells using fluorescence-activated cell sorting technique (FACS). They found that 17% of the cells were L type and bound the hu-r-Anx A1, and 3% of the cells were C type and bound hu-r-Anx A1. John et al. suggest in 2008 that the mechanism involved in inhibiting hormone release from the endocrine cells requires interaction with SNARE[9] proteins, which are critical to exocytosis.

[9] SNARE - soluble NSF attachment protein receptor, plays an essential role in vesicle fusion and thus exocytosis

Table 3: Tissue distribution of Fpr receptors in man and mouse. Abbreviations: Astro, astrocytes; CHO, chinese hamster ovary; DC, dendritic cells; EC, endothelial cell; Ep, epithelia; Hepato, hepatocytes; iDC, immature dendritic cells; LC, lung alveolar carcinoma cells;Mo, monocytes; NB, neuroblastoma; NS, nervous system; PMN, polymorphonuclear neutrophil; SF, synovial fibroblast; T, T cells. (Modified from Le et al., 2002.)

| Receptor | Cell and/or tissue expression[a] | Major responses |
|---|---|---|
| FPR | Mo, PMN, DC | $Ca^{2+}$ mobilization, migration, mediator release and desensitization of other chemoattractant receptors |
| | Hepato, LC | release of acute phase proteins |
| | Astro | $Ca^{2+}$ flux, migration, cytokine production |
| | EC, thyroid, Adrenal, NB, NS | unknown |
| FPRL1 (Synonyms: FPR2, FPRH1 hLXA4R) | Mo, PMN, iDC | $Ca^{2+}$ flux, migration, mediator release and desensitization of other chemoattractant receptors |
| | microglia | $Ca^{2+}$ flux, migration, cytokine production |
| | astro | cytokine production |
| | T | Chemotaxis |
| | Ep | Inhibition of cytokine production by LXA4 |
| | NB, SF, spleen, lung, testis | unknown |
| | | Distinct signaling pathways in monocytes versus neutrophils by interacting with the lipid agonist LXA4. The precise mechanism remains to be determined. |
| FPRL2 | Mo, DC | $Ca^{2+}$ mobilization, chemotaxis, oxidase Activation |
| mFPR1 | PMN | $Ca^{2+}$ mobilization, migration, mediator Release |
| | microglia, spleen, lung, liver | unknown |
| Fpr-rs1 | PMN, spleen, lung, heart, liver | Mostly unknown. In transfected CHO cells, LXA4 activates GPTases. |
| mLXA4R | | |
| mFPR2 | PMN, microglia | $Ca^{2+}$ mobilization, chemotaxis, |
| | spleen, lung | unknown |

## 4.8 Anx A1 and the fs cells

Anx A1 is present in fs cells (Christian et al., 1996). Taylor et al. have implicated that Anx A1 contributes to the inhibitory action of GC on hormonal release of ACTH, PRL, and TSH (Taylor et al., 1995a; 1995b; 1995c; 1997). Traverso et al. published in 1999 findings about Anx A1 localization in the TtT/GF cell line.

## 4.9 Anx A1 and ACTH

GC inhibit the ACTH release in a 1) rapid; 2) early delayed, and 3) late delayed mechanism (Keller-Wood and Dallman, 1984; Buckingham et al., 2006). The rapid answer to GC provocation raises in minutes and lasts less than 15min; the delayed phases involve occupation of intracellular steroid receptors and subsequent modulation of protein synthesis; early delayed (1-2h) influence the protein synthesis; late delayed response (12-24h) involves gene suppression of two ACTH stimulators (CRH and AVP) in the hypothalamus and POMC in the anterior pituitary lobe ( Arimura et al., 1969; Portanova and Sayers, 1974; Keller-Wood and Dallman, 1984; Jones and Gillham,

1988; Dayanithi and Antoni, 1989; Schlatter and Dokas, 1989; Buckingham et al., 2006).

## 4.10 Anx A1 and PRL

GC application *in vivo* leads to decrease in serum PRL (Euker et al., 1975; Fang and Shian, 1981). Adrenalectomized animals have increased PRL which is inversed by treatment with Dex (Watanobe, 1990). Taylor et al. (1995; 2000) showed that Anx A1 Ab or antisense oligonucleotides act inhibitory on PRL release from pituitary slices.

*In vitro* studies on GH3 cells showed that Dex suppresses PRL release and this action could be reversed by anti-Anx A1 polyclonal serum (Dannies and Tasjian, 1976; Perrone et al., 1980; Taylor et al., 1995; 2000). Human recombinant Anx A1 mimics and anti-Anx A1 mAb reverses the Dex effect (Taylor et al., 1995; 2000). It has been further shown, that Anx A1 blocks the GC independent PRL release from the decidual cells of the placenta ( Wilber and Utiger, 1969; Handwerger et al., 1991; Pihoker et al., 1991).

## 4.11 Anx A1 and the ECS

Anx A1 influences negatively the synthesis of EC from AA. The influence is indirect, since Anx A1 inibits the enzyme (PLA2) in charge for supplying the substrate (AA).

## 4.12 Pathological conditions involving Anx A1

**Cancer**

Anx A1 was discovered as one of the main cellular substrate for phosphorylation on tyrosine by the EGF receptor (Gerke and Moss, 2002). Mutations in this receptor underly various cancer diseases. Moreover, Anx A1 is involved in the regulation of the mitogen-activated protein (MAP) kinase pathway essential for events like proliferation, gene expression, differentiation, mitosis, cell survival, and apoptosis (Alldridge et al., 1999). These facts could explain the dysregulation of Anx A1 in breast, epithelial, prostate cancer and leukemia.

In breast cancer, Anx A1 is believed to function as a tumor suppressor (Cao et al., 2008; Ang et al., 2009; Nair et al., 2010; Wang et al., 2010).

Analysis of surgical tissue from patients with laryngeal squamous cell carcinoma, showed *in vivo* down-regulation of Anx A1 expression in the tumor and increased in mast cells and laryngeal squamous carcinoma cell line treated with Anx A1 peptide. Combined *in vivo* and *in vitro* analysis demonstrated that Anx A1 plays a regulatory role in laryngeal cancer cell growth (Silistino-Souza et al., 2007; Alves et al., 2008). The Anx A1 expression was dysregulated in lung squamous cell carcinoma (Nan et al., 2009; Wang et al., 2014). In invasive squamous cell carcinoma, Anx A1 may be an effective candidate for detecting cervical intraephitelial neoplasia lesions and for evaluating tumour cell differentiation in squamous cell carcinoma of the cervix (Wang et al., 2008; Guerrera et al., 2014). Anx A1 could be used as a negative biomarker for gastric cancer development and progression as its expression is reversely correlated (Yu et al., 2008). Anx A1 is up-regulated in high grade urinary bladder urothelial carcinoma as compared to non-high grade carcinomas (Li et al., 2010).

The Anx A1 reduced expression is an important parameter in prostate cancer as well (Inokuchi et al., 2009; D'Acunto et al., 2010).

Anx A1 may also play a tumor suppressor role in peripheral blood cells (Faria et al., 2010; Zhu et al., 2013). Anx A1 regulation is controversial in leukemia events – on one hand Anx A1 has been identified as upregulated in hairy cell leukemia (Falini et al., 2004), on the other, Anx A1 was downregulated and possibly contributes to the drug resistance in chromic myeloid leukemia (CML) cell line ( Zhu et al., 2009; Faria et al., 2010).

**Inflammatory and autoimmune diseases**

Anx A1 has anti-inflammatory properties shown *in vitro* and *in vivo*. It inhibits prostaglandin production, iNOS and influences the NF-κB complex formation (Cirino et al., 1987; Goulding et al., 1990; Perretti and Flower, 1993; Minghetti et al., 1999; Zhang et al., 2010).

Anx A1 is present in peripheral blood phagocyte and is strongly decreased in patients with rheumatoid artritis, it is influenced by GC compared to healthy control subjects (Goulding et al., 1992). The last parameter is close to its normal range (as in healthy subjects) after a therapy with disease modifying anti-rheumatic drugs. (Goulding and Guyre, 1992) and Perretti and Ahluwalia (2000) proposed that Anx A1 acts as a barrier

to inappropriate inflammatory and autoimmune stressors. Anx A1 modulates the adaptive immune system and plays a certain role in T-cell activation (D'Acquisto et al., 2007). It is highly expressed in T cells from rheumatoid arthritis patients (D'Acquisto et al., 2008; Perretti and Dalli, 2009). Treatment of rheumatoid arthritis patients with steroids decreased Anx A1 expression in T cells. Stevens et al. (1993) detected high levels of Anx A1 Ab in patients with inflammatory bowel disease (IBD). GC are widely used as a treatment for this condition but with uncertain success, since many patients do not respond well to the therapy. Beattie et al. (1995) proposed that it could be Anx A1 that is involved in the detrimental effect GC have on some patients. Sena et al. (2013) investigated the immunomodulatory interaction Anx A1 has during therapy of IBD with the chimeric anti-TNFα mAb infliximab. Downregulation and degradation of Anx A1 was found in the bronchoalveolar lavage fluid of patients with cystic fibrosis. Anx A1 may be a key protein involved in cystic fibrosis pathogenesis especially in relation to inflammation (Tsao et al., 1998). Decreased expression of Anx A1 contributes to the worsening of the cystic fibrosis phenotype (Bensalem et al., 2005). There are indications linking Anx A1 to Parkinson's disease as well. Anx A1 immunoreactivity has been found in ameboid microglia within the astrocytic envelope of neurons adjacent to or within glial scars in the parkinsonian substantia nigra (Knott et al., 2000). Anx A1 expression has been identified in the lesions of multiple sclerosis plaque and correlated with the degree of the disease (Probst-Cousin et al., 2002). Studies on mice let Paschalidis et al. (2009) suggest Anx A1 as a novel therapeutic approach for multiple sclerosis.

Currently, there is information on one clinical trial from 2006 involving Anx A1 and its potential as oral cancer marker. However, even that the study is accomplished, there is no information published on its outcome[10].

[10] ClinicalTrials.gov Identifier: Study the Expression of Annexin A1 and Its Potential Usage as a Prognostic Marker in Oral Cancer, NCT00364715

# 5 Nitric oxide (NO)

NO is a small, gaseous, paramagnetic radical, that freely diffuses through cell membranes and interacts preferably with ferrous hemoproteins such as soluble guanulate cyclase (Gc) and hemoglobin. The biological functions of NO include actions as a vasodilator, neurotransmitter, cytotoxic agent, inhibitor of platelet aggregation, and activator of smooth muscle proliferation (Dawson and Dawson, 1995).

## 5.1 Nitric oxide synthases (NOS)

Nitric oxide synthases (NOS) catalyze the conversion of L-arginine to NO and citrulline, and thus represent the main supplier of NO for the organism (Moncada and Higgs, 1993). The reaction is a two-step oxygenation (Fig. 15) with N-hydroxyarginine as an intermediate. The electrons necessary for these processes are supplied by a cofactor, the reduced form of nicotinamide adenine dinucleotide phosphate (NADPH; Fig. 16; Dawson and Dawson, 1995).

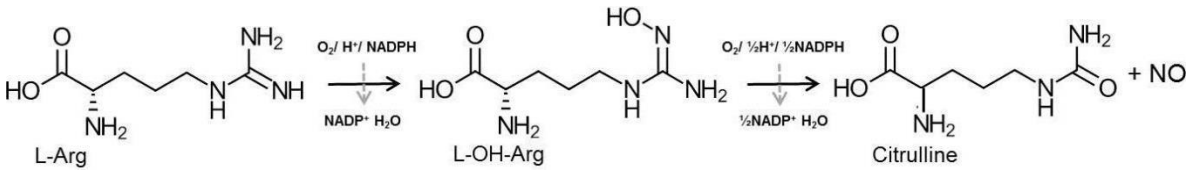


Fig. 15: Conversion of L-arginine to NO and citrulline with N-hydroxyarginine as an intermediate.

NOS is a voluminous enzyme and divided into two parts. One half, the oxygenase domain, receives electrons to permit the conversion of arginine and oxygen into citrulline and NO. This domain contains further cofactors: tetrahydrobiopterin (BH) and haem. They are bound strongly within the protein structure of the enzyme. Substrate oxygen binds to the iron of the haem cofactor before it oxygenates arginine to N-hydroxyarginine and then to citrulline, but the exact role of BH4 is yet not fully clarified. In the other half of the enzyme, the reductase domain, there are yet more cofactors: flavin mononucleotide (FMN) and flavin adenine dinucleotide (FAD). FMN and FAD receive electrons from the conversion of NADPH into NADP' and H' and pass them to the haem cofactor of the oxygenase domain, turning the oxygen bound to its iron centre into a highly reactive form that reacts with the arginine substrate. Calmodulin/$Ca^{2+}$ appears to facilitate the passage of electrons from FAD to FMN (Fig. 16; Butler and Nicholson, 2003).

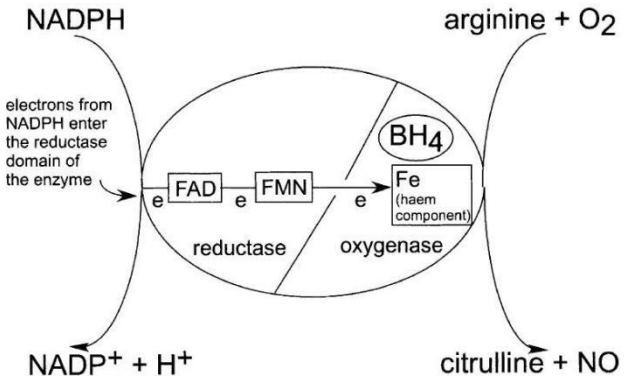


Fig. 16: Scheme representing the domains of the NOS enzyme and necessary cofactors. (From Dawson and Dawson, 1995.)

## NOS isoforms

There are three NOS isoforms with ca. 50% homology in humans. Named after the sequence in which they were discovered and after the tissues they were identified in and where they predominately occur. nNOS (also known as type I, NOS-I, NOS-1) being the first isoform found (and predominating) in neuronal tissue, iNOS (also known as type II, NOS-II, NOS-2) being the isoform which is inducible in a wide range of cells and tissues, and eNOS (also known as type III, NOS-III, NOS-3) being the last identified isoform, found in vascular endothelial cells.

## NOS inhibitors

There is a great variety of NOS inhibitors available for pharmacological studies. L-arginine analogues, such as $N^G$-nitro-L-arginine methyl ester (L-NAME; Fig. 17) are the most potent ones and inhibit all NOS isoforms (Palacios et al., 1989; Rees et al., 1990). The inhibitory constant (Ki) of L-NAME for nNOS, eNOS, and iNOS, is 15nM, 40nM, and 4.5nM, respectively. As for selective NOS inhibitors, curcumin inhibits the gene expression of iNOS, (Fig. 18; Brouet and Ohshima, 1995).

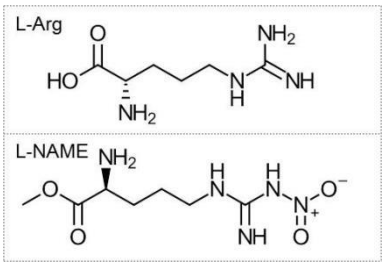


Fig. 17: Structural formulae of L-Arginine as leading structure and its analogue and NOS inhibitor L-NAME.

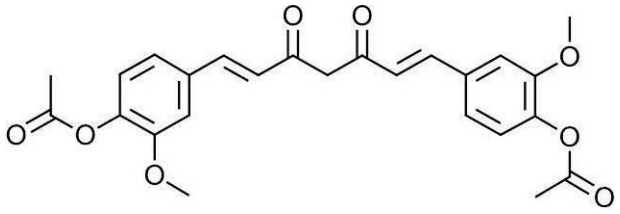

Fig. 18: Structural formula of curcumin (keto form).

**NOS activators**

LPS originate from the outer membrane of gram-negatve bacteria and elicit exorbitant activation of the immune system. These lipopolyglycan chains activate iNOS to produce NO (Mori et al., 1998; Boucher et al., 1999). Ionomycin (Fig. 19) as a Ca ionophore causes Ca release from the intracellular storages (Liu and Hermann, 1978) and subsequent activation of all NOS isoforms.

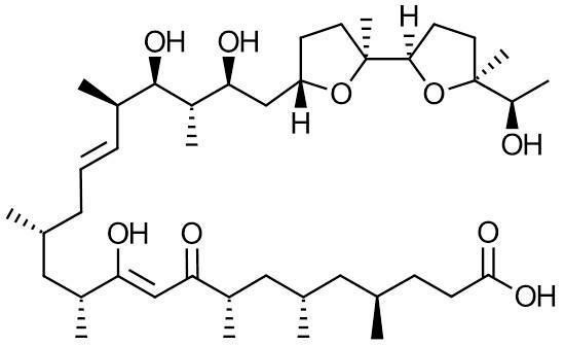

Fig. 19: Structural formula of ionomycin.

## 5.2 Detection of NO

The detection of NO is insidious because of its low concentration in tissues and cells and its short half-time of about 3 sec. NO can be either detected directly, or its amount can be deduced from the side products, the converted substrate or affected amount of catalyzing enzyme (Archer, 1993; Schmidt, 1994).

In solution, NO reacts with molecular oxygen to form nitrite ($NO^-_2$), and with oxyhemoglobin and superoxide anion ($O_2^-$) to form nitrate ($NO^-_3$). NO also reacts with thiols to form S-nitroso compounds, amines to form nitrosamines, and metals to form metalnitrosyl complexes. In gas phase, NO reacts with high concentrations of oxygen to form nitrogen dioxide ($NO_2$).

Its direct detection can be performed with ozone-chemiluminescence (Zafiriou and McFarland, 1980); NO microelectrodes (Shibuki, 1990); electron paramagnetic resonance (EPR) (Wennmalm et al., 1990); gas chromatography; mass spectroscopy, and flow cytometric analysis with fluorescent probes. Indirectly, NO can be detected via its oxidated form nitrite/ nitrate with diazotization (Griess reaction); via radioactively labeled L-arginine substrate conversion; via cyclic guanosine monophosphate (cGMP) that results after NO affects the cell, and via the reductive activity of NOS (NADPH diaphorase formazan assay).

The methods used in this work include gas-phase ozone-chemiluminescence, diazotization (Griess reaction), and fluorescent labeling with DAF-2DA (see Methods and Materials).

## 5.3 Molecular mechanisms involving NO

NO diffuses freely into the target cell through the cell membrane and activates the cytosolic guanylylcyclase (Gc), that converts guanosine triphosphate (GTP) into cGMP. cGMP activates the protein kinase G (PKG) that causes a decline in the intracellular Ca concentration, which leads to muscle relaxation and inhibition of exocytosis (Fig. 20).

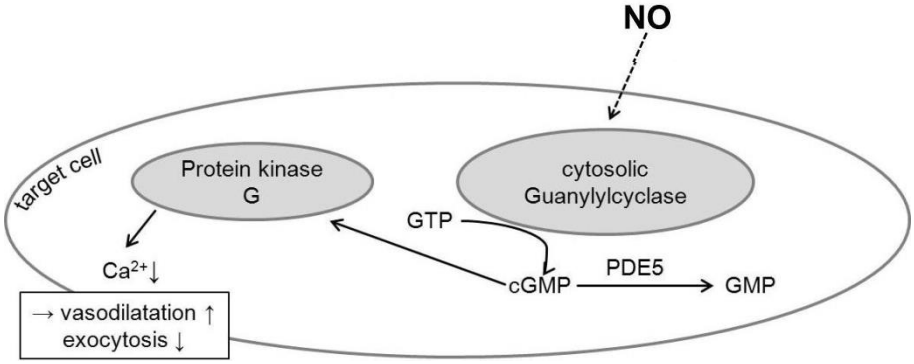


Fig. 20: Molecular mechanism of NO in a target cell. It activates the cytosolic guanylylcyclase (Gc) thus increasing the cyclic guanosine monophosphate (cGMP) which then activates the protein kinase G (PKG). That causes a decline in the intracellular Ca concentration and muscle relaxation and inhibition of exocytosis.

# 6 The endocannabinoid system (ECS)

## 6.1 Brief history

The plant Cannabis sativa (C. sativa), also known as marihuana, is considered as one of the very first plants grown for therapeutic and recreative purposes (Peters and Nahas, 1999). First historical reports of the use of C. sativa were found in China nearly 5000

years ago, where it was grown rather for fibers than for production of psychoactive extracts. From China, C. sativa propagated to all continents over the ages and became more and more important for medical applications besides its usage as pleasure-inducing drug.

C. sativa contains more than 60 compounds belonging to the chemical family of cannabinoids (Iversen, 2000), although the major psychoactive constituent is $\Delta^9$-tetrahydrocannabinol ($\Delta^9$-THC) (Gaoni and Mechoulam, 1964). Other compounds found in C. sativa include cannabidiol and cannabinol. Following the isolation of $\Delta^9$-THC from C. sativa, numerous synthetic cannabinoids, based on the structure of $\Delta^9$-THC, were synthesized. These were shown to induce behavioral effects such as hunger, hypothermia, catalepsy and hypomobility, similar to the *in vivo* effects of $\Delta^9$-THC, when injected into animals (Howlett et al., 2002).

Upon the identification and cloning of a specific cannabinoid receptor in the brain ($CB_1$) that mediated the effects of $\Delta^9$-THC (Devane et al., 1988; Matsuda et al., 1990), an endogenous agonist of this receptor, anandamide (AEA; Devane et al., 1992), was identified. In 1995, a second type of EC, 2-arachidonoyl glycerol (2-AG), was discovered, also a derivative of AA (Mechoulam et al., 1995; Sugiura et al., 1995). Also other derivatives of AA, e.g. docosatetraenoylethanolamide (DEA), di-homo-γ-lineoylethanolamide (DLEA), and oleoylethanolamine (OEA) have been reported to bind to $CB_1$ (Hanus et al., 1993) and 2-arachidonoyl glyceryl ether (noladin ether) was reported to act as an EC as well (Hanus et al., 2001). This suggested the presence of an ECS in the CNS.

## 6.2 The system organization

AEA and 2-AG are not stored in synaptic vesicles, but are synthesized "on-demand" from their membranal precursors *N*-arachidonoylphosphatidylethanolamine and diacylglycerol through *N*-arachidonoylphosphatidylethanolamine-specific phospholipase D (NAPE-PLD) and sn-1-selective diacylglycerol lipase (DAGL) (Di Marzo et al., 1994; Mechoulam et al., 1998; Piomelli, 2003; Di Marzo et al., 2004).

AEA is inactivated by reuptake via a membrane-bound transport protein and subsequent intracellular enzymatic degradation by fatty acid amide hydrolase (FAAH)-mediated

hydrolysis (Cravatt et al., 1996; Day et al., 2001; Deutsch et al., 2001; Giuffrida et al., 2001).

FAAH and the AEA transporter are distributed in brain areas in a pattern corresponding to that of $CB_1$, i.e. high concentration in hippocampus, cerebellum, and cerebral cortex (Egertova et al., 1998; Tsou et al., 1998b; Ueda and Yamamoto, 2000).

2-AG undergoes similar FAAH-mediated hydrolysis (Ueda and Yamamoto, 2000) and carrier-mediated transmembrane transport (Beltramo and Piomelli, 2000), possibly through the same AEA transporter (Bisogno et al., 2001). In addition, 2-AG can be hydrolyzed by monoacylglyerol lipase (MAGL) as well.

## 6.3 Cannabinoids

**Cannabinoid receptor agonists**

Cannabinoid receptor agonists can be classified into four groups based on their chemical structure: eicosanoid cannabinoids, classical cannabinoids, nonclassical cannabinoids, and aminoalkylindoles (Fig. 21).

Eicosanoids are derivatives of AA and were discovered as endogenous ligands of the cannabinoid receptors (Devane et al., 1992). Representatives of this group are anandamide (arachidonoylethanolamide, AEA) and 2-arachidonoylglycerol (2-AG), the two major ECs so far isolated from mammalian tissue.

Classical cannabinoids include compounds isolated from cannabis, mainly $\Delta^9$-THC, cannabidiol, and cannabinol.

CP-55.940 is an example for the nonclassical cannabinoids and has been used to demonstrate the existence of the cannabinoid receptors (Howlett et al., 1986).

Aminoalkylindoles are structurally different from classical and nonclassical cannabinoids and the EC themselves. The representative of this group is WIN 55.212-2 (WIN) (Ki 2 nM). As soon as cannabinoid receptors were discovered, several newly synthesized compounds were tested as putative specific antagonists of $CB_1$ or $CB_2$.

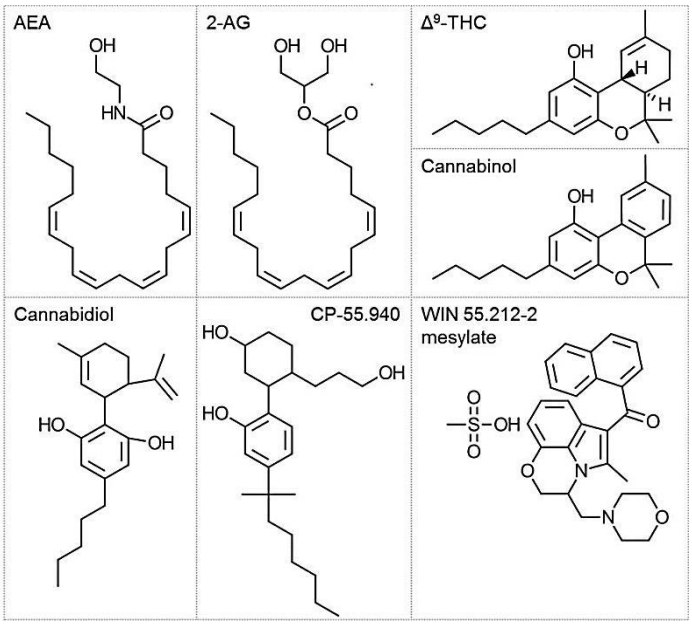


Fig. 21: Structural formulae of $CB_1$ agonists.

## Cannabinoid receptor antagonist

Otenabant (CP-945,598) (Fig. 22) developed at Pfizer, is a selective, highly competitive $CB_1$ receptor antagonist that inhibits both basal and cannabinoid agonist-mediated $CB_1$ receptor signaling. Its Ki is 2.8 nM for the rodent (rat) model, which is lower than that of 2-AG (472 nM) and AEA (89 nM), resulting in higher binding affinity of the synthetic antagonist to $CB_1$. The compound has low affinity (Ki 7600 nM) for $CB_2$ receptors. Otenabant reverses *in vivo* cannabinoid agonist-mediated CNS-driven responses such as hypo-locomotion, hypothermia, analgesia, and catalepsy. It furthermore exhibits dose and concentration-dependent anorectic activity in rodent models and was withdrawn from phase 3 clinical trial with obesity indication (Ward and Raffa, 2011).

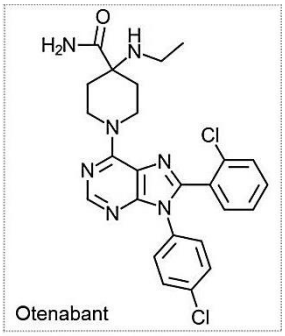


Fig. 22: Structural formula of otenabant ($CB_1$ antagonist).

## 6.4 The cannabinoid receptor

$CB_1$ was first identified in the brain (Devane et al., 1988; Matsuda et al., 1990). A second cannabinoid receptor ($CB_2$) was cloned from a leukaemic cell line and has a relatively low sequence identity with $CB_1$ (44% overall the whole protein, 68% in the transmembrane regions; Munro et al., 1993). Its expression is limited to cells and organs of the immune system suggesting that the ECS may also play a role in modulating the immune system. Both $CB_1$ and $CB_2$ are seven transmembrane G protein-coupled receptors, mostly coupled to Gi/o pertussis toxin-sensitive proteins. $CB_1$-mediated signaling pathways have been extensively characterized. *In vitro* studies, using different neuronal and non-neuronal culture systems have revealed that $CB_1$ exerts its functions presumably through two main intracellular pathways: inhibition of adenylate cyclase (AC) which generates the second messenger cyclic adenosin monophosphate (cAMP) and alterations of ion channel activities. However, also other intracellular pathways could be triggered by $CB_1$. The cannabinoid receptor distribution was first shown by autoradiography of ligand-receptor binding on rat brain sections with different radiolabeled agonists (Herkenham et al., 1990; Herkenham, 1991; Jansen et al., 1992; Glass et al., 1997b). As the quantity of receptors in the brain is very high, $CB_1$ can be considered as one of the most abundant G protein-coupled receptors in the mammalian brain (Herkenham et al., 1990), comparable in quantity and density with glutamate receptors. The highest density of cannabinoid receptors has been demonstrated in the basal ganglia (substantia nigra, globus pallidus, entopeduncular nucleus and dorsolateral caudate putamen) and in the cerebellum. $CB_1$ is also present in the periaqueductal gray (PAG). $CB_1$ was furthermore detected in the VMH, thalamic nuclei and pituitary gland (Matsuda et al., 1993; Tsou et al., 1998a; Bayatti et al., 2005; Yasuo et al., 2010a). With a closer look at the hypophysis, $CB_1$ is present in PD and absent from PT, as found in our institute (Yasuo et al., 2010a; 2010b). Only a restricted number of L cells were $CB_1$-positive, whereas C and fs cells readily expressed the $CB_1$ receptor (Yasuo and Korf, 2011).

## 6.5 Interaction of ECS with hormonal secretion

There is an enhancement of CRH expression in the hypothalamus and anterior pituitary lobe after chronic exposure to cannabinoids (Corchero et al., 1999a; 1999b). Exogenous (Δ9-THC and WIN) and endogenous ligands (AEA) increases the release of ACTH in

the pituitary gland via the secretion of CRH through $CB_1$ (Weidenfeld et al., 1994; Pagotto et al., 2001).

Moreover, EC (AEA, 2-AG) inhibit PRL secretion in rodents (rats: Scorticati et al., 2003; mice: Murphy et al., 1998; Oláh et al., 2008). Concerning cell cultures, Ho et al. (2000) showed that PRL release from GH4C1 is inhibited in a $CB_1$- mediated manner, while Kolesnick et al. (1984) had shown that AA stimulates PRL release from GH3 cells.

Since those findings are based on the involvement of the $CB_1$ receptor, that is mostly Gi coupled, one would suggest that $CB_1$ agonists would inhibit the exocytotic procession of hormones, while a $CB_1$ antagonist would not influence hormonal secretion. The molecular mechanism (Fig. 23) involves an indirect inhibitory action (via adenylyl cyclase, AC) and a direct way (via Ca-channels). The indirect path involves inhibition of AC, so that less cAMP is produced which arrests the protein kinase A (PKA). PKA cannot then be recruited into the cell nucleus where CREB dependent hormonal gene expression can take place. $CB_1$ receptor influences negatively the exocytosis in a direct way by inhibiting the Ca channels, so that the low intracellular $Ca^{2+}$ concentration is not sufficient for the exocytosis of hormone vesicles.

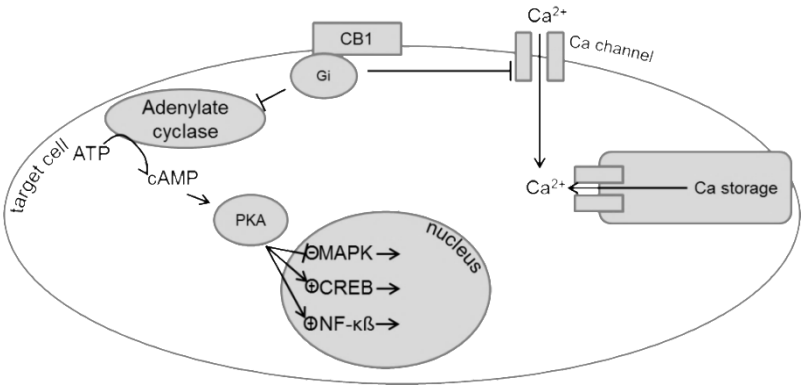


Fig. 23: Molecular mechanism involving $CB_1$ receptor inhibition of hormonal exocytosis. The adenylate cyclase (AC) is inhibited by the Gi subunit of the $CB_1$ receptor after a $CB_1$ agonist binds. In this way, less cyclic adenosine monophosphate (cAMP) is formed and the protein kinase A (PKA) cannot be activated to initiate hormonal gene expression. $CB_1$ receptor blocks the Ca channels and intracellular $Ca^{2+}$ concentration does not allow exocytosis of hormone vesicles.

# Methods and Materials

All materials, recipes, and facilities used are listed in section Materials. All experiments were performed at least in triplicates, if not specifically stated otherwise.

## 1 Methods

### 1.1 Cell lines, maintenance

The fs TtT/GF cell line derived by Kinji Inoue, were a gift from Prof. Dr. U. Renner (Max-Planck-Institute for Psychiatry, Dept. Endocrinology, Munich, Germany). The fs Tpit/F1 cell line, derived by Kinji Inoue as well, was purchased from Riken bioresource center cell bank, Japan. The C cells AtT20/D16v-F2 developed by Gumbiner and Kelly in 1982 from the AtT20, an ACTH secreting cell line established from a murine pituitary tumor, were a gift from Prof. Dr. G. Auburger (Klinikum der Universität Frankfurt, Molekulare Neurogenetik, Neuroscience Center). The L cells GH4C1 developed by Tashjian from pituitary PRL and GH positive pituitary cells of female Whistar-Furth rats, were purchased from Leibnitz Institute, Deutsche Sammlung von Mikroorganismen und Zellkulturen GmbH, Braunschweig, Germany.

The cell cultures were kept and treated as stated in established protocols of suppliers of the cells and chemical reagents for the cells. The aseptic conditions while working with the cells were assured by using sterile material, decontaminating the incubators at short intervals, treating the working area with 70% ethanol and monitoring. The latter contains visual examinations of the cell cultures and all the solutions for particles, performing tests for mycoplasma infection with MycoProbe ® mycoplasma detection kit and MycoAlert ™ mycoplasma detection kit, and applying contact agar tests with Roti ® DipSlides (all listed in Table 4) for bacterial and fungal infections.

The cell colonies were cultured to a maximum of 45 passages and the experiments were performed at the phase between passage 3 and 35. The cells were grown to a sub-confluent level, then further either diluted or stepwise frozen in a high serum percentage medium. The controlled decrease of temperature (-1 °C/minute) was assured by the usage of Mr. Frosty ® freezing container, in which the cells were kept at -80 °C overnight. The following day the cell vials were transferred to the vapor phase of a liquid nitrogen storage vessel. The thawing procedure includes bringing the cell vials to

37 °C in a water bath and changing the cryoprotective medium with serum-rich new medium.

TtT/GF and Tpit/F1 are strictly adherent, AtT20/D16v semi-adherent and GH4C1 were grown in a suspension, which further defined the different types of culture flasks and deviations in the cell protocol. TtT/GF, AtT20/D16v, and GH4C1 cells were kept at 37 °C/ 5%CO2; Tpit/F1 cells at 33 °C/ 5%CO2.

The vitality of the cells was proven at certain intervals in the following way – 10 µl 0.4% trypan blue solution was added to 40 µl cell suspension. The cell number was determined using the Neubauer improved cell counting chamber. Cells stored at -80 °C are vital up to 2 years, when kept in liquid nitrogen indefinitely.

For the purpose of imaging techniques, floating cells (GH4C1 and partly AtT20/D16v) were immobilized by using poly-L-lysine coated glass coverslips. The coverslips were later gathered with the adhered cells and according to the protocol either directly frozen or fixed with 4% PFA solution and kept at 4 °C.

## 1.2 Mice

Wild type C3H mice from Charles River GmbH, Sulzfeld, Germany were used. The mice were kept and processed according to the Directive 2010/63/EU. The animals were housed in cages with controlled light, humidity, and temperature. Food (Altromin Spezialfutter GmbH& Co. KG, Lage, Germany) and water were available *ad libitum*.

Animals were adapted to a photoperiod of 12 hours light (L; 250 lux), 12 hours dark (D) with lights on at zeitgeber time (ZT) 0 for two weeks. One day before the experiments, animals were transferred to constant darkness. Circadian time (CT) 0 was defined as lights on at the previous light-dark schedule.

**Cryopreservation**

Tissue was preserved according to the protocol of the experiment to be later performed. ISH, IB, (q) PCR and some IHC analysis were performed on tissue not treated with a fixative prior to freezing in ice-cold isopentane. For all other experiments, the tissue was kept in succrose solutions or 4% PFA before storage at -25 or -80 °C.

## 1.3 Cell stimulations

Stimulations of the fs cells with 2-AG, AEA, WIN, otenabant (Table 5) and subsequent measurement of Anx A1 and NO were performed. The hormonal cells were treated with 2-AG, Anx A1 and NO Additionally, stimulations with NOS activators, ionomycin and LPS, and inhibitors, L-NAME and curcumin (Table 6) were conducted.

To establish standardized stimulation conditions, a validation process based on measurements of produced NO and Anx A1 of TtT/GF was performed. Stimulations with different cell medium content (without any serum supplement and supplemented with 1% fetal bovine serum (FBS)) and with different duration (from 10 to 30 minutes and from 20 to 24 hours) took place.

The results reveal distinguishable dependency on serum content and time duration. The stimulations were performed with 1 µM 2-AG and 300 µM L-NAME, (Fig. 24).

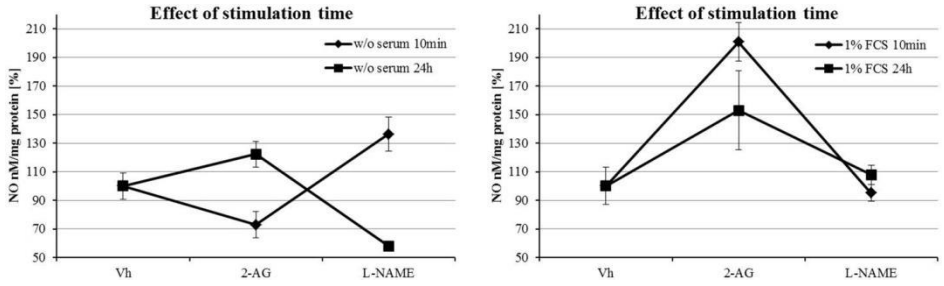


Fig. 24: Analysis of NO from TtT/GF cells treated with 2-AG and L-NAME. Plotted are the relative NO/ protein ratios of the cells treated with 1 µM 2-AG and 300 µM L-NAME for t=10min; 24h, and with 1% serum or without serum.

The data is plotted as line charts to express more evidently the outcome influence (Fig. 24). Short stimulations resulted with more consistent levels of NO in regard of deviation. Long stimulations result in greater deviation that could be due to the individual cell cycle turnover within one cell culture. The levels of Anx A1 did not differ (data not shown).

Serum was omitted to equilibrate most cells to arrest their cell cycle at G0. However, essential processes involved in regulation and secretion of products, require nutrients introduced to the cell as part of the serum mixture. The solution was to serum starve the cells from four hours to maximum one night for the purpose of cell cycle arrest and supplement the cell medium with B-27 ®, a predefined serum substitute, for two hours before stimulation to ensure cell factor production and release. The stimulation

conditions were tested again in terms of NO production on another cell line – AtT20/D16v (Fig. 25).

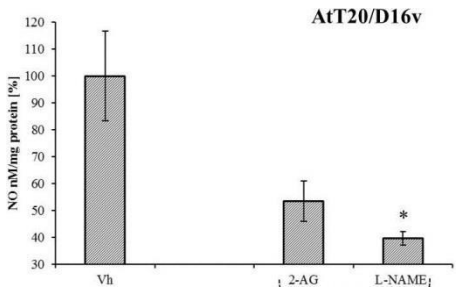


Fig. 25: Analysis of NO from AtT20/D16v cells treated with 2-AG and L-NAME. Plotted are the NO/ protein ratio of the cells treated with 1 µM 2-AG and 300 µM L-NAME under validated conditions (t=30min, B-27 supplemented cell medium).

After the stimulation cells were harvested with a rubber policeman and kept at -80 °C and the cell media at -25 °C. The stimulation concentrations of all compounds were chosen according to their Ki or according to obtained results. However, the validation phase of the stimulation experiment revealed that WIN in concentrations close to its Ki did not exert an effect. Therefore the used WIN concentration range was increased. After the stimulations cell media and cell extracts were collected for further Anx A1 and NO determination.

## 1.4 Anx A1 determination

Samples containing Anx A1 protein from the cell extract, cell membrane, and cell medium were processed in IB and in ELISA. Cell membranous Anx A1 was collected with EDTA buffer after Tierney (2003), consisting of 1 mM EDTA/ PBS, supplemented with protease inhibitors and phosphatase inhibitors (1 µM NaF and 1 µM Na-o-vanadate). Cell medium contained Anx A1 had to be concentrated with a vacuum centrifuge to achieve detectable limits. Eventhough I was able to detect membranous and secreted Anx A1, due to the intricate handling, only cytoplasmic Anx A1 could be quantified.

## 1.5 Immunoblotting (IB)

The term “blotting” refers to the transfer of biological samples from a gel to a membrane and their subsequent detection on the surface of the membrane. “Immuno” because an antibody is used to specifically detect its antigen, the particular protein of interest. The method described is also called Western blotting and was introduced by

Towbin et al. in 1979 and has meanwhile turned routine for qualitative and semi-quantitative protein analysis.

The cells were harvested with a rubber policeman, suspended in lysis buffer and disrupted through sonification. The cell debris was removed through centrifugation and the protein content was assayed after Bradford. This protein assay method was first described by Marion Bradford in 1976. Afterwards 40 µg of protein extract was mixed with Laemmli buffer, heated at 70 °C for 10 min in denaturing and reducing conditions to destroy the tertiary structure of the protein molecules and loaded onto a polyacrylamide gel. The SDS (sodium dodecyl sulfate) reagent in the sample buffer coats the protein molecules with detergent, assigning a high net negative charge that is proportional to the length of the polypeptide chain. When loaded onto a gel matrix and placed in an electric field, the negatively charged proteins migrate towards the positively charged electrode and are separated due to their size by a molecular sieving effect. The separated proteins were transferred or blotted onto a positively charged second matrix, a nitrocellulose membrane. Immediately after blotting, the membrane was treated with a signal enhancer Qentix. Subsequent rinse in 0.1% ponceau S solution visualized the blotted proteins. The membrane was further blocked with 5% bovine serum albumin (BSA)/TBST to prevent any non-specific binding of antibodies to the surface of the membrane. The transferred protein was detected indirectly. It was complexed with a primary antibody/ 0.5% BSA/TBST incubation over night at 4 °C. After a washing step, a second HRP (horseradish peroxidase) enzyme labeled antibody/ 0.5% BSA/TBST was added. (The second antibody is directed against IgGs from the species of origin of the primary antibody.) Super Signal West pico Chemiluminescent Substrate was added to the membrane. The substrate (luminol) and peroxide are oxidized by HRP. Luminol is converged in its excited state 3-aminophthalate, that decays to a lower energy state by releasing photons of light.

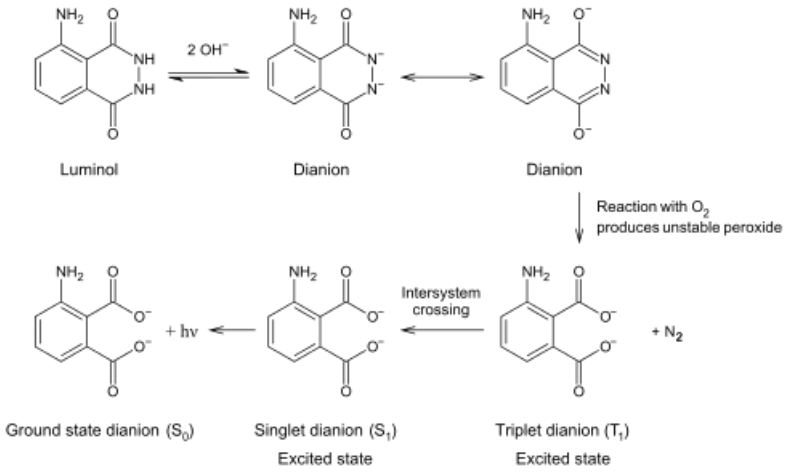


Fig. 26: Luminol turnover to a chemiluminescent dianion. (From a Bio-Rad western blot manual.)

The light output was captured using Kodak BioMax ® MR film. The film was developed with Agfa Rodinal developer and fixed with Roentgen Superfix fixer.

The IB results were analyzed by densitometry. The films were scanned with an Epson device and the images were processed with ImageJ (NIH, Bethesda, MD, USA). Each band of the protein of interest was encompassed and the optical density (OP) of the contained pixels was determined as "mean grey value" and multiplied by the area of the band. Thus the unit of the obtained value is [mean grey value*area]. The value was then corrected for background and adjusted to actin. For the purpose of statistical analysis, the value was then normed to the average of at least 3 repetitions and then presented as percentage of the basal level (set up to 100%).

**Statistical analysis**

The statistical analysis was conducted with GraphPad Prism 5 (San Diego, CA, USA). One-way analysis of variance (ANOVA) with Bonferroni correction was used when 3 and more groups were compared. Student's T-test with Welch's correction was used to compare 2 groups. The results are presented as mean relative OD +/- standard error of the mean (SEM).

## 1.6 ELISA

ELISA (enzyme-linked immunosorbent assay) is used for the quantitative measurement of a target antigen. This assay employs an antibody specific for the target protein coated on a 96-well plate. Standards and samples are pipetted into the wells and the target

protein present in a sample is bound to the wells by the immobilized antibody. The wells are washed and biotinylated secondary antibody is added. After washing away unbound biotinylated antibody, HRP-conjugated streptavidin is pipetted to the wells. The wells are again washed, a 3, 3', 5, 5'-tetramethylbenzidine (TMB) substrate solution is added to the wells and color develops in proportion to the amount of target protein bound. A stop solution is added and the intensity of the color is read at the certain wavelength.

Mouse Anx A1 ELISA kit (Cusabio Life Sciences, Wuhan, China) was applied for cell extracts and cell media from WIN and otenabant treated TtT/GF cells. Mouse ACTH ELISA kit (MyBioSource, San Diego, CA, USA) was applied for cell extracts and cell media from 2-AG, Anx A1 and NO treated AtT/D16v cells. Rat PRL ELISA kit (Sigma Aldrich Chemie GmbH, Germany) was applied for cell extracts and cell media from 2-AG, Anx A1 and NO treated GH4C1 cells.

**Calculation**

The instructions in the manuals supplied with the kits were strictly followed and the results from measuring the samples at a Multi scan plate reader were calculated with a four parameter logistic function:

$y = d + (a - d)/(1 + (x/c)^b)$, respectively $x = c * \sqrt[b]{\frac{a-d}{y-d} - 1}$, where

y = optical intensity

b = slope

x = concentration

c = inflection point

a = minimum asymptote

d = maximum asymptote.

The resulted values were normalized upon the amount of protein in the samples and after averaging over the arithmetic mean were subjected to statistical analysis and presented as a percentage of the basal value that corresponds to 100%. One-way ANOVA with Bonferroni correction was used to compare 3 and more groups, and Student's T-test with Welch's correction was used to compare 2 goups.

## 1.7 PCR method

Polymerase-chain reaction (PCR) method is applied to detect genes that are actively expressed at the point of measurement. Total RNA was extracted using Trizol and reversely transcribed to complementary DNA (cDNA) using a *Taq* enzyme. A 2% agarose gel electrophoresis was run to ensure genomic DNA is absent in the samples. The resulting DNA was measured spectrophotometrically and used for conventional PCR or qPCR.

**Primers generation**

Coding RNA (hence mRNA) segments from the genes of interest were sought in data base of the NCBI (National Center for Biotechnology Information, NIH) and converted into FASTA format, which is a text based description of nucleotide sequences. The FASTA data of one particular gene was further compared to the sequences of the other genes of the host organism to prevent non-specific binding of the primers later. The sequence comparison algorithm used was BLAST (Basic Local Alignment Search Tool) (Altschul et al., 1990) provided by NIH. After possible alignment with non-specific nucleic sequences was excluded, suitable primers were designed with the software tool PRIMER3 (Whitehead Institute for Biomedical Research, Steve Rozen) (Untergasser et al., 2012). All designed primers were synthetized by Eurofins MWG Operon, Ebersberg, Germany.

**Conventional PCR**

Conventional PCR was applied to confirm the presence of mRNA of Anx A1, FAAH in the FS cells TtT/GF and Tpit/F1; POMC (a precursor of ACTH) in the C cells AtT20/D16v, and PRL in the L cells GH4C1. The used PCR run schemes are shown below (Fig. 27). The amplified cDNA fragments were visualized by performing a 2% agarose – etidium bromide gel electrophoresis at PowerPac Universal for 40 min at 110 V and subsequent UV exposure at Gel Imaging System red ® device ProteinSimple and image acquisition with the Pronto software.

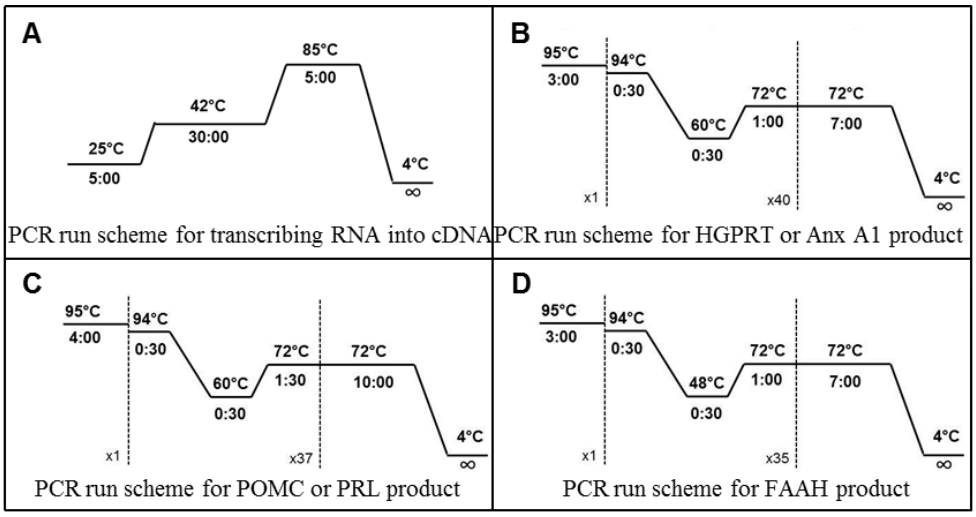


Fig. 27: PCR schemes for (A) transcribing RNA into cDNA; (B) amplifying HGPRT or Anx A1 cDNA; (C) amplifying POMC or PRL cDNA, and (D) amplifying FAAH cDNA.

### RNA extraction

The cells were rinsed with PBS and Trizol. One ml Trizol per 10 $cm^2$ of cell dish or culture flask was added. The detached cells were gathered and left for 5 minutes at room temperature to permit the complete dissociation of nucleoprotein complexes. After cell debris was removed via centrifugation, 0.2 ml chloroform per 1 ml Trizol was added and the tube was vortexed. After a 3 min – incubation, centrifugation at 12000 x g for 15 min followed. Three phases were built: lower red, phenol-chloroform phase, an interphase, and a colorless upper aqueous phase. The extracted total RNA is in the aqueous phase and had to be transferred in a new tube. At this step 0.5 ml isopropyl alcohol per 1 ml Trizol was added to the tube and centrifuged at 12000 x g for 10 min at 4 °C after an incubation of 10 min. The RNA pellet was washed 3 times with 1 ml 70% EtOH per 1 ml Trizol and left air-drying for 20 min. The final step was resolving the RNA pellet in DEPC-treated water.

### Nucleic acid quantification

Isolated RNA, copy DNA, but also DIG-labeled primers were analyzed spectrophotometrically for purity, integrity, and quantification. Two µl of the nucleic acid samples were loaded air bubles-free onto the measurement pedestal of NanoDrop ND 1000. The UV absorbance was measured at 260 and 280 nm. The concentration of nucleic acid was determined using the Beer-Lambert law, which predicts a linear change in absorbance with concentration. RNA and DNA have its absorption maximum

at 260 nm and their ratio is used to assess the purity of a given preparation. Pure RNA has “2”as ratio of the absorbance at 260 and 280 nm (A260/A280). As this ratio decreases, protein contamination rises (purity decreases). DNA pure samples have A260/A280 ratio of 1.8. Protein and phenol absorb at 230 nm.

### 1.7.1 qPCR

Real-time or quantitative (q) PCR allows the quantification of amplified complementary DNA in process by measuring the intensity of intercalated fluorescent dye (SYBR ® green). This method was applied to assay the different NOS types (brain, endothelial, and inducible) in the fs TtT/GF and Tpit/F1, and C AtT20/D16v cells. (Fig. 28 shows the run scheme that was used for qPCR.)

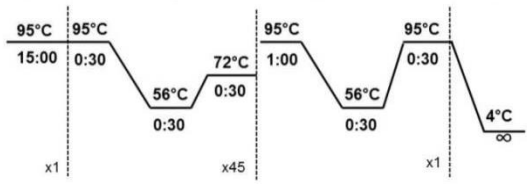


Fig. 28: qPCR scheme for amplifying the cDNA of NOS isoforms and EFa1.

**Calculation**

One uses the detected threshold cycle (Ct) when the level of fluorescence gives signal over the background and is in the linear portion of the amplified curve. Since it is a relative value, an internal control is used. I chose to use the house keeping gene elongation factor-1α (EF-1α). The resulted Ct values of the triplicate samples for the NOS enzymes were averaged and the difference from the averaged values for EF-1α was obtained (dCt). The background was substracted to yield ddCt that was presented logarithmically as $2^{-ddCt}$.

## 1.8 Staining techniques

### 1.8.1 *In situ* hybridization (ISH)

ISH is a highly sensitive mRNA detection method. Labeled with a radioactive isotope or with digoxigenin DNA probes hybridize with their matching mRNA segments. The detection is either with a radioactivity-sensitive film or with an antibody directed against digoxigenin.

**Procedure**

The cell or tissue material to be subjected to ISH was frozen fresh and fixed with 4% PFA only prior to performing the technique. After rinsing the samples with PBS, an acetylation step with acetic anhydride and triethanolamine removes the positive charge on the glass surface and thus prevents non-specific probe binding. It further allows better access to the cell RNA. The samples are dehydrated in alcohol and incubated at 42 °C over night with the probes in hybridization buffer. Afterwards the non-specifically bound probes were removed by stringency washes with saline-sodium citrate (SSC) buffer. The final detection step was performed according to the labeling of the probes used.

**Radioactively labeled probes**

The radioactive method was used to validate the ISH method on cell samples. Radioactive ISH was performed on the fs cells TtT/GF and C cells AtT20/D16v to confirm the presence of Anx A1- and POMC-mRNA.

All operations involving radioactive material were performed in a specialized laboratory environment under frequent controls with a radiation counter Contamat FHT 111M. [α-$^{33}$P]-dATP with radioactive activity of 10mCi/ml (Perkin Elmer, MA, USA) was tailed on the 3' end of the designed ISH primers using terminal deoxytransferase (TdT) enzyme. $^{33}$P is a relative stable phosphorus isotope with half-life of 25 days and beta emission as decay mode. Its decay product is $^{33}$S. The designed DNA primers were mixed with the components from the table below and incubated at 37 °C for 2h. The reaction was stopped with 80 µl Tris-EDTA (TE) buffer. The non-labeled $^{33}$P-dATPs were removed in a gel matrix as follows. A 1 ml sterile syringe was filled with a pea-size quantity of RNAse-free glass wool (Carl Roth GmbH, Karlsruhe, Germany) and stabilized in a 15 ml falcon tube. The glass wool was washed once with TE buffer. The next step involved polymerization of Sephadex ® G-50 fine (GE Health, Uppsala, Sweden) in the syringe. Sephadex is a gel filtration medium prepared by crosslinking dextran with epichlorohydrin and thus suitable for the gentle and quick purification of the probes. The probes were eluated in the column at 2000 rpm for 90 sec and collected in a 1.5 ml tube with previously added 1 µl 0.1 M DTT. The purificated probes were measured in a scintillation counter (2500 TR Packard Tri-Carb ®) to ensure their sufficient quality. One µl of the radioactive probe was mixed with 1 ml scintillation

cocktail Rotiszint eco plus (Carl Roth GmbH, Karlsruhe, Germany) and the counts per minute (cpm) were determined. Only probes with 200 000 and higher cpm were used. The detection was performed by exposing the samples to a X-ray sensitive film Kodak BioMax ® MR film. The film was developed with Agfa Rodinal developer and fixed with Roentgen Superfix fixer.

**Non-radioactively DIG labeled probes**

The non-radioactive method was established afterwards as a safer alternative. The designed primers were subjected to a digoxigenin labeling with a DIG tailing kit 2$^{nd}$ generation to yield the probes. After hybridization with the specific RNA sequences in the samples, the probes were detected indirectly using alkaline phosphatase coupled Fab fragments from an antibody raised against digoxigenin. The dye substrate that was then added to the samples, nitro-blue tetrazolium (NBT) and 5-bromo-4-chloro-3'-indolyphosphate (BCIP), was converted to a blue precipitate by the enzyme. The ISH procedure was run using DIG Wash and Block Buffer Set, anti-digoxigenin-AP Fab fragments, and NBT/BCIP substrate from Roche, according to the instructions supplied.

### 1.8.2 Immunocytochemistry (ICC)

The ICC method is used to obtain an image of the localization of a certain antigene in cell samples. The cells were fixed with 4% PFA and incubated in serum to mask the non-specific binding sites. A primary antibody raised against the protein of interest was then added with a detergent, triton x-100, that permeabilizes the cell membrane. The incubation at room temperature lasted one night. After rinsing with PBS solution, a secondary antibody raised against the species of the primary antibody was added. The secondary antibody was conjugated to either biotin or a fluorescent dye, depending on the method of detection. In the case of 3, 3'-diaminobenzidine (DAB) based detection, an avidin coupled peroxidase enzyme (ExtrAvidin ®) was then given to the biotin conjugate for 1h. After forming the stable avidin-biotin complex, DAB substrate was added. The peroxidase oxidizes DAB and an addition of $H_2O_2$ initiates its polymerization to a brown precipitate. The cells were mounted with Kaiser's glycerol gelatine and observed through light microscopy. In the case of a fluorescent conjugate of the secondary antibody, after incubation, the samples were rinsed and mounted with Dako fluorescent mounting medium. The specimen were kept at 4 °C, protected from light and observed through confocal microscopy.

### 1.8.3 Immunohistochemistry (IHC)

IHC follows the same principles as ICC, involving detection based on an antibody bound to a specific antigen. However, the specimen for this technique is tissue. Fluorescent IHC was performed on tissue slices of 8 to 20 µm thickness. It was conducted after the fluorescent ICC protocol with an additional antigen retrieval step with citrate buffer at the beginning. The specimen were immersed in pre-heated (to 95-100 °C) citrate buffer for 10 min, then rinsed and processed as described in the fluorescent ICC section.

### 1.8.4 Microscopy

The imaging procedure for samples subjected to DIG labeling and DAB precipitation involved light microscopy. The process included image acquisition with Axiovert Vision 2 software and Axioplan light microscope, and recording with an AVT Horn camera system. The acquired image data was converted to grey 8 bit scaled TIFF format files that were analyzed with ImageJ with white color corresponding to the value of 255 and black color to 0. The number of specifically stained cells per area unit was obtained by introducing a background-corrected threshold filter.

Confocal microscopy was used for samples subjected to fluorescent labeling. A laser scanning microscope converges the laser beam into a small spot using an objective and scans the specimen in the X-Y direction using the laser beam. The microscope then captures the fluorescent light and reflected light from the specimen using light detectors and provides the specimen image on an image monitor. The confocal system used in this study was FluoView™ FV1000 obtained and supported by Olympus, Japan. It comprises fluorescence illumination unit, laser diodes, an Argon laser, a Helium laser, thus covering multiple emissions from 405 to 635 nm wavelength, a laser combiner that incorporates the independent laser beams, and a simultaneous (SIM) scanner. The image acquisition was performed at the following scanning mode: 12 µs/pxl speed; automatic offset value, confocal aperture, and transmission light control; frame averaged to 5; Kalman filtering, and sequential scanning.

## 1.9 NO detection

NO reacts with dissolved oxygen to form nitrite ($NO_2^-$). In the absence of oxyhemoglobin (as in cell cultures), nitrite will be the major oxidation product of NO. Thus the applied techniques in this work - gas-phase ozone-chemiluminescence, diazotization (Griess reaction), and fluorescent labeling with DAF-2DA, are indirectly detecting NO over its end product nitrite.

### 1.9.1 Ozone-chemiluminescence method

The ozone-chemiluminescence method detects a gas-phase chemiluminescent reaction between NO and ozone:

$NO + O_3 \rightarrow NO_2^* + O_2$

$NO_2^* \rightarrow NO_2 + hv$

Emission from electronically excited nitrogen dioxide ($NO_2^*$) is in the red and near-infrared region of the spectrum, and is detected by a thermoelectrically cooled, red-sensitive photomultiplier tube. To measure nitrite, a reducing agent, such as KI in glacial acetic acid was added to convert nitrite to NO:

$I^- + NO_2^- + 2H^+ \rightarrow NO + 1/2I_2 + H_2O$

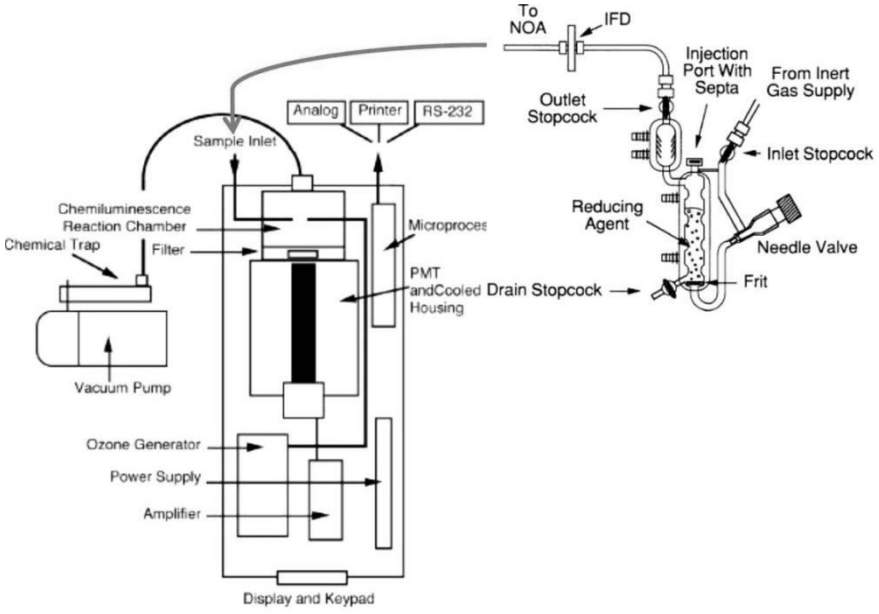


Fig. 29: Scheme of the apparatus Sievers NO analyzer used for chemoluminescent detection of NO. (From the manual NOA® 280i)

The device with which the detection was performed is a Sievers NO analyzer (NOA® 280i) (Fig. 29). The calculated values were obtained with NoaWin32® version 1.5f (DeMeTec, Hannover, Germany). A standard curve was used to calculate the NO concentration according to the following formula:

$$x = \frac{y + a}{b}$$

where

x = calculated concentration a = slope

y = value obtained with Sievers i280 b = intercept

The resulted values were normalized upon the amount of protein in the samples and after averaging over the arithmetic mean were subjected to statistical analysis and presented as a percentage of the basal value that corresponds to 100%. One-way ANOVA with Bonferroni correction was used to compare 3 and more groups, and Student's T-test with Welch's correction was used to compare 2 goups.

**Deproteinization**

The cell medium samples had to be protein-free when measured with 280i NOA. For this purpose absolute ethanol protein precipitation took place. 9 parts ice-cold 99% ethanol was added to 1 part cell sample. The mixture was kept over night at -80 °C and centrifuged at at least 14000 rpm for 30 min. The protein-free liquid phase was transferred to a new 1.5 ml tube.

### 1.9.2 Diazotization

Griess developed a two-step diazotization reaction for detecting NO in 1864 (Griess, 1879; described in detail by Fox et al., 1987). The mechanism involves generation of the NO-derived nitrosating agent from the acid-catalyzed formation of nitrous acid from nitrite, that further reacts with sulfanilamide (Griess reagent 1) to produce a diazonium ion that is then coupled to *N*-(1-napthyl)ethylenediamine (Griess reagent 2) to form a chromophoric pink azo product that absorbs at 540 nm (Fig. 30).

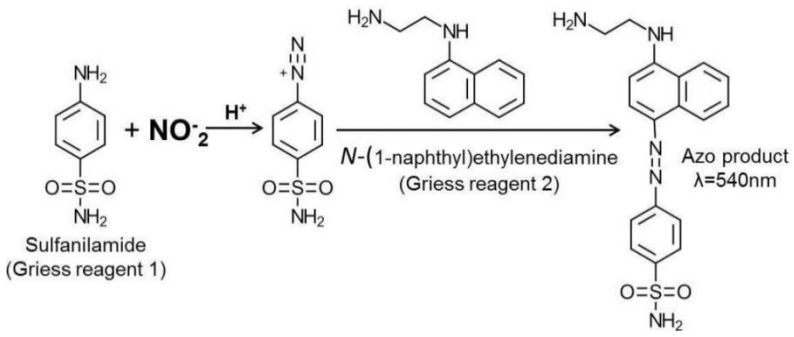


Fig. 30: Reaction mechanism of the Griess diazotization.

The NOS cofactor NADPH that is needed for converting nitrate into nitrite through nitrate reductase (NR) interferes with the Griess reagents and disturbs the reaction. A way to circumvent this, is to oxidize the excess NADPH with lactate dehydrogenase (LDH) (Sun et al., 2003). A Nitrate/Nitrite Colorimetric assay kit (LDH method) from Cayman Chemical Company, Ann Arbor, MI, USA was used to measure nitrite in cell medium. The samples were read at 550 nm at a Multiscan RC device and a standard curve was used to calculate the NO concentration according to the following formula:

$$x = \frac{y + a}{b}$$

where

x = concentration

a = slope

y = read absorbance

b = intercept

The resulted values obtained with Ascent software version 2.6 (Thermo Fisher Scientific, Darmstadt, Germany) were normalized upon the amount of protein in the samples and after averaging over the arithmetic mean were subjected to statistical analysis and presented as a percentage of the basal value that corresponds to 100%. One-way ANOVA with Bonferroni correction was used to compare 3 and more groups, and Student's T-test with Welch's correction was used to compare 2 goups.

### 1.9.3 Fluorescent labeling with DAF-2DA

DAF-2DA (4,5-diaminofluorescein-2-diacetyl) is a dye, that deacetylates upon penetration into the cell by cytosolic non-specific esterases to DAF-2 and is then trapped in the cell (Fig. 31; Nagano, 1999). NO that has been oxidized to nitrite in the

cell, forms with the non-fluorescent DAF-2 the strongly fluorescent DAF-2T that can be photometrically detected.

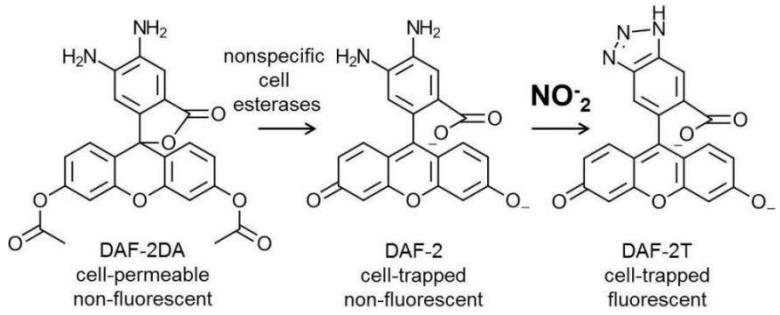


Fig. 31: Mechanism of the deacetylation of DAF-2DA leading to cell-trapping of the substance, which after conversion with nitrite, results in its fluorescent DAF-2T form.

**DAF-2DA fluorescent imaging**

For performing the DAF-2DA staining technique PD tissue slices from C3H mice were immersed after biopsy in B-27 supplemented HBSS medium. FS cells (TtT/GF and Tpit/F1) were kept in DMEM/F-12 without phenol red. Ten µM DAF-2DA was added to the culture medium of tissue and cells for 1 h. Afterwards the specimen were fixed in 2.5% glutaraldehyde at 4 °C for 30 min. Images of the tissue slices and cell cultures were taken through confocal microscopy at 488 nm excitation. The procedure was described by Schwendemann et al. (2008).

**DAF-2DA cell sorting**

Furthermore DAF fluorescent cells can be sorted using flow cytometry, as suggested by Lampiao et al. (2006) and Katrin Schroeder (oral communication). This technique was applied to AtT20/D16v cells *a priori* incubated with 10 µM 2-AG.

Fluorescence-activated cell sorting (FACS) separates the cells according to their excitation by a laser of certain wavelength and their respective emission. The analysis delivers information on the size and morphological complexity of the sorted cells. A Forward Scatter (FSC) is a detector of emitted light directed parallel to the cell suspension stream and provides information on the cell volume, while a Side Scatter (SSC) is directed perpendicular to the streamed cells and measures the level of scattered light according to the granularity of the cells.

Fresh AtT20/D16v cell cultures at the 2$^{nd}$ day after their passage were divided into 2 groups. The cells were incubated in serum and phenol red free HEPES-Tyrode (HT)

buffer since the mentioned compounds interfere with the DAF-2DA substance. Ten µM of 2-AG were given to one group of 3 cell cultures 30 min prior to measurement. The other group of 8 cell cultures was used as a control. Three µl DAF-2DA (yielding 5 mM end concentration) were given to all cells 30 min prior to 2-AG stimulation. The 50 µl cell suspension containing ca. 10000 cells was measured at 488 nm a FACSCalibur Becton, Dickinson and Company device and analyzed per BD FACSDiva™ software. The calculated output represents the DAF-2DA fluorescent positive cell counts. The background was subtracted from the values that were then averaged and subjected to an unpaired Student's T-test comparison with a Welch correction.

**Validation of NO measurement**

The Griess and NOA NO detecting methods were compared by the values being normed to reduce as far as possible side effect bias. Even with indisputable standard deviations, the measurements performed with NOA and Griess method showed centered arithmetic mean behavior.

## 1.10 Fura Calcium measurement

The intracellular $Ca^{2+}$ concentration after $CB_1$ receptor activation was measured with the fura method. Fura-2-acetoxymethyl ester (fura-2AM or acetoxymethyl 2-[5-[bis[(acetoxymethoxy-oxo-methyl)methyl]amino]-4-[2-[2-[bis[(acetoxymethoxy-oxo-methyl)methyl]amino]-5-methyl-phenoxy]ethoxy]benzofuran-2-yl]oxazole-5-carboxylate) (Fig. 32) is membrane-permeable and when added to cells, crosses the cell membrane. Once inside the cell, the acetoxymethyl groups are removed by cellular esterases thus the compound is converted to fura-2 a pentacarboxylate calcium indicator. Measurement of the level of fluorescence at both 340 nm (fura-2-$Ca^{2+}$ complex) and 380 nm (unbound fura-2) allows calculation of the $Ca^{2+}$ concentration-based 340/380 ratios.

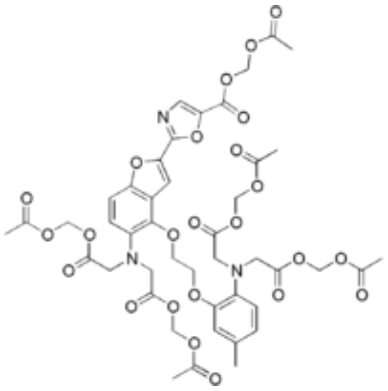

Fig. 32: Structural formula of fura-2-acetoxymethyl ester (fura-2AM or acetoxymethyl 2-[5-[bis[(acetoxymethoxy-oxo-methyl)methyl]amino]-4-[2-[2-[bis[(acetoxymethoxy-oxo- methyl)methyl]amino]-5-methyl-phenoxy]ethoxy]benzofuran-2-yl]oxazole-5-carboxylate).

TtT/GF cells (1.5 x $10^4$ cells per well) and Tpit/F1 (15 x $10^4$ cells per well) were seeded in µClear plates. At least 24 h later the cell medium was changed with HT buffer supplemented with 1% serum. Cell permeant fura-2AM with final concentration 1.25 µM was added for 30 min. After a rinse step with PBS, HT buffer supplemented with 1 µM probenecid was added to the cells to block the fura-2 transport out of the cell. The wells were measured 15 times to obtain the baseline. Immediately after, 2-AG (1 µM, 2 µM) and AEA (1 µM, 2 µM) were added a measurement cycle with 50 repeats was initiated. At last saturated $MnCl_2$ solution was added and a measurement cycle with 10 repeats was performed to acquire the background that was later subtracted from the calculated values. The triplicate samples were averaged and plotted as 340 nm/380 nm ratios with (+/- SEM). The measurements took place on a Perkin Elmer EnVision/ 2104 Multilabel Reader device and the software used to obtain the data was Wallac EnVision ® Manager (Life Technologies). The data was later processed in Excel (Microsoft Co., Redmont, WA, USA).

# 2 Materials

Table 4: Consumables used for the cell cultures.

| **chemicals for cell culture** | **source** |
|---|---|
| amphotericin B | Gibco, Karlsruhe, Germany |
| B-27 ® | Gibco, Karlsruhe, Germany |
| DMEM/Ham's F-12 | Gibco, Karlsruhe, Germany |
| DMEM high glucose/ with stable glutamine | Gibco, Karlsruhe, Germany |
| DMEM/F-12 without phenol red | Gibco, Karlsruhe, Germany |
| Ham's F-10 | PAA Laboratories, Pasching, Austria |
| HBSS | Gibco, Karlsruhe, Germany |
| HEPES | Sigma Aldrich Chemie GmbH, Germany |
| Hi FBS | Gibco, Karlsruhe, Germany |
| MycoAlert ™ mycoplasma detection kit | Lonza Group AG, Basel, Switzerland |
| MycoProbe ® mycoplasma detection kit | R&D Systems Inc., Bristol, UK |
| NaF | Carl Roth GmbH, Karlsruhe, Germany |
| Na-o-vanadate | Carl Roth, GmbH Karlsruhe, Germany |
| NHS | Sigma Aldrich Chemie GmbH, Germany |
| PBS | PAA Laboratories, Pasching, Austria |
| penicillin-streptomycin | Sigma Aldrich Chemie GmbH, Germany |
| PFA | Merck AG, Darmstadt, Germany |
| poly-L-lysine | Sigma Aldrich Chemie GmbH, Germany |
| purified water | Gibco, Karlsruhe, Germany |
| Roti ® DipSlides | Carl Roth GmbH, Karlsruhe, Germany |
| trypan blue solution | Sigma Aldrich Chemie GmbH, Germany |
| trypsin | Gibco, Karlsruhe, Germany |
| **disposables** | |
| µClear plates, sterile pipettes, falcon tubes; multidish plates, culture flasks | Greiner Bio-One GmbH, Frickenhausen, Germany |
| sterile filter systems | Corning Holding, Wiesbaden, Germany |

Cannabinoid substances for cell stimulation with indicated function, binding constant, used concentration, and source.

Table 5: Cannabinoid substances for cell stimulation with indicated function, binding constant, used concentration, and source.

| compound | function | Ki | concentration | source |
|---|---|---|---|---|
| 2-AG | endogenous CB1 agonist | 472 nM | 0,05/ 0,5/ 5 µM; 1 µM | Tocris, Bristol, UK |
| AEA | endogenous CB1 agonist | 89 nM | 0,001/ 0,01/ 0,1 µM | Tocris, Bristol, UK |
| WIN 55.212-2 | exogenous CB1 agonist | 2 nM | 0,1/ 1/ 10 µM | R&D Systems Inc., Bristol, UK |
| otenabant | exogenous CB1 antagonist | 2.8 nM | 1 nM | Selleck Chemicals, Dallas, TX, USA |

Stimulation substances with indicated function, reference, used concentration, and source.

Table 6: Stimulation substances with indicated function, reference, used concentration, and source.

| compound | function | reference | concentration | source |
|---|---|---|---|---|
| ionomycin (A23187 HCl) | Ca ionophore<br>NOS activator | Stefanie Oess, Igor Kovacevic oral communication; data sheet Enzo Inc. | 1 µM | Enzo Life Sciences Inc., Farmingdale, NY, USA |
| LPS from E. coli | NOS activator | Brouet and Ohshima, 1995 | 1 µM ($8.10^6$ eu[11]/ml) | Sigma Aldrich Chemie GmbH, Germany |
| L-NAME | NOS inhibitor | Katrin Schröder oral communication; Rees et al., 1990; Boucher et al., 1999 | 300 µM | Sigma Aldrich Chemie GmbH, Germany |
| curcumin | iNOS inhibitor | Brouet and Ohshima, 1995 | 10 µM | S. Cruz Biotechnology Inc., Dallas, TX, USA |

[11] eu - endotoxin units

| | | | | |
|---|---|---|---|---|
| rAnx A1 hn GST tagged | Anx A1 mimetic | semi-quantitative analysis Anx A1 collected from cultured fs cells | 13 µM | Abnova GmbH, Heidelberg, Germany |
| NO-2 | NO mimetic | Venkelekom et al., 2002 | 1 µM | Sigma Aldrich Chemie GmbH, Germany |

## 2.1 Recipes

### Cell media

Table 7: Cell media composition for each of the cell lines used.

| cell line | cell medium composition |
|---|---|
| TtT/GF | DMEM/Ham's F-12, 10% NHS, 2.5% FBS, 1% HEPES, 1% penicillin, 1% streptomycin, 1% amphotericin B |
| Tpit/F1 | DMEM/Ham's F-12, 10% NHS, 2.5% FBS, 1% HEPES, 1% penicillin, 1% streptomycin, 1% amphotericin B |
| AtT20/D16v | DMEM high glucose/ with stable glutamine, 10% FBS, 1% HEPES, 1% penicillin, 1% streptomycin, 1% amphotericin B |
| GH4C1 | Ham's F-10, 10% NHS, 2.5% FBS, 1% HEPES, 1% penicillin, 1% streptomycin, 1% amphotericin B |

**IB**

| lysis buffer | |
|---|---|
| 50 mM Tris HCl pH 8 | 3200µl |
| 1 mM NaCl | 1096µl |
| 0,5 M EDTA | 80µl |
| 85% glycerol | 800µl |
| 1% triton ™ X-100 | 80µl |
| 0,5 M DTT | 16µl |
| 0,2 M sodium o-vanadate | 40µl |
| 1M ß-glycerolephosphate | 80µl |
| cOmplete Mini protease inhibitor (Roche Diagnostics, Mannheim, Germany) | 1 |
| aq. dest. | ad 8ml |

**Protein quantification**

Coomassie Plus ™ (Bradford) assay kit, Thermo Fisher Scientific, Darmstadt Germany

Photometry cuvettes, Sarstedt, Nümbrecht, Germany

| sample buffer | |
|---|---|
| 0.5 M Tris pH 6.8 | 1 ml |
| 10% SDS | 1.6 ml |
| 0.1 M glycerol | 800 µl |
| 1% bromphenol blue | 400 µl |
| ß-mercapto EtOH | 400 µl |
| aq. dest. | ad 8 ml |

**Gel electrophoresis**

MiniProtean ® TGX stain-free ™ precast gels, Bio-Rad GmbH, Dreieich, Germany

Running buffer: Tris/ Glycine/ SDS, Bio-Rad GmbH, Dreieich, Germany

Marker: Precision Plus Protein ™ WesternC ™ Standard and StrepTactin-HRP conjugate, Bio-Rad GmbH, Dreieich, Germany

Marker: MagicMark ™ XP Western Protein Standard, Invitrogen, Carlsbad, CA, USA

Incubation buffer

Blocking buffer: 5% Albumin from bovine serum (BSA) (Sigma Aldrich, Germany) in TBST

Antibody buffer: 0.5% Albumin from bovine serum (BSA) (Sigma Aldrich, Germany) in TBST

**PCR**

| components | vol per rct |
|---|---|
| nuclease-free water | 40.5-x µl |
| 10x ThermoPol ® buffer | 5 µl |
| 5 mM dNTP Qiagen | 2 µl |
| primer FW | 1 µl |
| primer RV | 1 µl |
| Thermo *Taq* polymerase | 0.5 µl |
| cDNA template | x µl |
| total volume | 50 µl |

**RNA extraction**

TRI ® reagent, Sigma Aldrich Chemie GmbH, Germany, RNeasy ® kit, Qiagen, Venlo, Holland

Long term storage buffer: 10% Roti ®-Block (Carl Roth GmbH, Karlsruhe, Germany) in TBST

**Visualization**

Qentix ™ Western Blot signal enhancer, Pierce, Rockford, IL, USA

Super Signal ™ West pico Chemiluminescent Substrate, Thermo Fisher Scientific, Darmstadt, Germany

Kodak ™ BioMax ® MR Film, Kodak GmbH, Stuttgart, Germany

Developer: 1:50 Agfa Rodinal, Agfa Photo, Leverkusen, Germany, in aq. dest.

Fixer: 1:8 Tetenal Roentogen Superfix, Tetenal, Norderstedt, Germany, in aq. dest

Restore Western blot stripping buffer, Thermo Fisher Scientific, Darmstadt, Germany

**cDNA synthesis**

*Taq* DNA polymerase, New England BioLabs Inc., Ipswitch, MA, USA

iScript ™ cDNA synthesis kit, Bio-Rad

| components | vol per rct |
|---|---|
| 5x iScript ™ reaction mix | 4 µl |
| iScript ™ Reverse Transcriptase | 1 µl |
| nuclease-free water | 15-x µl |
| RNA template | x µl |
| total volume | 20 µl |

**Electrophoresis**

Agarose, AppliChem GmbH, Darmstadt, Germany, etidium bromide, Sigma Aldrich Chemie GmbH, Germany

RedSafe ™, iNtRON Biotechnology Inc., Kyungki-Do, South Korea

**qPCR**

Reagents with given volume for performing 1 qPCR reaction.

| components | vol per rct |
|---|---|
| nuclease-free water | 22-x µl |
| iQ ™ SYBR ® Green Supermix (Bio-Rad) | 25 µl |
| primer FW | 1.5 µl |
| primer RV | 1.5 µl |
| cDNA template (10 ng) | x µl |
| total volume | 50 µl |

Contains of iQ ™ SYBR ® Green Supermix.

| iQ ™ SYBR ® Green Supermix (Bio-Rad) contents |
|---|
| 100 mM KCl |
| 40 mM Tris HCl pH 8.4 |
| 0.4 mM dNTP |
| 50 u/ml iTaq ™ polymerase |
| 6 mM MgCl2 |
| SYBR ® green |
| 20 nM fluorescein |

**ISH**

DIG oligo tailing kit 2$^{nd}$ generation; DIG Wash and Buffer kit, Roche Diagnostics, Mannheim, Germany, was used.

Recipe for the hybridization buffer.

| hybridization buffer | volume |
|---|---|
| deionized formamide | 5 ml |
| 1 M Tris HCl pH 8 | 0.33 ml |
| 2 mg/ml yeast tRNA (Sigma Aldrich) | 1 ml |
| Denhardt‘s solution x 50 (Sigma Aldrich) | 0.2 ml |
| 5 M NaCl (Sigma Aldrich) | 1.2 ml |

| | |
|---|---|
| 10% SDS (Sigma Aldrich) | 0.25 ml |
| 0.5 M EDTA pH 8 (Sigma Aldrich) | 0.02 ml |
| DEPC water | 2 ml |
| total volume | 10 ml |

TE buffer recipe.

| TE buffer | volume |
|---|---|
| 1 M Tris HCl pH 8 | 1 ml |
| 0.5 M EDTA | 200 µl |
| 5 M NaCl | 4 ml |
| DEPC water | ad 100 ml |

Reagents with given volume for performing 1 reaction of synthetizing [α-33P]-dATP containing DNA probes.

| components | volume per rct |
|---|---|
| 5x TdT buffer (Invitrogen) | 4 µl |
| 2 pmol/l primer | 1.5 µl |
| [α-33P]-dATPs | 3 µl |
| 15 u/ml TdT (Invitrogen) | 1 µl |
| DEPC water | 10.5 µl |
| total volume | 20 µl |

**ICC/IHC**

Dako fluorescence mounting medium, Agilent Technologies, Santa Clara, CA, USA

entellan; Kaiser's glycerol gelatine, Merck AG, Darmstadt, Germany

ExtrAvidin ®, Sigma Aldrich Chemie GmbH, Germany

triton x-100, Sigma Aldrich Chemie GmbH, Germany

Antigen retrieval citrate buffer recipe.

| 10 mM citrate buffer pH 6 | |
|---|---|
| 9 ml citric acid solution | (21.01 g citric acid ad 1 L with Aq. dest) |
| 41 ml tri-sodium citrate solution | (29.41 g tri-sodium citrate dehydrate ad 1 L with Aq. dest) |
| 450 ml aq. dest. | |

**NO**

Nitrite standard, Sigma Aldrich Chemie GmbH, Germany

4, 5-diaminofluorescein diacetate (DAF-2DA), Sigma Aldrich Chemie GmbH, Germany

Potassium iodide, Sigma Aldrich Chemie GmbH, Germany

Nitrate/ Nitrite Colorimetric Assay Kit (LDH Method), Cayman Chemical Company, Ann Arbor, MI, USA,
NADPH powder, Trevigen ® Inc., Gaithersburg, MD, USA

| Tyrode HT buffer pH 7.4 | amount |
|---|---|
| HEPES | 2.38 g |
| NaCl (Sigma Aldrich) | 8 g |
| KCl (AppliChem) | 0.2 g |
| MgCl2x6H2O | 0.1 g |
| CaCl2x2H2O | 0.26 g |
| NaH2PO4xH2O | 0.05 g |
| glucose (Sigma Aldrich) | 0.9 g |
| aq. dest. | ad 1 l |

**Ca imaging**

Probenecid HCl, Molecular Probes ®, Dallas, TX, USA

Fura-2AM, Molecular Probes ®, Dallas, TX, USA

MnCl2, Carl Roth GmbH, Karlsruhe, Germany

µClear ® plate, Greiner Bio-One GmbH, Frickenhausen, Germany

## 2.2 Antibodies and primers

**Primary antibodies**

| antigenity | clonality | source | concentration | company |
|---|---|---|---|---|
| anti-actin | pc | ms | 1:20000 IB | Sigma Aldrich Chemie GmbH, Germany |
| anti-S100 | mc | ms | 1:1000 ICC, 1:200 IHC | Millipore, Merck AG, Darmstadt, Germany |
| Anx A1 | pc | rb | 1:1000 IHC, 1:2000 IB | Cell Signaling Technology Inc., Cambridge, UK |
| CB1 | pc | rb | 1:200 ICC, 1:500 IB | Frontier Science Co. Ltd., Hokkaido, Japan |
| DAGL a | pc | rb | 1:100 IHC | S. Cruz Biotechnology Inc., Dallas, TX, USA |
| FAAH | pc | rb | 1:200 ICC, 1:500 IB | Cayman Chemical Company, Ann Arbor, MI, USA |
| FAAH | pc | gt | 1:100 IHC | S. Cruz Biotechnology Inc., Dallas, TX, USA |

| | | | | |
|---|---|---|---|---|
| PRL | mc | ms | 1:1000 IB | QED Bioscience Inc., CA, USA |
| PRL | pc | gt | 1:500 IHC, 1:1000 IB | S. Cruz Biotechnology Inc., Dallas, TX, USA |

**Control peptides**

| control peptide | company |
|---|---|
| rAnx A1 hn GST tagged | Abnova |
| CB1 | Frontier Science |
| DAGL a | S. Cruz Biotechnology Inc., Dallas, TX, USA |
| FAAH | Cayman Chemical Company, Ann Arbor, MI, USA |
| FAAH | S. Cruz Biotechnology Inc., Dallas, TX, USA |
| PRL | S. Cruz Biotechnology Inc., Dallas, TX, USA |

**Secondary antibodies**

| antigenity | source | conjugate | concentration | company |
|---|---|---|---|---|
| Gt IgG | rb | biotin | 1:100 ICC | Sigma Aldrich Chemie GmbH, Germany |
| Rb IgG | gt | biotin | 1:100 ICC | Sigma Aldrich Chemie GmbH, Germany |
| Gt-IgG | dk | Alexa Fluor ® 488 | 1:200 IHC | Molecular Probes ®, Dallas, TX, USA |
| Gt-IgG | dk | Alexa Fluor ® 546 | 1:500 IHC | Molecular Probes ®, Dallas, TX, USA |
| Rb-IgG | dk | Alexa Fluor ® 488 | 1:200 IHC | Molecular Probes ®, Dallas, TX, USA |
| Rb-IgG | dk | Alexa Fluor ® 546 | 1:500 IHC | Molecular Probes ®, Dallas, TX, USA |
| Ms-IgG | gt | Alexa Fluor ® 488 | 1:200 IHC | Molecular Probes ®, Dallas, TX, USA |
| Gt IgG | dk | HRP | 1:5000 IB | S. Cruz Biotechnology Inc., Dallas, TX, USA |
| Ms IgG | Gt | HRP | 1:5000 IB | S. Cruz Biotechnology Inc., Dallas, TX, USA |

| | | | | |
|---|---|---|---|---|
| Rb IgG | Gt | HRP | 1:5000 IB | S. Cruz Biotechnology Inc., Dallas, TX, USA |
| Rt IgG | Gt | HRP | 1:5000 IB | S. Cruz Biotechnology Inc., Dallas, TX |

**ISH primers**

| gene | direction | sequence (5'-3') |
|---|---|---|
| ANXA1 | fw | GCC GAG AAG CTG TAC GAA GCC ATG AAG GGT GCC GGA ACT CGC CAT |
| ANXA1 | rv | CGG CTC TTC GAC ATG CTT CGG TAC TTC CCA CGG CCT TGA GCG GTA |
| Fpr-rs1 | fw | GTC CTG CAT CCA GTC TGG GCT CAG AAC CAC CGC ACT GTG AGC CTG |
| Fpr-rs1 | rv | CAG GAC GTA GGT CAG ACC CGA GTC TTG GTG GCGC TGA CAC TCG GAC |
| POMC | fw | CCA GAG CCG AGT CCA CGC GAG GGC AAG CGC TCC TAC TCC ATG GAG |
| POMC | rv | CTC CAT GGA GTA GGA GCG CTT GCC CTC GCG TGG ACT CGG CTC TGG |

**PCR primers**

| gene | direction | sequence (5'-3') |
|---|---|---|
| ANXA1 | fw | GGG AAG ACA AGC AAA TAC AAA GAT |
| ANXA1 | rv | GAT ACA TTG AAG GAA GGG TAG GG |
| FAAH | fw | TAA CTA GGC AGT CTG ACT CTA G |
| FAAH | rv | ACT CAA GGT CAG CCT GAA ACC |
| FAAH | neo | TTT GTC ACG TCC TGC ACG ACG |
| HRPT | fw | GCT GGT GAA AAG GAC CTC T |
| HRPT | rv | CAC AGG ACT AGA ACA CCT GC |
| POMC | fw | GTG CCA GGA CCT CAC CAC |
| POMC | rv | AAC GTT GGG GTA CAC CTT CA |
| PRL | fw | CTC AGG CCA TCT TGG AGA AG |
| PRL | rv | GAA GTG GGG CAG TCA TTG AT |

**q PCR primers**

| gene | direction | sequence (5'-3') |
|---|---|---|
| nNOS (NOS 1) | fw | CTC CCG CCT CGG GCA AAC AG |
| nNOS (NOS 1) | rv | GTG CAC CCC GTT TCC AGC GT |
| eNOS (NOS 3) | fw | CTG CCC TGG CCG AGG AGA CT |
| eNOS (NOS 3) | rv | CAG CAC GTC GAA GCG ACC GT |
| iNOS (NOS 2) | fw | GCT CGC TTT GCC ACG GAC GA |
| iNOS (NOS 2) | rv | AAG GCA GCG GGC ACA TGC AA |
| eEF-α1 | fw | TTG GAG GAA TCT CCC AAC ATG |
| eEF-α1 | rv | AAC GGA CTT GAC TTC AGT AGT C |

## 2.3 Facilities, apparatuses

analytical scale: Mettler P1200, Mettler Toledo, Switzerland

animal cages MH&L, USA

AVT Horn camera system, Horn Imaging GmbH, Aalen, Germany

autoclave: Technoklav 50, Integra Biosciences GmbH, Tecnomara, Fernwald, Germany

bench: Laminar Flow, Heraeus, LaminAir HB 2448, Hanau, Germany

Ca-fura measurement: Perkin Elmer EnVision ®/ 2104 Multilabel Reader, Rodgau, Germany

cell counter chamber: Neubauer improved, Marienfeld, Germany

cell cryopreservation: MrFrosty ® Thermo Fisher Scientific, Darmstadt, Germany; liquid N2 storage vessel

centrifuges: Heraeus, Hanau, Germany, Eppendorf AG, Hamburg, Germany

confocal microscope: FluoView ® FV1200 Laser Scanning Confocal Microscope Olympus (water objectives: UMPlanFl 20x/NA 0.50 W, LUMPlanFl/IR NA 0.90 ∞/0), Japan

cryostat: Leica cryostat, Solms, Germany

developing cassettes: Hypercassette ™, Amersham Life Science, GE Healthcare, Freiburg, Germany

electrophoresis: Mini-PROTEAN ® 3, Bio-Rad PowerPac ™ 300, Bio-Rad PowerPac ™ Universal, blotting Trans-Blot ® Turbo ™ Transfer system, Bio-Rad GmbH, Dreieich, Germany

FACSCalibur ™, Becton, Dickinson and Company, Heidelberg, Germany

fridges, Bosch, Stuttgart, Germany

incubator: HeraCell ™ 150 BS, Heraeus, Hanau, Germany

light microscopes: Zeiss Axioplan, Göttingen, Germany, Leica Axiovert, Solms, Germany

NOA: Sievers Nitric Oxide Analyzer 280i, GE analytical instruments, Manchester, UK

PCR apparatuses: Stratagene MX3005P Agilent Technologies Inc., Santa Clara, CA, USA, MyCycler ™, MyiQ ™ Cycler, Bio-Rad GmbH, Dreieich, Germany

PCR visualization: red ® device ProteinSimple, San Jose, CA, USA

photometer (ELISA, NO): Multiskan RC 351, Labsystems Genesis, Finland

photometer (nucleic acid): NanoDrop 1000 spectrophotometer, PEQLAB Biotechnologie GmbH, Erlangen, Germany

photometer (protein): Bio-Rad SmartSpec ™ Plus spectrophotometer

radiation counter: Contamat FHT 111M, Thermo Fisher Scientific, Darmstadt, Germany

scanner: Epson Perfection ™ V750, Japan

scintillation counter: 2500 TR Packard Tri-Carb ®, San Diego, CA, USA

shaker: Thermomixer ® Comfort, IKA ® table shaker KS 250 basic, Staufen, Germany

soonificator: IKA ® Ultra-Turrax ® T8 homogenizer, Staufen, Germany

water bath: Memmert GmbH & Co KG, Schwabach, Germany

# Results

## 1 Cellular localization of components of the ECS

Our group has proposed that the ECS, as a major regulative system, mediates signals from the PT to the PD of the pituitary gland. According to the hypothesis presented in this work, the presence of the $CB_1$ receptor in the used cell lines was analyzed. Furthermore, the fs TtT/GF and Tpit/F1 cell lines were analyzed for FAAH (EC hydrolyzing enzyme).

### 1.1 $CB_1$ receptor

As stated in the introduction section the $CB_1$ receptor is expressed in the PD of the pituitary gland. More precisely, it has been detected on the fs, C, and on few L cells. Confirmation of these findings has been sought by the means of ICC and IB using the cell models TtT/GF, Tpit/F1, AtT20/D16v, and GH4C1.

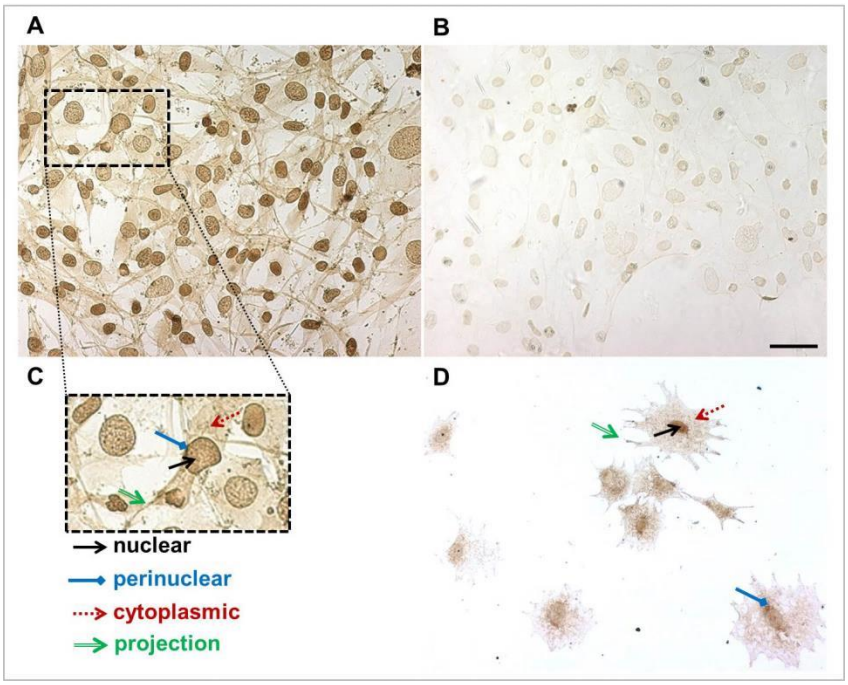


Fig. 33: DAB ICC analysis of $CB_1$ in TtT/GF and Tpit/F1 cells. The staining is positive in (A) TtT/GF cells; (C) enlarged segment of (A). The negative control TtT/GF cells (B) resulted in weaker staining. The Tpit/F1 cells were also positive for $CB_1$ (D). The black solid arrow indicates nuclear staining, the blue solid arrow indicates perinuclear, the red dashed arrow shows cytoplasmic, and the green interrupted arrow points at $CB_1$ staining on the cell processes. (Scale bar 50 µm)

$CB_1$ receptor was detected using DAB ICC not only on the cell membrane, but also in the cell cytoplasm and perinuclear space of fs cells (TtT/GF, Tpit/F1) as shown by the

following images (Fig. 33). These findings were further confirmed by fluorescent ICC (Fig. 35), and IB (Fig. 36). Furthermore, the C AtT20/D16v and L GH4C1 cells appeared positive for the $CB_1$ receptor in the ICC (Fig. 34, Fig. 35) and IB (Fig. 36) analysis.The C AtT20/D16v cells and L $GH_4C_1$ cells also displayed a positive $CB_1$ DAB ICC reaction (Fig. 34).

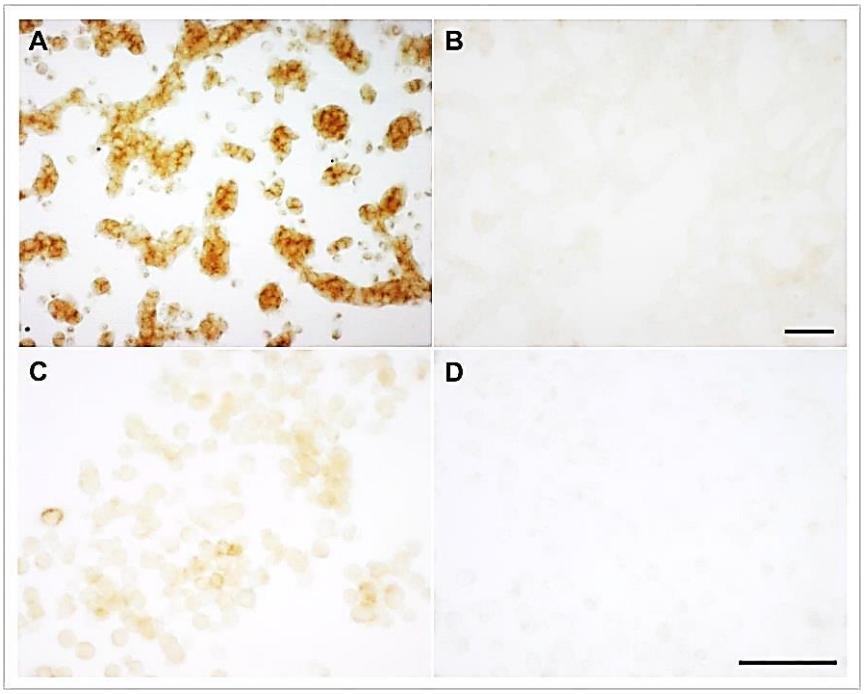


Fig. 34: DAB ICC analysis of $CB_1$ in AtT20/D16v and GH4C1 cells. The images demonstrate (A) perinuclear and cytoplasmic staining of AtT20/D16v cells; (B) AtT20/D16v negative control; (C) cytoplasmic positive $CB_1$ staining in GH4C1 cells; (D) GH4C1 negative control. (Scale bar 50 µm)

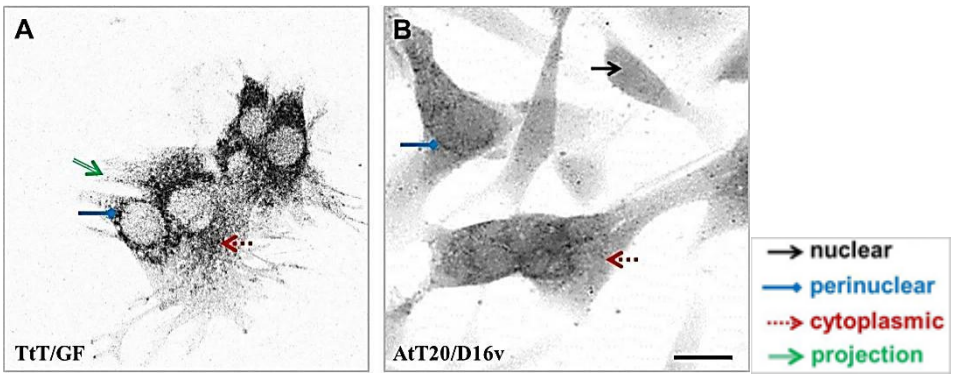


Fig. 35: Fluorescent ICC analysis of $CB_1$ in (A) TtT/GF and (B) AtT20/D16v cells. The green fluorescent signal was inverted into grayscale for better visibility. The black solid arrow indicates nuclear staining, the blue solid arrow – perinuclear, the red dashed arrow – cytoplasmic, and the green interrupted arrow points at $CB_1$ staining on the cell processes. (Scale bar 20 µm)

IB for the $CB_1$ receptor was performed in duplicate on lysates of the cell lines. The analysis revealed $CB_1$ positive bands in all four cell models: TtT/GF, Tpit/F1, GH4C1, and AtT20/D16v.

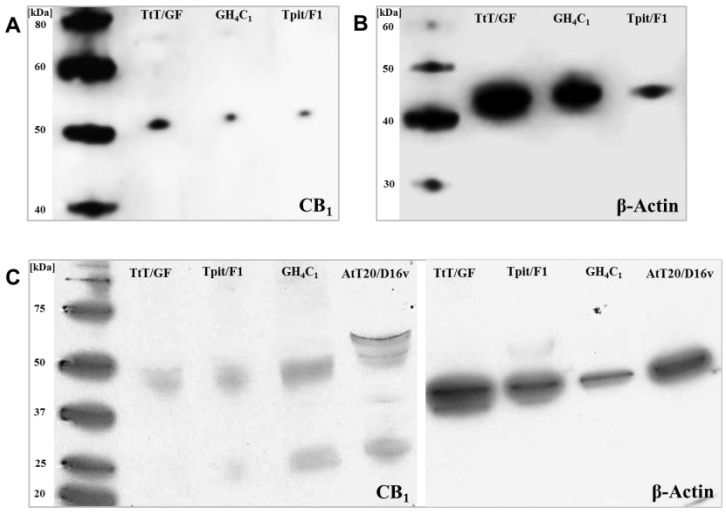


Fig. 36: IB analysis of $CB_1$ (48, 52, (75) kDa) and ß-actin (42 kDa) on TtT/GF, Tpit/F1, GH4C1, and AtT20/D16v cell lysates. (A) Glycosylated $CB_1$ receptor reactivity is seen as a band at 52 kDa in the TtT/GF, GH4C1, and Tpit/F1 cells; (B) a ß-actin control blot of the TtT/GF, GH4C1, and Tpit/F1 cells; (C) A detection of $CB_1$ without glycosylation at 48 kDa in the TtT/GF, Tpit/F1, and GH4C1 cells. The AtT20/D16v cells are positive for the glycosylated variant of $CB_1$ at around 52/ 54 kDa. The control blot for ß-actin on the TtT/GF, Tpit/F1, GH4C1, and AtT20/D16v cell lysates is displayed adjacent on the right side.

## 1.2 FAAH

The fs (TtT/GF, Tpit/F1) cells were analysed for FAAH, an enzyme hydrolyzing EC. Fig. 37 demonstrates images of the PCR analysis of FAAH nucleic acid (performed in duplicate) and Fig. 38 shows images of DAB ICC for FAAH protein in TtT/GF and Tpit/F1 cells.

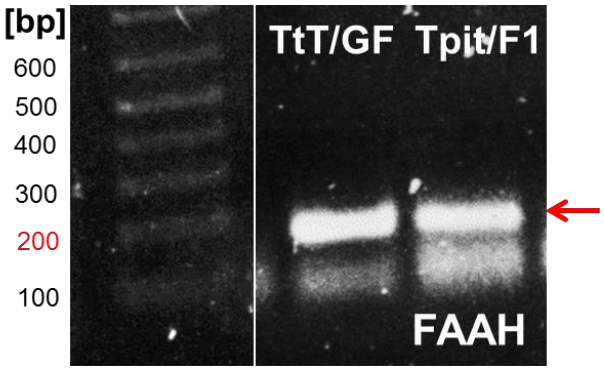


Fig. 37: PCR analysis of FAAH cDNA (200 bp) from TtT/GF and Tpit/F1 cells. The arrow indicates the PCR product for FAAH.

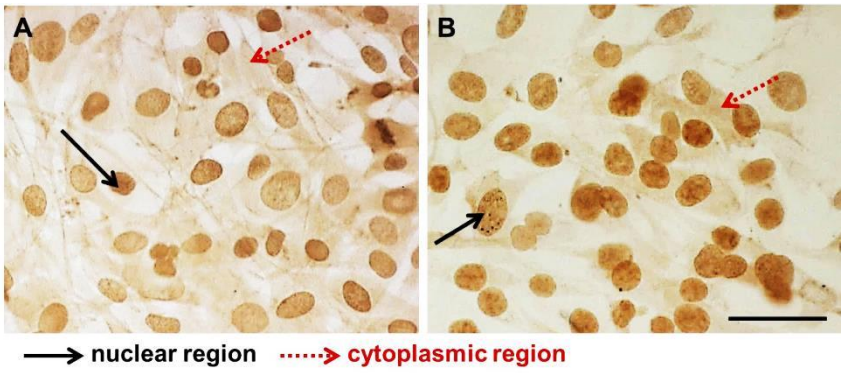


Fig. 38: DAB ICC analysis of FAAH in the fs cells (A) TtT/GF; (B) Tpit/F1. ICC yielded positive FAAH nuclear (black solid arrow) and cytoplasmic (red dashed arrow) staining. (Scale bar 50 µm)

# 2 Detection of Anx A1

Anx A1 has been proposed to act as a messenger molecule from the fs cells to transmit information to hormone producing cells. In this section results of the Anx A1 nucleic acid and protein detection in cell and tissue material are presented.

Anx A1 nucleic acid was detected by PCR analysis of cDNA from the fs cell lines TtT/GF and Tpit/F1 (Fig. 39). Furthermore, mRNA for Anx A1 was detected by the BCIP/NBT ISH method (Fig. 41).The dark violet 5-bromo-4-chloro-3-indolyl phosphate (BCIP) and nitro blue tetrazolium chloride (NBT) product of an alkaline phosphatase reaction was used to detect Anx A1 mRNA. The Anx A1 protein was confirmed by IB of cell extracts (Fig. 40) and fluorescence IHC of murine tissue from areas proximal to and including the PD (Fig. 45) and the PT (Fig. 51).

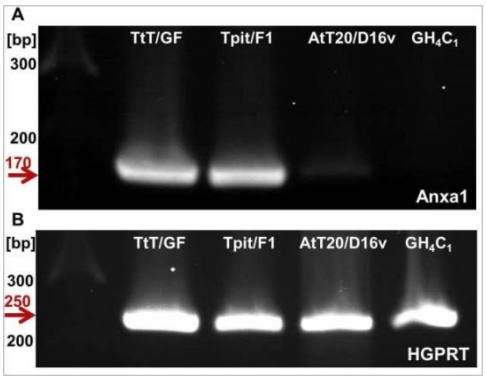


Fig. 39: PCR analysis of (A) Anx A1 cDNA in extracts from TtT/GF, Tpit/F1, AtT20/D16v, and GH4C1 cells with the product visible at 170 bp and for (B) HGPRT as a housekeeping gene with its product visible at 250 bp.

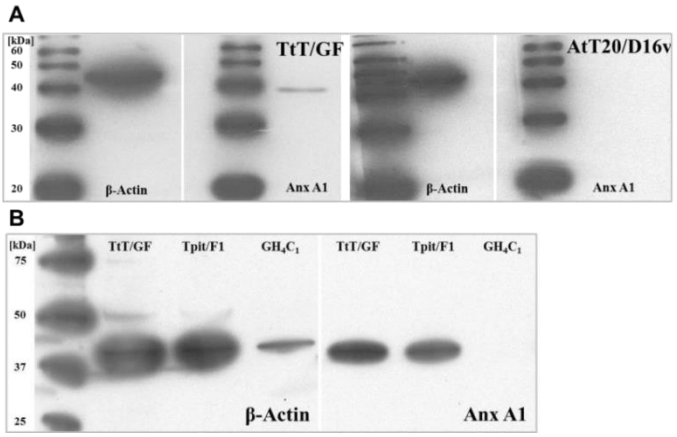


Fig. 40: IB analysis of Anx A1 (37 kDa) and β-actin (42 kDa) in lysates from (A) TtT/GF and AtT20/D16v cells; (B) TtT/GF, Tpit/F1, and GH4C1 cells.

The fs cell lines TtT/GF and Tpit/F1 were confirmed to express Anx A1, whereas the controls – the C AtT20/D16v cells and L GH4C1 cells, yielded negative results.The BCIP/NBT ISH analysis yielded positive reactions in the cell nuclei (black solid arrow), cytoplasm (red dashed arrow) and cell processes (green interrupted arrow) of TtT/GF and Tpit/F1 cells (Fig. 41).

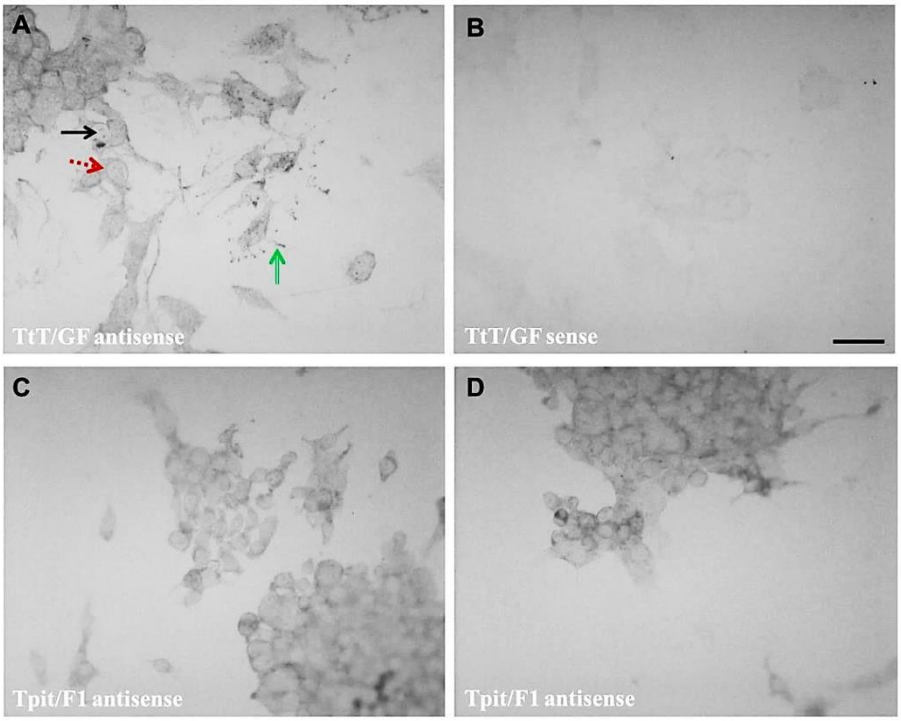


Fig. 41: BCIP/NBT ISH analysis of Anx A1 mRNA in TtT/GF and Tpit/F1 cells. (A) Hybridization of Anx A1 antisense probes on TtT/GF samples yielded dark BCIP/NBT product; (B) Anx A1 sense probes on TtT/GF samples as a negative control; (C, D) hybridization of Anx A1 antisense probes on Tpit/F1 samples. The black solid arrow indicates nuclear staining, the red dashed arrow – cytoplasmic, and the green interrupted arrow points at Anx A1 staining on the cell processes. (Scale bar 50 μm)

The AtT20/D16v cells proved consistently negative for Anx A1 mRNA in the BCIP/NBT ISH analysis (Fig. 42).

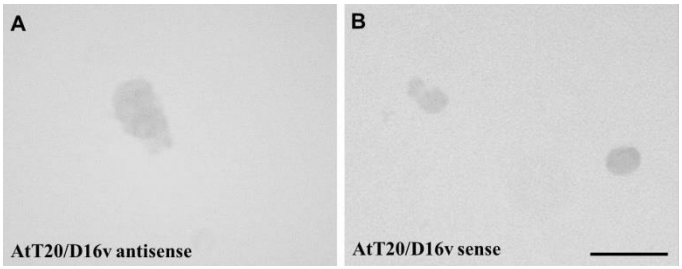


Fig. 42: BCIP/NBT ISH analysis of Anx A1 mRNA in AtT20/D16v cells. (A) Anx A1 antisense probes on AtT20/D16v samples and (B) Anx A1 sense probes on AtT20/D16v samples. (Scale bar 50 µm)

Slices of murine pituitary gland tissue revealed positive detection of Anx A1 mRNA according to the ISH method. Tissue material from mice sacrificed at ZT04 and at ZT16 was used to detect possible fluctuations of Anx A1 mRNA expression according to time. The PD area was positive for Anx A1 mRNA in all tissue slices (Fig. 43; images from ZT16-slices are not shown).

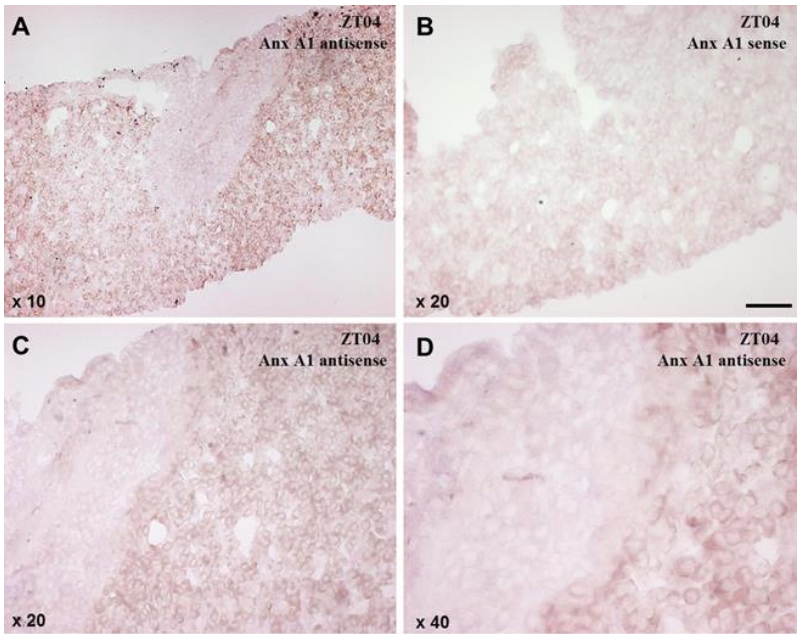


Fig. 43: BCIP/NBT ISH analysis of Anx A1 mRNA in murine tissue slices of PN, PI, and PD. (A) Anx A1 antisense probes on tissue taken at ZT04 with 10 fold magnitude; (B) Anx A1 sense probes on tissue taken at ZT04 as a negative control with 20 fold magnitude; (C) Anx A1 antisense probes on tissue taken at ZT04 with 20 fold magnitude; (D) Anx A1 antisense probes on tissue taken at ZT04 with 40 fold magnitude. (Scale bar 50 µm)

The images were processed with the software tool Image J to determine the intensity of the BCIP/NBT reaction in positive cells (count) for a defined area (pxl^2) and the results were run in a statistical analysis (Student's T-test).The statistical analysis revealed no significant difference in relation to the ZT timepoint (Fig. 44).

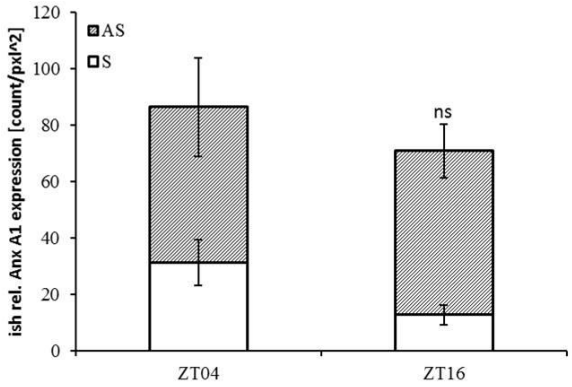


Fig. 44: Analysis of the level of Anx A1 mRNA detected in murine PD. The bars display relative Anx A1 mRNA expression in cells for defined area in the PD. The statistical analysis proved no significance of the comparison between positive cells regions from the PD at ZT04 and corresponding positive cells regions from the PD at ZT16. (The white bars show calculated Anx A1 mRNA intensity after application of the Anx A1 sense probes, hence negative controls. The striped bars show calculated Anx A1 mRNA intensity after application of the Anx A1 antisense probes.)

Fluorescent IHC analysis was performed (in duplicate) on murine pituitary gland. The tissue samples included the PN, PI, and PD regions To localize the Anx A1 protein. To investigate the proximity of the Anx A1-expressing cells to hormone-producing cells, PRL labeling was added. The following drawing represents a map of the used tissue slices (Fig. 45). (I) maps a 10-fold overview image shown in Fig. 46, while (II) corresponds to a 60-fold image of structures in the PD, shown in Fig. 47, and (III) shows a 40-fold image containing structures from the PD shown in Fig. 48. 4',6-diamidino-2-phenylindole (DAPI) was used to visualize the cell nuclei in blue. Anx A1 was labeled red and PRL green. Colocalization is indicated by an arrow.

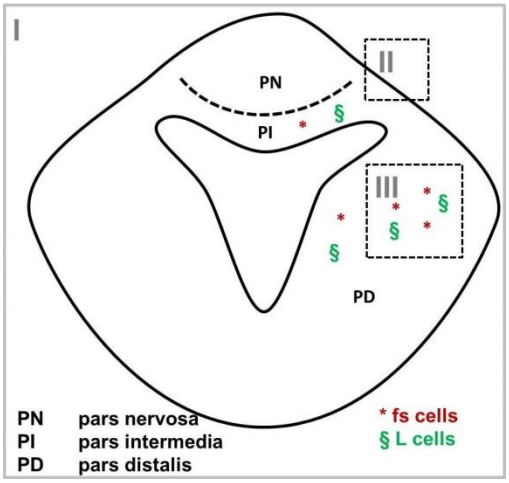


Fig. 45: Overview of the tissue structures and mapping of the performed confocal imaging. (I) 10 fold; (II) 60 fold; (III) 40 fold images.

Fluorescent images from the IHC analysis of Anx A1 and PRL on the pituitary gland slices taken with confocal microscopy are presented in the following figures. Fig. 46 displays imaging corresponding to (I) mapped in Fig. 45. It contains areas from the PN, PI, and PD. The Anx A1 protein was detected prevalently in the PD area, but there were also some Anx A1-positive cells in the PI. The PRL signal was prevalent in the PD area with some PRL-positive cells in the PI as well. Colocalization of Anx A1 and PRL was detected in the PD.

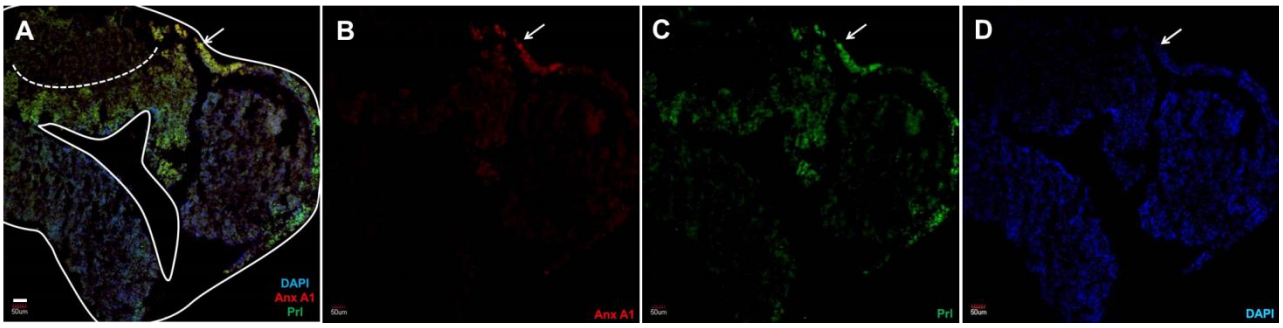


Fig. 46: Fluorescent IHC analysis of Anx A1 and PRL in murine tissue (I). Displayed is a 10-fold image of tissue sample subjected to specific antibodies labeled in red (Anx A1) and green (PRL). DAPI visualizes the cell nuclei in blue. The arrow indicates a colocalization. (A) A combined image with Anx A1, PRL, and DAPI staining; (B) an image showing only the Anx A1 staining; (C) an image showing only the PRL staining; (D) an image showing only the DAPI staining. (Scale bar 50 µm)

Fig. 47 demonstrates imaging corresponding to the (II) region mapped in Fig. 45. It displays the PD area, wheret Anx A1 was particularly prevalent. The distribution of the PRL signal was similar to that of Anx A1 and many cells indicate a colocalization of the two proteins.

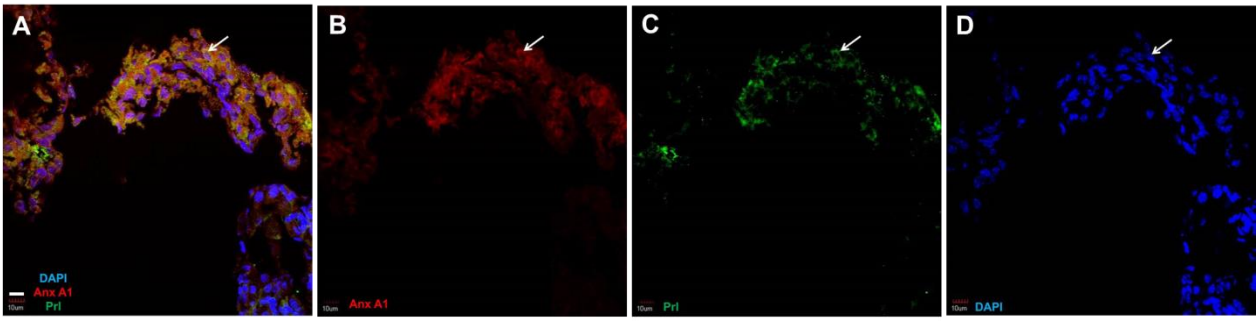


Fig. 47: Fluorescent IHC analysis of Anx A1 and PRL in murine tissue (II). Displayed is a 60-fold image of tissue sample subjected to specific antibodies labeled in red (Anx A1) and green (PRL). DAPI visualizes the cell nuclei in blue. The arrow indicates a colocalization. (A) A combined image with Anx A1, PRL, and DAPI staining; (B) an image showing only the Anx A1 staining; (C) an image showing only the PRL staining; (D) an image showing only the DAPI staining. (Scale bar 10 µm)

Fig. 48 shows imaging corresponding to the (III) region from the PD mapped in Fig. 45. The region contains cell clusters with low colocalization, but high proximity of PRL- and Anx A1-expressing cells.

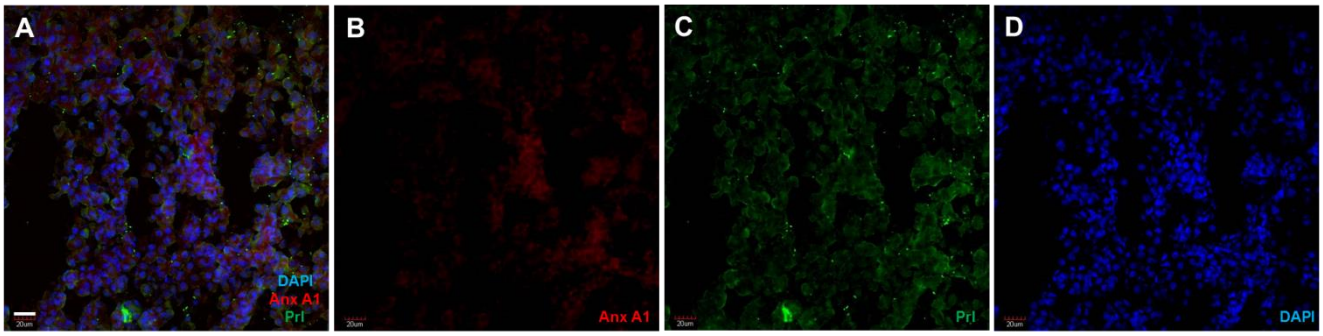


Fig. 48: Fluorescent IHC analysis of Anx A1 and PRL in murine tissue (III). Displayed is a 40-fold image of tissue sample subjected to specific antibodies labeled in red (Anx A1) and green (PRL). DAPI visualizes the cell nuclei in blue. (A) A combined image with Anx A1, PRL, and DAPI staining; (B) an image showing only the Anx A1 staining; (C) an image showing only the PRL staining; (D) an image showing only the DAPI staining. (Scale bar 20 µm)

Further IHC fluorescent imaging of Anx A1 was performed (in duplicate) on coronal slices of murine brain from rostral to distal direction. The structures where Anx A1 was detected, include PT, ME, the cell layer outlining the third ventricle (V3), and parts of the hypothalamus, such as the Arc and the ventromedial and dorsolateral nuclei (VMH, DMH). Anx A1 was labeled in green and DAPI in blue.

The most rostral image is demonstrated in Fig. 49. It shows positive staining for Anx A1 throughout the VMH close to the V3.

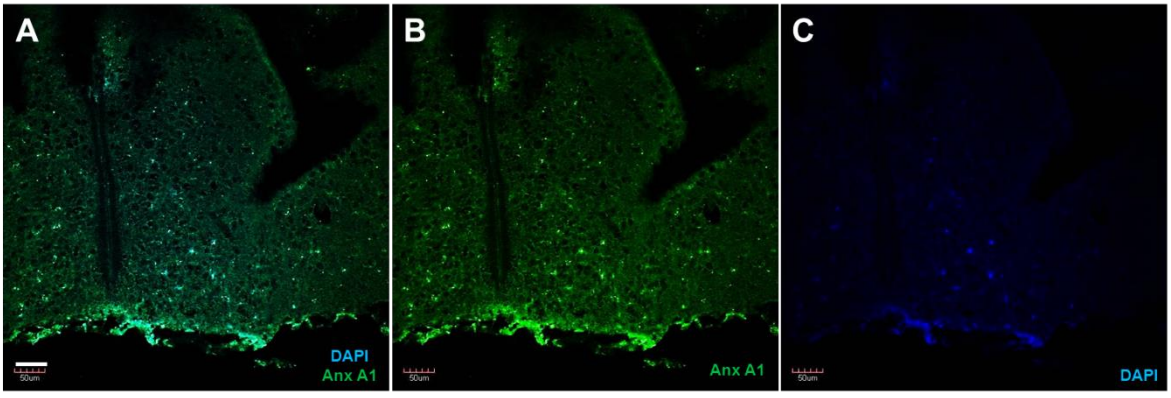


Fig. 49: Fluorescent IHC analysis of Anx A1 in murine tissue. Displayed is a confocal image of a coronal slice of brain samples subjected to specific antibodies raised against Anx A1 and labeled in green. The depicted areas include positive Anx A1 signal in cells in the V3 and in the VMH. (A) A combined image of Anx A1 and DAPI staining; (B) an image showing only the Anx A1 staining; (C) an image showing only the DAPI cell nuclei staining. (Scale bar 100 µm)

Distally located is the next image, displayed in Fig. 50. It shows a positive Anx A1 signal in cells in the periventricular area of the V3 and in cells dispersed in the VMH situated laterally to the V3. Part of the Arc with positive Anx A1 cells is situated adjacent to the bottom ending of the V3. There are Anx A1-positive cells scattered in the PD that is below the section as a detached oval body. Furthermore, there is a strong Anx A1 signal in the periaqueductal gray, displayed as a round body on the upper side of the image.

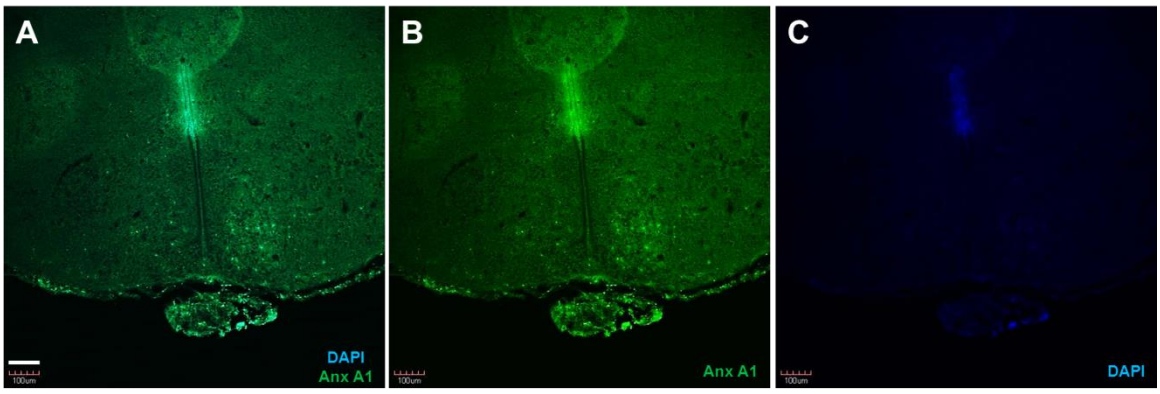


Fig. 50: Fluorescent IHC analysis of Anx A1 in murine tissue. Displayed is a confocal image of a coronal slice of brain samples subjected to specific antibodies raised against Anx A1 and labeled in green. The depicted areas display Anx A1-positive signal in the V3, VMH, Arc, PD, and in the periaqueductal gray. The enlarged region includes a colocalization, indicated by an arrow. (A) A combined image of Anx A1 and DAPI staining; (B) an image showing only the Anx A1 staining; (C) an image showing only the DAPI cell nuclei staining. (Scale bar 50 µm)

The next coronal plane is imaged in Fig. 51. It demonstrates Anx-A1-positive reactivity in cells lying along the V3, in the DMH next to the V3, in the Arc close to the tip of the V3, and in the ME and the PT outlining the vault of the section.

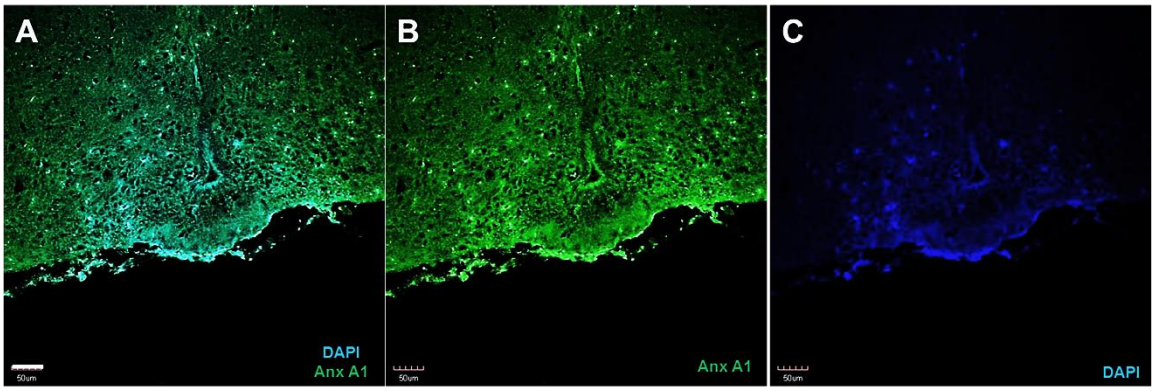


Fig. 51: Fluorescent IHC analysis of Anx A1 in murine tissue. Displayed is a confocal image of a coronal slice of brain samples subjected to specific antibodies raised against Anx A1 and labeled in green. The depicted areas with Anx A1-positive cells include the V3, DMH, Arc, ME, and the PT. The enlarged region includes a colocalization, indicated by an arrow. (A) A combined image of Anx A1 and DAPI staining; (B) an image showing only the Anx A1 staining; (C) an image showing only the DAPI cell nuclei staining. (Scale bar 50 µm)

The most distally lying investigated plane with fluorescent labeling for Anx A1 is displayed in Fig. 52. There are Anx A1-positive cells situated in the posterior part of the periventricular hypothalamic area along the V3, in the Arc, in the ME, and in the PT.

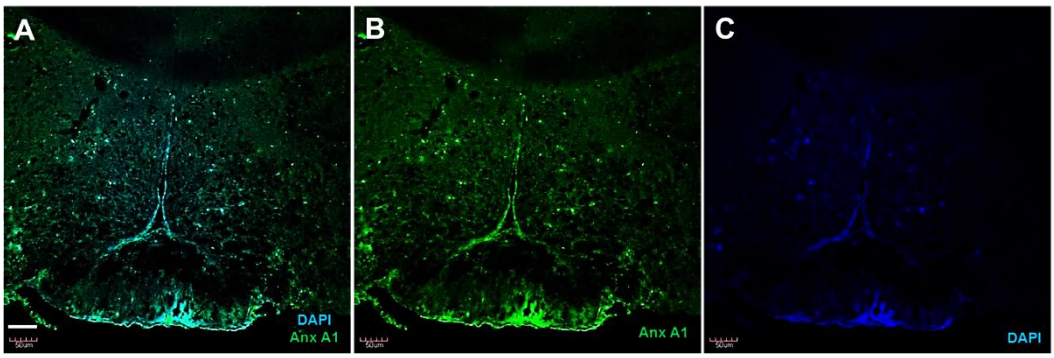


Fig. 52: Fluorescent IHC analysis of Anx A1 in murine tissue. Displayed is a confocal image of a coronal slice of brain samples subjected to specific antibodies raised against Anx A1 and labeled in green. The depicted areas include the V3, Arc, ME, and the PT. The enlarged region includes a colocalization, indicated by an arrow. (A) A combined image of Anx A1 and DAPI staining; (B) an image showing only the Anx A1 staining; (C) an image showing only the DAPI cell nuclei staining. (Scale bar 50 µm)

# 3 Detection of the Anx A1 receptor, Fpr-rs1

As Anx A1 was detected in fs cells and structures connected to fs cells, the next step was to investigate the presence of the Anx A1 receptor, Fpr-rs1. The available cell models and murine tissue samples of the pituitary gland were subjected to a BCIP/NBT ISH analysis with Fpr-rs1 specific DNA-probes. The C AtT20/D16v cells, the L GH4C1 cells, and some regions of the tissue proved positive, whereas the fs Tpit/F1 cells appeared negative for Fpr-rs1 mRNA.

Images from BCIP/NBT ISH analysis with Fpr-rs1 probes on AtT20/D16v and GH4C1 cells are demonstrated in Fig. 53.

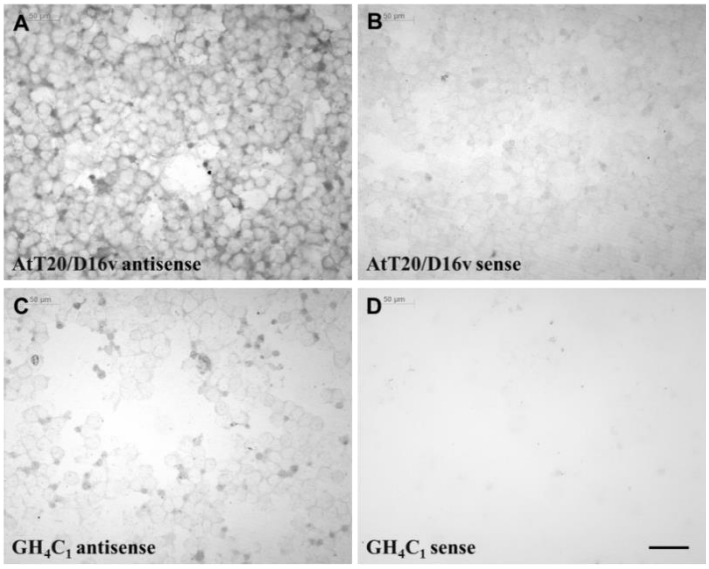


Fig. 53: BCIP/NBT ISH analysis of Fpr-rs1 mRNA in AtT20/D16v and GH4C1 cells. (A) Hybridization of Fpr-rs1 antisense probes in AtT20/D16v samples yielded dark BCIP/NBT product; (B) Fpr-rs1 sense probes in AtT20/D16v samples yielded a weaker reaction and served as a negative control; (C) hybridization of Fpr-rs1 antisense probes in GH4C1 samples yielded dark BCIP/NBT product; (D) Fpr-rs1 sense probes in GH4C1 samples yielded only a weak reaction and served as a negative control. (Scale bar 50 µm)

The Tpit/F1 cells turned negative in the ISH analysis of Fpr-rs1 mRNA. The images from the samples subjected to sense probes were close in their signal intensity to those from samples with no probes, and to those samples with antisense probes (Fig. 54).

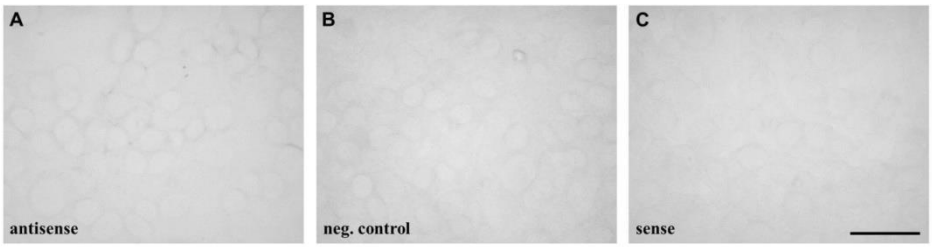


Fig. 54: BCIP/NBT ISH analysis of Fpr-rs1 mRNA in Tpit/F1 cells. (A) Fpr-rs1 antisense probes; (B) no probes used and (C) Fpr-rs1 sense probes. (Scale bar 50 µm)

Slices of murine pituitary gland revealed a positive reaction of Fpr-rs1 mRNA (images from ZT16-slices are not shown; Fig. 55). However, one cannot distinguish a particular Fpr-rs1 distribution pattern. The most intensive Fpr-rs1 reaction was located in the PD area with some positive cells in the PI. The images were processed with the software tool Image J to determine the intensity of the BCIP/NBT reaction in positive cells (count) for a defined area (pxl^2) and the results were run in a statistical analysis (Student's T-test). The statistical analysis revealed a significant difference in relation to the ZT timepoint (Fig. 56).

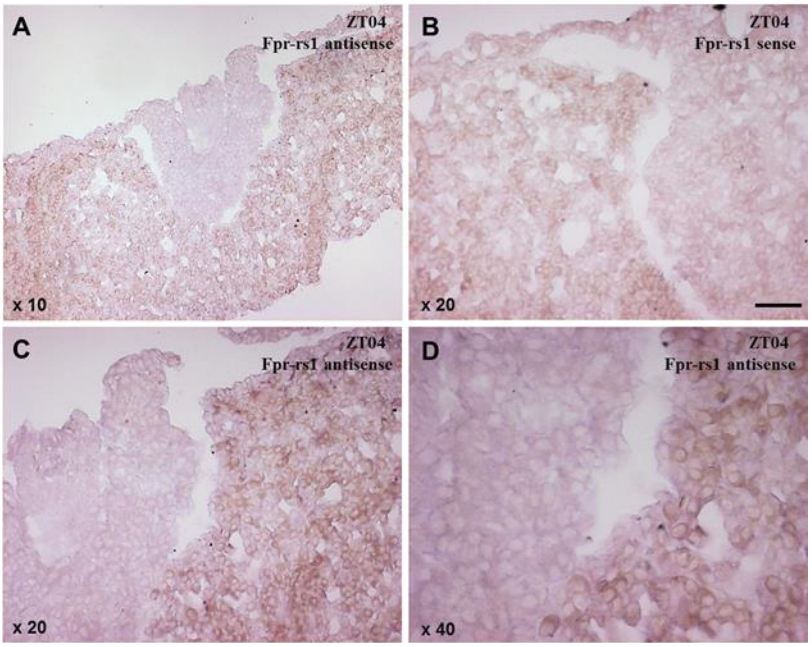


Fig. 55: BCIP/NBT ISH analysis of Fpr-rs1 mRNA in murine tissue slices. (A) Hybridization of Fpr-rs1 antisense probes in tissue taken at ZT04 with 10 fold magnitude; (B) of Fpr-rs1 sense probes in tissue taken at ZT04 as a negative control with 20 fold magnitude; (C) of Fpr-rs1 antisense probes in tissue taken at ZT04 with 20 fold magnitude; (D) of Fpr-rs1 probes in tissue taken at ZT04 with 40 fold magnitude. (Scale bar 50 µm)

The significant dependence on the time point of Fpr-rs1 mRNA expression in murine PD tissue is shown in Fig. 56. The analysis revealed that the Fpr-rs1 mRNA signal was lower at ZT16 (subjective day) as compared to ZT04 (subjective night).

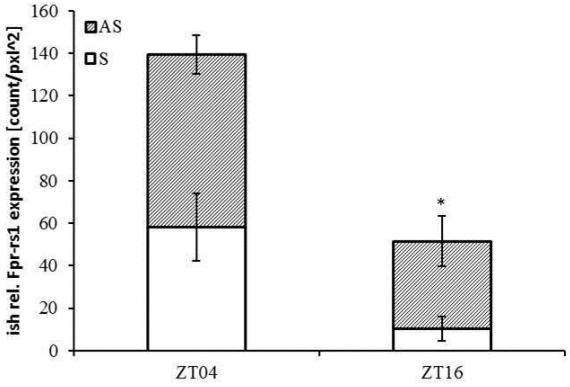


Fig. 56: Analysis of the level of Fpr-rs1 mRNA in murine PD at different time points. The bars display relative Fpr-rs1 mRNA expression in cells for defined area in the PD. The statistical analysis proved a significance of the comparison between positive cells regions from the PD at ZT04 and corresponding positive cells regions from the PD at ZT16. (The white bars show calculated Fpr-rs1 mRNA intensity after application of the Fpr-rs1 sense probes, hence negative controls. The striped bars show calculated Fpr-rs1 mRNA intensity after application of the Fpr-rs1 antisense probes.)

# 4 Analysis of NO

NO, the other proposed messenger was investigated by means of direct (using the fluorofor DAF-2DA) and indirect detection (analyzing NOS or products of NO). Results

obtained from detection of NO products (such as $NO^{-2}$) with the photometric Griess or chemiluminescent method are further presented in section 8.

## 4.1 Direct detection of NO with DAF-2DA

### 4.1.1 The FACS DAF-2DA method

A DAF-2DA coupling method was used to detect NO in AtT20/D16v cells with a FACS apparatus. The cells were divided in two groups. A vehicle was applied to the first one and 10 µM 2-AG to the second one. A statistical t-test analysis of the measured positive events, did not show any significant difference compared to the vehicle group (Fig. 57). However, the scatter plots delivered from the software of the sorting apparatus indicate changes in the cell granulation and cell shape of the cells treated with 2-AG (Fig. 58).

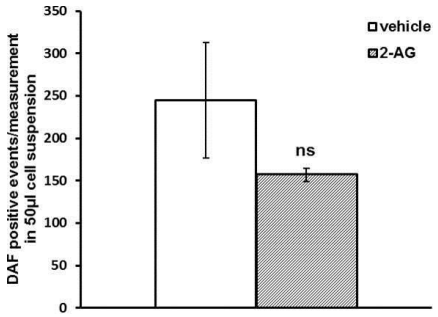


Fig. 57: Analysis of FACS of AtT20/D16v cells treated with 2-AG and DAF-2DA. The bars represent fluorescent DAF-2DA cells counts indicating the presence of NO in the measured AtT20/D16v cells. The white bar corresponds to cells incubated with the vehicle only; striped bar corresponds to the cells treated with 10 µM 2-AG.

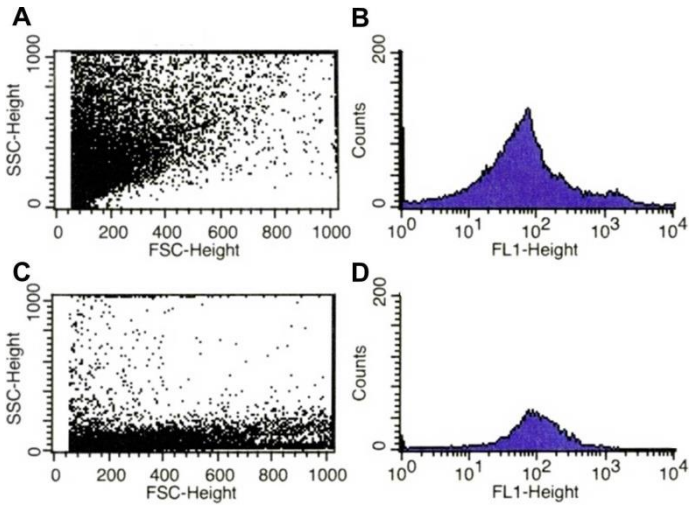


Fig. 58: Scatter plots and histograms of FACS measurements of NO producing AtT20/D16v cells treated with (A)/ (B) vehicle, and with (C)/ (D) 10 µM 2-AG.

The AtT20/D16v cells that reacted to the treatment with 2-AG contained fewer granules and appeared bigger, compared to the cells to which the vehicle was added. (FSC is forward-scattered light signal and is proportional to the size of the cells, while SSC is side-scattered light signal and is a parameter for the granularity of the cells).

### 4.1.2 DAF-2DA imaging

Since the DAF-2DA-NO product is fluorescent, cell and murine pituitary gland samples containing NO, to which the DAF-2DA was added, could be directly observed under a fluorescence microscope. Fig. 59 contains confocal images of the fs TtT/GF, Tpit/F1 cells, and cells of the PDregion. The positive cells are green with the signal for NO that is coupled to DAF-2DA.

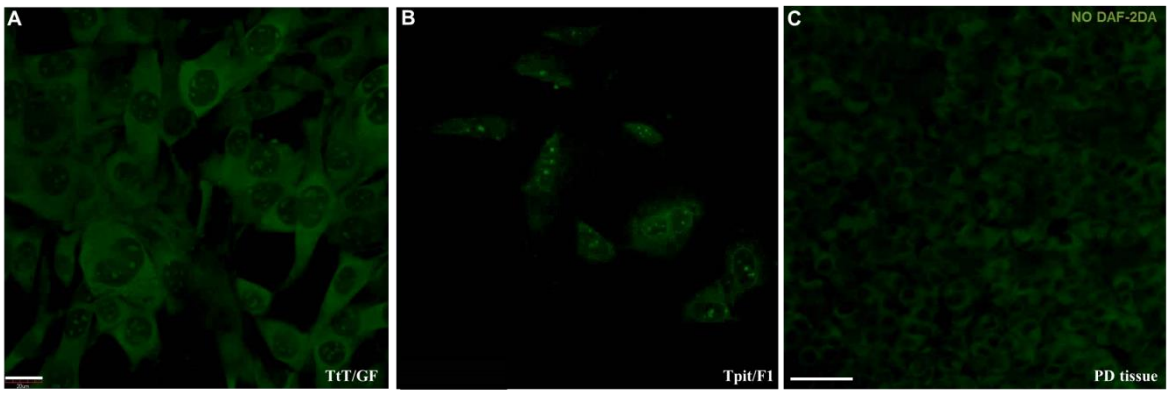


Fig. 59: Confocal imaging of NO in (A) TtT/GF, (B) Tpit/F1 cells, and (C) murine tissue (PD) subjected to DAF-2DA (Scale bar 20 µm)

## 4.2 Indirect detection of NO through NOS

### 4.2.1 qPCR analysis

To investigate the presence of (e), (i), and (n) NOS, in the fs TtT/GF and Tpit/F1 and C AtT20/D16v cells, qPCR analysis was performed. Eukaryotes translocation elongation factor 1-α1 (EF-α1) was used for the control house keeping gene detection. Fig. 60 depicts the quantity of qPCR cDNA products for (e), (i), (n) NOS standardized upon the EF-α1 cDNA product of Huvecs, TtT/GF, Tpit/F1, AtT20/D16v, and murine brain extracts. eNOS expression was highest in the Huvecs and in the AtT20/D16v cell nuclear extract. iNOS expression was highest in the Huvecs and in the brain preparations and nNOS was most expressed in the brain tissue and in the Tpit/F1 cells.

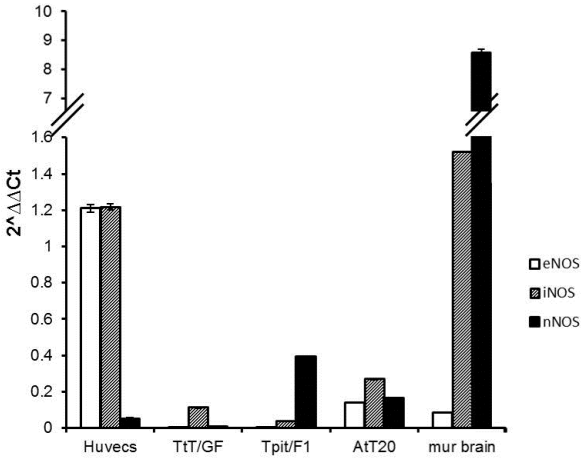


Fig. 60: qPCR analysis of the level of cDNA of the NOS isoforms in extracts from Huvecs, TtT/GF, Tpit/F1, AtT20/D16v cells, and murine brain. The bars represent 2^ddCt values yielded by qPCR analysis of the level of expression of eNOS (white bar), iNOS (striped bar) and nNOS (black bar).

# 5 Detection of POMC, a precursor of ACTH

The AtT20/D16v cells were screened for POMC, a precursor of ACTH, in a PCR analysis of cDNA (Fig. 61). Those results were confirmed by an ISH analysis of POMC mRNA. The ISH POMC analysis was performed using radioactively labeled probes (Fig. 62) and digoxygenin labeled probes (Fig. 63).

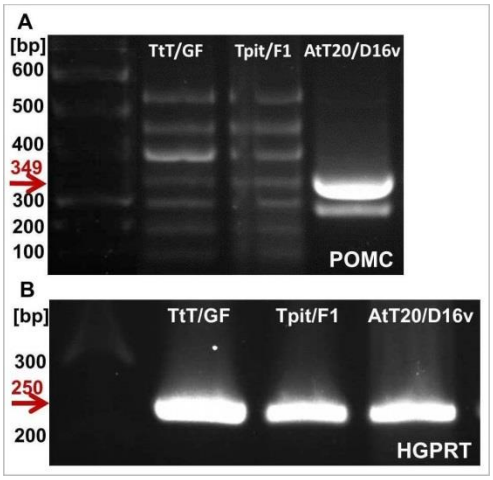


Fig. 61: PCR analysis of POMC and HGPRT cDNA from TtT/GF, Tpit/F1, and AtT20/D16v cells. The POMC product is visible at 349 bp and the HGPRT product at 250 bp.

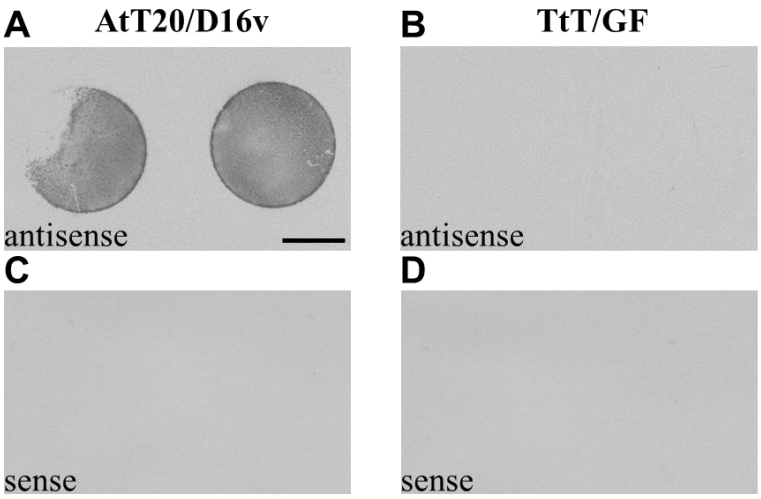


Fig. 62: Radioactive ISH analysis of POMC mRNA in AtT20/D16v and TtT/GF cells. (A) POMC antisense probes hybridization on coverslips with AtT20/D16v cells; (B) POMC antisense probes on coverslips with TtT/GF cells as a negative control; (C) POMC sense probes on coverslips with AtT20/D16v cells as a negative control; (D) POMC sense probes on coverslips with TtT/GF cells as a negative control. (Scale bar 60 µm)

The BCIP/NBT ISH analysis for POMC mRNA in AtT20/D16v cells (Fig. 63) confirmed the results obtained by the radioactive ISH method.

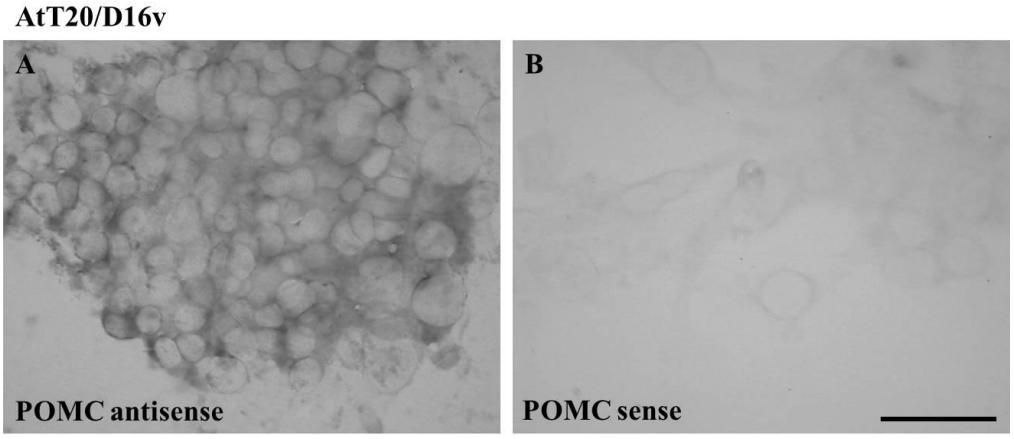


Fig. 63: BCIP/NBT ISH analysis of POMC mRNA in AtT20/D16v cells. (A) POMC antisense probes hybridization; (B) POMC sense probes as a negative control. (Scale bar 50 µm)

# 6 Detection of PRL

The GH4C1 cells were screened for PRL nucleic acid as shown in the following image from PCR cDNA analysis (Fig. 64). Furthermore, the PRL protein was confirmingly detected in IB analyses of cell extracts (Fig. 65) and IHC analyses of murine pituitary gland tissue.

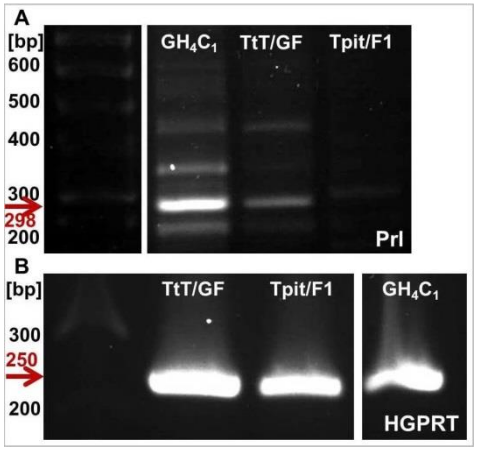


Fig. 64: PCR analysis of PRL and HGPRT cDNA from GH4C1, TtT/GF, and Tpit/F1 cells. PRL product is visible at 298 bp and the HGPRT product at 250 bp.

The PRL protein was specifically detected in the lysates from GH4C1 cells by means of IB technique, using two different specific antibodies. (The IB analyses were performed each in unicate, using an antibody from QED and from S. Cruz). Cell extracts from TtT/GF and AtT20/D16v were used as negative controls (Fig. 65).

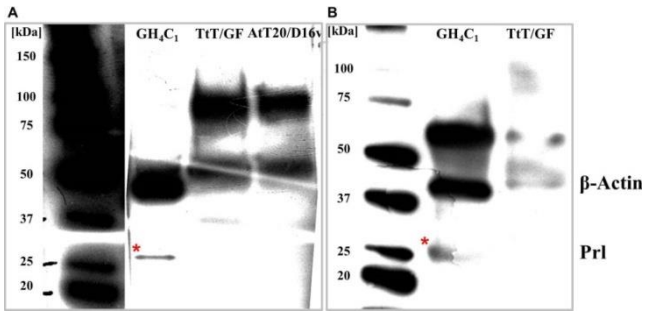


Fig. 65: IB analysis of PRL (27 kDa), marked with an asterisk*, and ß-actin (42 kDa) in lysates from (A) GH4C1, TtT/GF, and AtT20/D16v cells (S.Cruz Ab); (B) GH4C1 and TtT/GF cells (QED Ab).

# 7 Analysis of the influence of the cannabinoids on Anx A1 production in fs cells

After confirmation of the expression of $CB_1$ and that of Anx A1in the fs cells, the next step of the work comprised investigation of the influence cannabinoids have on Anx A1 protein levels. 2-AG, AEA, WIN, and otenabant were used as chemical agents to treat the cell cultures. 2-AG and AEA represented the physiologically native and faster inactivatable $CB_1$ agonists, whereas WIN was applied as a more stable, synthetic $CB_1$ agonist. Otenabant was added to investigate the potential role $CB_1$ antagonism might have on Anx A1 protein levels.

## 7.1 Influence of the endogenous agonists 2-AG and AEA

Incubations with increasing 2-AG concentration of both fs cell lines TtT/GF and Tpit/F1 revealed dose dependent significant increase in the level of the produced Anx A1 (Fig. 66).

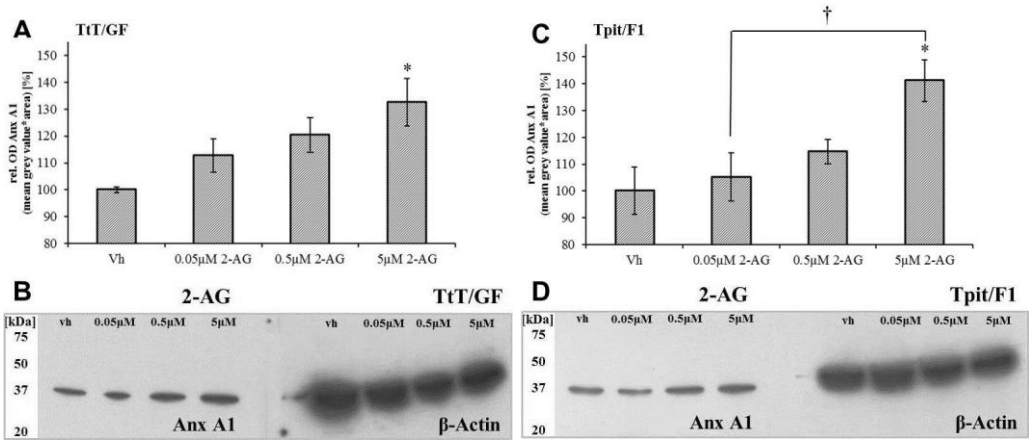


Fig. 66: Relative optic density diagrams of an IB analysis of Anx A1 in lysates of TtT/GF and Tpit/F1 cells treated with 2-AG. (A) Diagram for Anx A1 in the TtT/GF cells; (B) IB of TtT/GF cells; (C) diagram for Anx A1 in the Tpit/F1 cells; (D) IB of Tpit/F1 cells (Anx A1 (37 kDa) and ß-actin (42 kDa)).

Incubations performed with increasing AEA concentration of the TtT/GF and Tpit/F1 cells yielded a trend of an increase in the level of Anx A1 (Fig. 67).

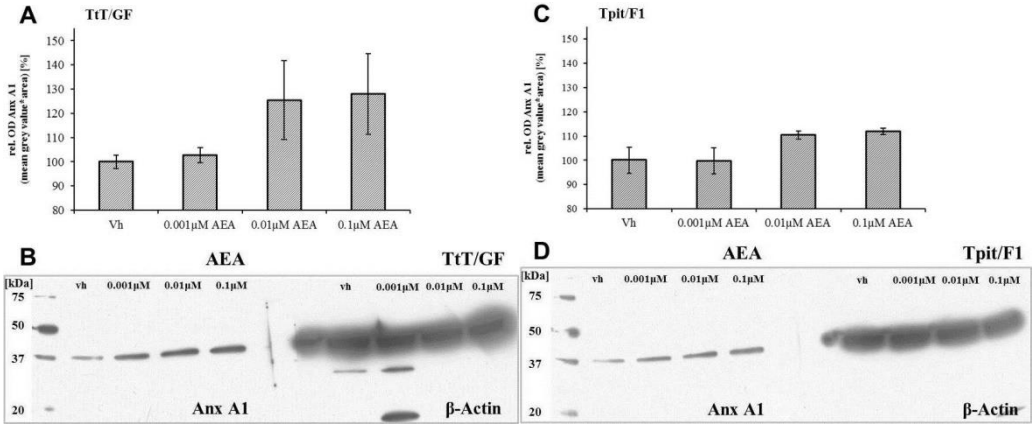


Fig. 67: Relative optic density diagrams of an IB analysis of Anx A1 in lysates of TtT/GF and Tpit/F1 cells treated with AEA. (A) Diagram for Anx A1 in the TtT/GF cells; (B) IB of TtT/GF cells; (C) diagram for Anx A1 in the Tpit/F1 cells; (D) IB of Tpit/F1 cells (Anx A1 (37 kDa) and ß-actin (42 kDa)).

### Distribution Anx A1 in the fs cell

The Anx A1 protein was detected not only in the cell cytoplasm and cell processes (ISH analysis), but also on the cell surface. IB analysis was performed of membranous Anx

A1 protein collected using the Tierney EDTA wash up method from TtT/GF and Tpit/F1 cells treated with EC. The resulting blots in Fig. 68, demonstrated an additional Anx A1 protein band at 33 kDa. However, one of the pitfalls of analyzing membranous Anx A1 protein samples with IB, was the sensitivity range of the method. The samples were subjected to vacuum centrifugation until at least 40 µg of protein were available for performing the IB analysis.

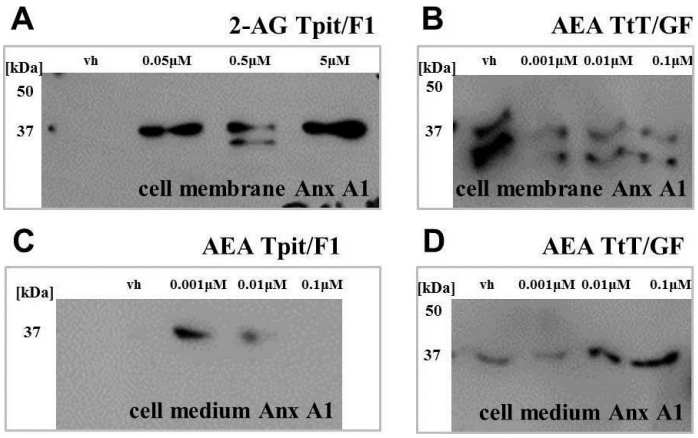


Fig. 68: IB analysis of Anx A1 from the cell surface of (A) Tpit/F1 cells treated with 2-AG; (B) TtT/GF cells treated with AEA, and excreted into the cell medium of (C) Tpit/F1 cells treated with AEA and (D) TtT/GF cells.

## 7.2 Influence of the exogenous agonist WIN and antagonist otenabant

The TtT/GF cells were also treated with the exogenous cannabinoid agonist WIN and the antagonist otenabant to confirm that the Anx A1 stimulating action of the EC involves the $CB_1$ receptor. Cell lysates were collected and subjected to IB (Fig. 69) and ELISA (Fig. 70) analyses. A significant increase in Anx A1 levels was detected after incubation with WIN while the antagonist otenabant caused no significant difference from the basal levels of the Anx A1 protein.

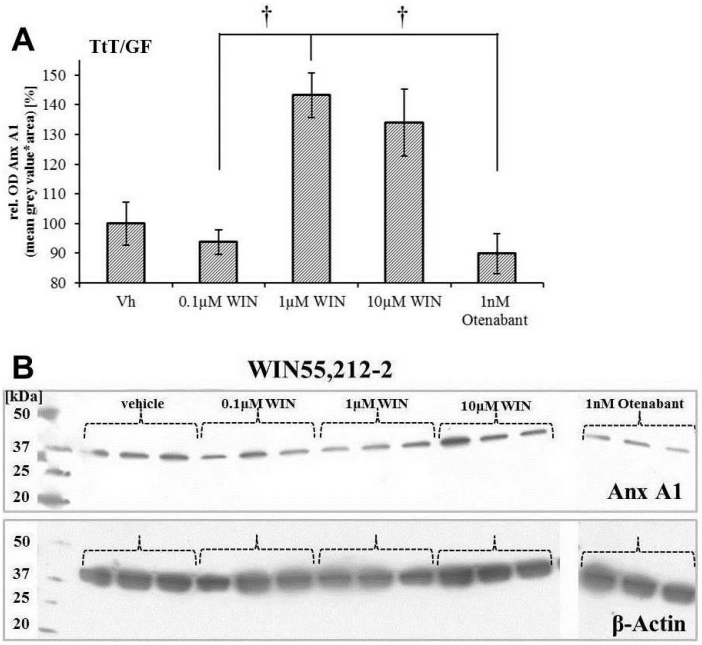


Fig. 69: Relative optic density diagrams of an IB analysis of Anx A1 in lysates of TtT/GF cells treated with WIN and otenabant. (A) Diagram of Anx A1 in TtT/GF cells; (B) IB of TtT/GF cells with Anx A1 (37 kDa) and ß-actin (42 kDa).

TtT/GF cell media samples were further analyzed by means of ELISA being a more sensitive method compared to IB (Fig. 70). The samples were analyzed untreated which represents the advantage of this technique for low protein measurements. The analysis revealed significantly increasing Anx A1 protein levels along increasing concentration of WIN and thus confirmed the IB data.

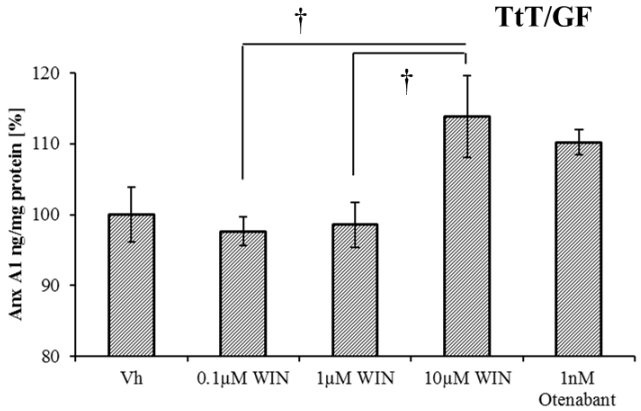


Fig. 70: ELISA analysis of Anx A1 in the cell media of TtT/GF cells treated with WIN and otenabant.

# 8 Analysis of the influence of cannabinoids on NO production

NO, as proposed messenger produced from the fs cells, was analyzed by means of chemiluminescent and photometrical (Griess) method. The validation of the used techniques is described in the Methods section.

## 8.1 Influence of the endogenous agonist AEA

Incubations with increasing AEA concentration strongly and significantly decreased the levels of produced and released NO in the cell medium of TtT/GF cells. This effect was absent in the case of the Tpit/F1 cell line.

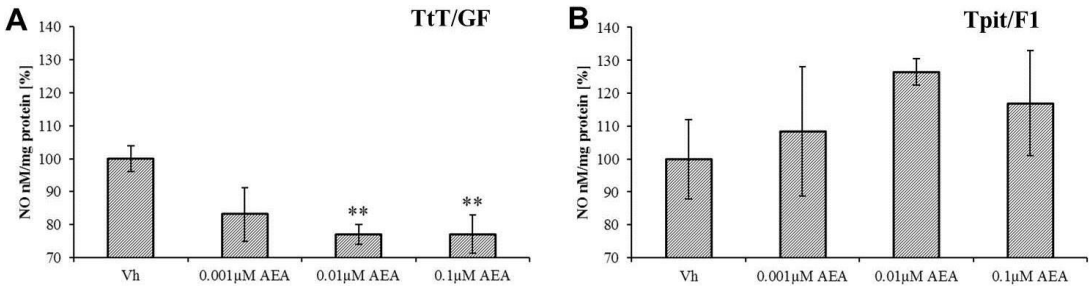


Fig. 71: Chemiluminescent analysis of NO produced from (A) TtT/GF and (B) Tpit/F1 cells treated with AEA.

## 8.2 Influence of the exogenous agonist WIN and antagonist otenabant

Incubations with increasing concentration of the exogenous $CB_1$ receptor agonist WIN and the antagonist otenabant were performed on TtT/GF cells. WIN decreased expectedly the NO levels in the cell medium of TtT/GF cells while otenabant did not cause an effect as compared to the vehicle.

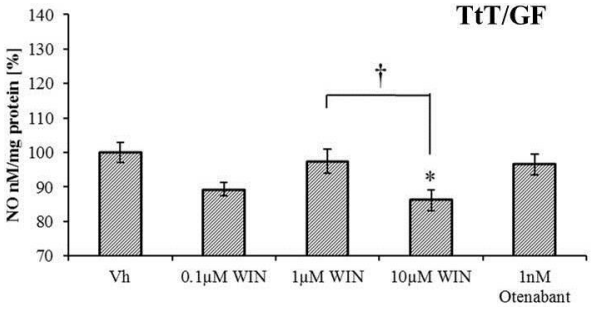


Fig. 72: Griess analysis of NO produced from TtT/GF cells treated with WIN and otenabant.

## 8.3 Influence of NOS activators or inhibitors

To underline that the observed changes in NO resulted from NOS dependent mechanisms, studies with NOS activators and inhibitors were performed on the TtT/GF cell line. Ionomycin and LPS (from E. coli) were applied as activators; L-NAME and curcumin as inhibitors. The collected cell media were processed in analysis of NO and the cell lysates were subjected to IB analysis of Anx A1 protein levels.

### 8.3.1 On the NO production

Chemiluminescent measurements of NO after incubation with ionomycin, LPS, L-NAME, and curcumin of TtT/GF cells demonstrated a significant decrease of NO after treatment with L-NAME.

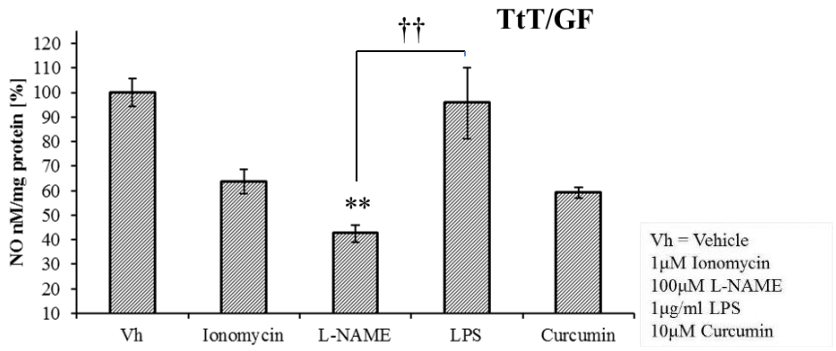


Fig. 73: Chemiluminescent analysis of NO produced from TtT/GF cells treated with NOS activators ionomycin, LPS and NOS inhibitors L-NAME and curcumin.

### 8.3.2 On the Anx A1 production

Cell lysates from TtT/GF cells analyzed in IB, revealed double bands for the Anx A1 protein at 33 kDa and at 37 kDa, after the cells were treated with NOS inhibitors (L-NAME, curcumin).


Fig. 74: IB analysis of isoforms of Anx A1 in lysates of TtT/GF cells treated with NOS activators ionomycin, LPS and NOS inhibitors L-Name and curcumin. The asterisk* emphasizes the double bands.

## 8.4 Influence of the EC on the $[Ca^{2+}]_i$ in fs cells

An investigation of the $[Ca2^{+}]_i$ after activation of $CB_1$ provided indication about the CB receptor and the signaling cascades. Treatments of TtT/GF cells with 1 µM 2-AG (A) led to delayed $[Ca^{2+}]_i$ increase, but not when subjected to 2 µM 2-AG. AEA did not trigger any change in $[Ca^{2+}]_i$ (B). The Tpit/F1 cells demonstrated $[Ca^{2+}]_i$ sensitivity at 1 µM 2-AG (C).

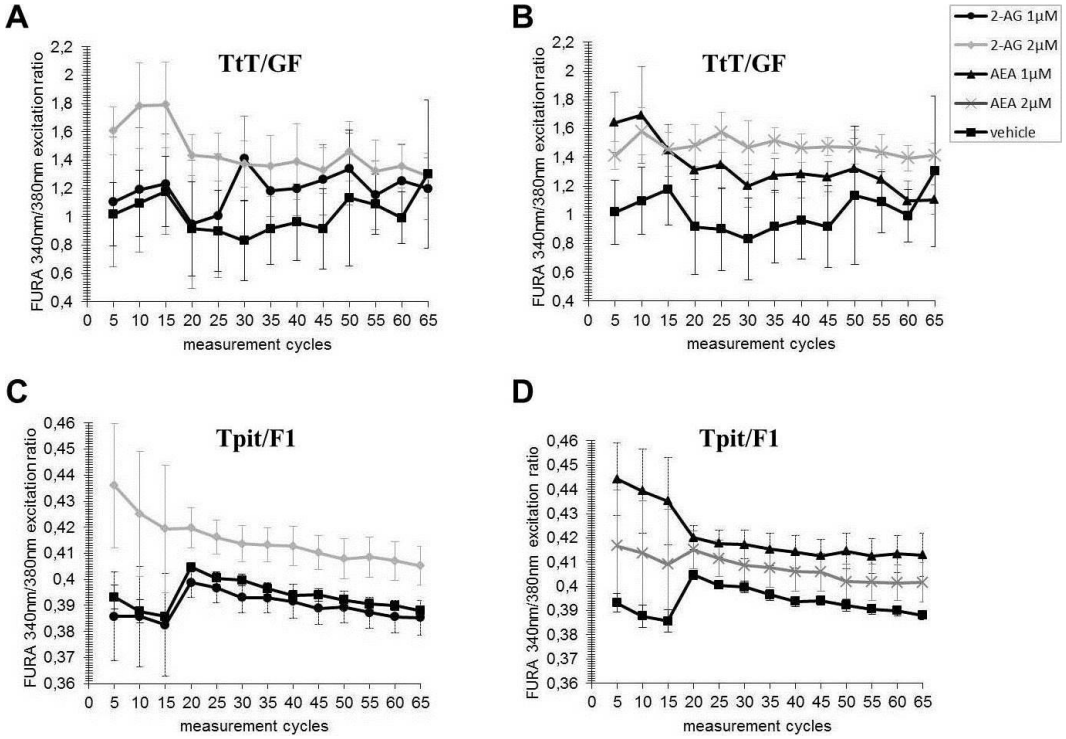


Fig. 75: $Ca^{2+}$-fura analysis of (A) TtT/GF cells treated with 2-AG; (B) TtT/GF treated with AEA; (C) Tpit/F1 treated with 2-AG; (D) Tpit/F1 treated with AEA.

# 9 Analysis of the influence of EC, Anx A1 and NO on the ACTH production and secretion in AtT20/D16v cells

ACTH production and release were investigated using an ELISA method. The cell media and lysates from AtT20/D16v cells subjected to Anx A1, 2-AG, and NO were collected and measured untreated.

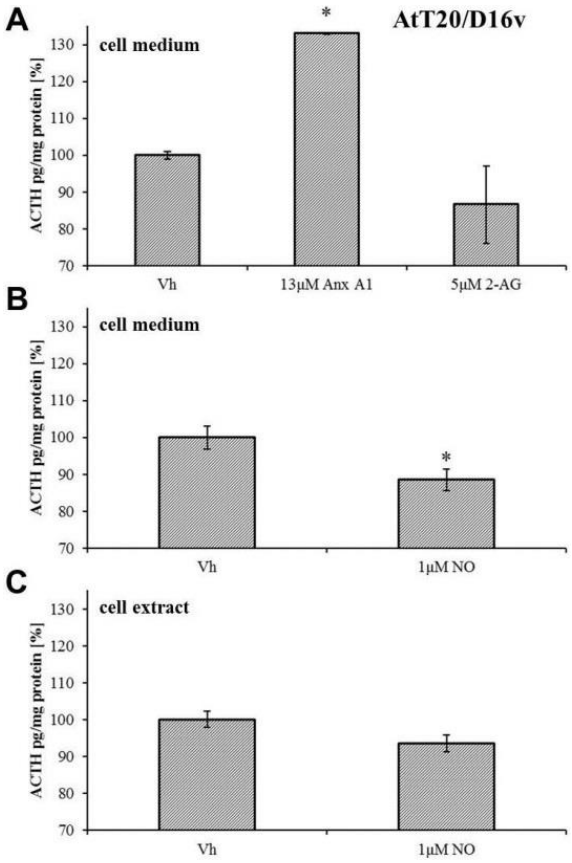


Fig. 76: ELISA analysis of ACTH from AtT20/D16v cells treated with (A) Anx A1 and 2-AG; (B) and (C) NO.

The calculated results presented in charts in Fig. 76 demonstrate that released ACTH in the cell medium was significantly increased when the C cells were incubated with Anx A1 (A). 2-AG supplementation caused great variations, but tended to act diminishing on the resulting ACTH (A). NO acted decreasing on the ACTH release into the cell medium (B) and intracellular ACTH levels did not differ from the untreated cells (C).

# 10 Analysis of the influence of the EC, Anx A1, and NO on the PRL production and secretion in GH4C1 cells

PRL production and release were analyzed by means of ELISA. Anx A1, 2-AG, and NO were added to GH4C1 cell cultures. The cell media and lysates were collected and measured untreated.

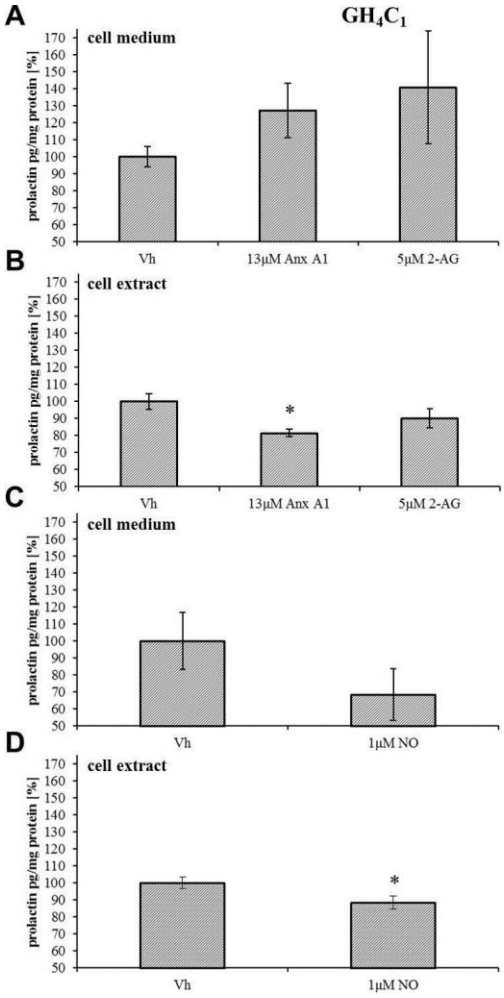


Fig. 77: ELISA analysis of PRL from GH4C1 cells treated with (A) and (B) Anx A1 and 2-AG, (C) and (D) NO.

The calculated results presented in charts in Fig. 77 demonstrate that released PRL levels were increased when the L cells were incubated with Anx A1 (A). 2-AG supplementation caused great variations, but tended to act stimulating on the released PRL (A). Anx A1 significantly decreased the PRL levels in the cell (B). NO caused a decrease on the PRL release into the cell medium (C) and intracellular PRL levels were lower than those in the untreated cells (D).

# Discussion

The aim of this study was to investigate the influence of EC on fs, C, and L cells. With the assumed existence of an intricate intercellular regulative mechanism involving the Anx A1 protein and the anorganic molecule NO as messengers the focus fell on their impact on ACTH and PRL release.

### Brief overview results

Even though the ICC and IB analysis demonstrated that the fs cells TtT/GF and Tpit/F1, the C cell line AtT20/D16v and the L cell line GH4C1 express $CB_1$, direct treatment of the endocrine cell lines with 2-AG did not yield significant change in the ACTH and PRL protein levels. An interesting finding, however, is the fact that 2-AG in the concentrations used for incubating the hormonal cells, produced a significant increase in Anx A1 protein levels in both fs cell lines – the TtT/GF and the Tpit/F1. Furthermore, Anx A1 stimulated ACTH release in the cell medium of AtT20/D16v cells. Anx A1 inhibited PRL in the cell (lysates)**,** but had a stimulatory effect in the cell medium from GH4C1 cells. NO concentration was inhibited by AEA and WIN in the TtT/GF cells, whereas otenabant caused as expected no change from the basal level. NO acted inhibitory on both ACTH and PRL protein levels. Another interesting finding is the detection of the EC degrading enzyme FAAH in the fs TtT/GF and Tpit/F1 cells with PCR and ICC analysis confirming the involvement of the fs cells in EC regulation.

### Ambiguity $CB_1$ receptor

Since $CB_1$ receptors were present on the endocrine cells, we hypothesized that EC could directly regulate hormonal production. The proposed mechanism was an inhibition through the adenylate cyclase (AC), which would generate cAMP and alterate the ion channel activities. Nevertheless, the pharmacology of the CB1 receptor is further confounded by the existence of various heterodimer forms ($A_{2A}CB_1$, $A_{2A}$, or $CB_1D_2$), receptor desensibilization, and internalization (reviewed by Pertwee, 2005; 2006). The phenomena of dimerization and desensibilization could provide an explanation for the controversial antagonistic effects of $CB_1$ agonists and the unexpected stimulatory effect of EC on Anx A1 production or the missing significance of the effect of EC on ACTH and PRL levels. The occurance of un/glycosylated CB1 isoforms as stated by Shire et al. (1995), Song and Howlett, (1995), and De Jesús et al. (2006), was confirmed by the

performed IB analysis. The bands at 45/ 48 kDa were due to unglycosylated $CB_1$ reactivity, while the bands at 52/ 54 kDa represented the glycosylated $CB_1$ receptor protein.

**$CB_1$ affecting HPA**

The appetite-stimulating effect of marihuana in humans has been well known for centuries (Abel, 1975). Furthermore, administration of cannabinoids stimulates food intake in animal models (Williams et al., 1998; Koch, 2001). On the basis of the observation that $CB_1$ and EC are present in the brain regions controlling food intake (Howlett et al., 2002), the ECS has been proposed as a putative modulator of feeding behavior (Mechoulam and Fride, 2001; Cota et al., 2003a).

It has been suggested that cannabinoids interact with CRH that controls energy metabolism, because $CB_1$ and CRH receptor 1 (CRHR1) are expressed to a high extent in the same brain regions such as hippocampus, cortex, and cerebellum (Raber et al., 1997; Gardner et al., 1998; Huang et al., 1998). Corchero et al. reported an enhancement of CRH expression in the hypothalamus and the anterior pituitary lobe after chronic exposure to cannabinoids (Corchero et al., 1999a; 1999b). The effects of hypothalamic EC on energy balance might partially be mediated by CRH (Cota et al., 2003b). It has been further found that exogenous (Δ9-THC and WIN) and endogenous ligands (AEA) increase the release of ACTH in the pituitary gland via secretion of CRH that was mediated by $CB_1$ (Weidenfeld et al., 1994; Pagotto et al., 2001). In this regard, my findings that EC induce Anx A1 and Anx A1 induces ACTH support the reported EC-mediated stimulatory effect on ACTH.

**$CB_1$ affecting PRL**

On one side, Ho et al. (2000) demonstrated with experiments involving WIN and rimonabant ($CB_1$ antagonists) that PRL release from GH4C1 is inhibited in a $CB_1$-mediated manner (Ho et al., 2000). Furthermore, EC (AEA, 2-AG) inhibited PRL secretion in rodents (rats - Scorticati et al., 2003), (mice - Murphy et al., 1998; Oláh et al., 2008). Those reports contradict my findings, according to which the EC 2-AG had a stimulatory, non-significant effect on PRL.

On the other side, Kolesnick et al. (1984) demonstrated that AA stimulates PRL release from GH3 cells. Furthermore, Bjøro et al. showed in 2009 that inhibitors of AA

attenuate the thyroliberin (TRH) stimulated PRL production without modifying the production of inositolphosphates in GH4C1 cells. Our group reported findings about high level of plasma PRL, associated with high level of 2-AG in the PT of hamsters kept under long day conditions, mimicking summer (Yasuo and Korf, 2011).

These contradictory effects include the dopaminergic turnover. There is inhibitory, dopaminergic control of PRL release by the anterior pituitary gland. The work of Scorticati et al. (2003) might shed some light on the process involved. They used male, ovariectomized, and ovariectomized, estrogen-substituted rats. AEA decreased plasma PRL in the first, showed little effect in the second, and increased PRL in the last group. Furthermore, the elevated PRL release and the response to AEA were blocked by the $CB_1$ antagonist AM 251 in the last group, indicating that AEA decreases the inhibitory control of PRL release. DA turnover has been increased in the male rats and decreased significantly in ovariectomized, and estrogen-primed rats.

**$CB_1$ affecting Anx A1 and NO**

The novel results in this work are that EC influence Anx A1 and NO through action on the $CB_1$ receptor. Anx A1 is known to be regulated by GC (Flower and Blackwell, 1979; Hirata et al., 1980; Russo-Marie and Duval, 1982). Anx A1 protein levels increase and NO levels decrease after incubation with synthetic and natural CB1 ligands. 2-AG caused a significant increase of Anx A1 in both TtT/GF and Tpit/F1 cells, while AEA had a stimulatory tendency upon Anx A1 in both fs cell lines. WIN, a potent synthetic $CB_1$ agonist and otenabant, a highly selective $CB_1$ antagonist led in TtT/GF to significant results on Anx A1 and NO levels, consistent with the expectations. AEA significantly decreased NO measured in the TtT/GF cell line.

That the ECS is involved in regulating Anx A1 is a novel notion, supported by the fact that Anx A1 is expressed in hypothalamic and pituitary areas where also $CB_1$ receptor has been detected (Woods et al., 1990; Weidenfeld et al., 1994).

The original assumption was that $CB_1$ receptor agonists act inhibitory via the Gi α subunit on Anx A1 production and release. Following this thought, $CB_1$ receptor agonists should yield a decrease in the level of Anx A1 protein. However, 2-AG had a significant stimulatory effect on Anx A1 in TtT/GF and Tpit/F1 and AEA exerted a stimulatory, non-significant tendency in both cell lines. WIN as a synthetic $CB_1$ agonist

mimicked the action of 2-AG on both Anx A1 and NO, while otenabant as a $CB_1$ antagonists yielded results that did not differ from the basal levels. On NO production, inhibitory effects were prevalent and consistent among natural and synthetic $CB_1$ receptor ligands. This leads to the thought that $CB_1$ on fs cells is not entirely Gi coupled (Fig. 78). Further measurement of an $[Ca^{2+}]_i$ increase after 2-AG binding to the $CB_1$ receptor let some room for speculations about a possible involvement of Gq, Go, or even Gs α subunits, possibly as part of a heterodimer $CB_1$ receptor complex. Moreover, it has been already noted that $CB_1$ readily forms heterodimers with adenosine and DA receptors (Pertwee 2005; 2006). The stimulatory effect of ECs could involve elevations of $Ca^{2+}$ concentration and interactions with ATP-dependent $K^+$ channels. The latter are necessary for the Anx A1 ABC-mediated export (Philip et al., 1998; Chapman et al., 2003; Solito et al., 2003; Solito et al., 2006). At low $Ca^{2+}$ concentrations, the unique N-terminal domain of Anx A1 is embedded within the pore formed by the protein structure, but elevations in $Ca^{2+}$ (≥1 mM, as in plasma or other biological fluids) expose this region and may thereby influence the biological activity of the protein (Rosengarth et al., 2001a; Rosengarth et al., 2001b; Gavins and Hickey, 2012).

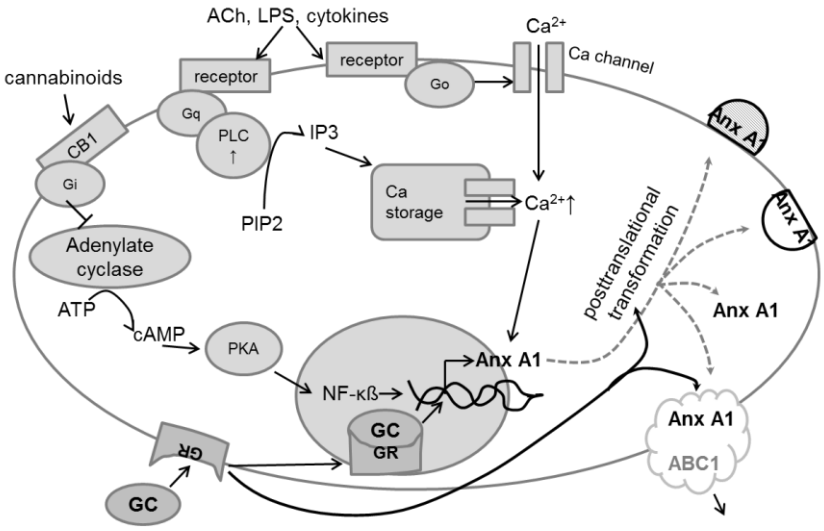


Fig. 78: Proposed mechanism of the influence of EC on Anx A1 in the fs cell. It has been assumed that ECs act upon Gi-coupled $CB_1$ receptors to trigger an inhibition of the adenylate cyclase and subsequent depletion of its product cAMP that would have caused the PKA to activate the NF-κβ complex to bind on the promoter region of the Anx A1 gene. On the other side, Go and Gq-coupled receptors would directly (through activation of N-/T-type voltage dependent $Ca^{2+}$ channels) or indirectly (through activating PLC to recruit more IP3 units to release $Ca^{2+}$ from the intracellular storages) lead to an increase of $Ca^{2+}$ in the cell. $Ca^{2+}$ interacts with Anx A1 by binding to its $Ca^{2+}$-affine sites and thus activates it and translocates it from the cytosol to the cell membrane. Further modificational processes lead to transformation of the Anx A1 molecule to export it from the cell through ABC1 transporter. GC induce and support the mechanism of Anx A1 production and release. ABC1 ATP-binding cassette transporter type 1; ACh acetylcholine; ATP adenosine triphosphate; cAMP cyclic adenosine monophosphate; GC glucocorticoids; GR GC receptor; IP3 inositol trisphosphate; LPS lipopolysaccharides; NF-κβ nuclear factor kappa-light-chain-enhancer of activated B cells; PIP2 phosphatidylinositol 4,5-bisphosphate; PKA protein kinase A; PLC phospholipase C.

Referring to the data demonstrated in this work, 2-AG causes elevations of $[Ca^{2+}]_i$ that lead to modification of membrane-bound Anx A1 protein, resulting in its mobilization and externalization.

NO production was inhibited as expected by AEA and WIN and was not changed by otenabant. The findings available in the literature are so far controversial. On one hand, incubation of decidual explants with m-AEA (a stable synthetic AEA analogue) led to an induction of iNOS and hence an increase in the NO level (Vercelli et al., 2009). On the other hand, NO production in rat microglia was inhibited in a $CB_1$ receptor-related mechanism (Waksman et al., 1999). That NO is inhibited through $CB_1$ receptor in spite of $Ca^{2+}$-increase, can be supported by evidence that NOS enzymes activation is not strictly dependent on high $Ca^{2+}$-concentration in the cell, as reviewed by Alderton et al. (2001). Another possible explanation would be that EC lead to an activation of Anx A1 that has been shown to inhibit NO. Anx A1 inhibits NO production by inhibiting iNOS (Minghetti et al., 1999; Ferlazzo et al., 2003) or eNOS (Paliege et al., 2011). Vakalopoulou et al. suggested in 1991 that Anx A1 binds to mRNA segments that are AU-rich at their 3' end and thus prevents their translation. iNOS mRNA has AU-repeats at its 3' end. There is reported evidence that Anx A1 negatively interacts with the iNOS gene in J774 macrophagial cell line (Wu et al., 1995; Ferlazzo et al., 2003). Moreover, Minghetti et al. showed in 1999 that LPS-induced iNOS was inhibited by Dex-induced Anx A1.

LPS and cytokines induce NO secretion. One way for unfolding an activatory stimulus is the increase of intracellular $Ca^{2+}$, either directly through activating $Ca^{2+}$ channels, or indirectly by activating the PLC. Cannabinoids in this work were demonstrated to constrain NO. A presumed mechanism could involve inhibition of the available $Ca^{2+}$, inhibition of NF-κβ that has been proved to induce and facilitate NO production, and/ or inhibition through the Anx A1 protein.

An interesting link, however, is the fact that NOS inhibitors like L-NAME and curcumin triggered 33 kDa Anx A1-variants. Analysis of membranous Anx A1 revealed the presence of the 33 kDa-Anx A1-variant as well. This could be an incentive to further investigate whether L-NAME/ curcumin-caused Anx A1 and membranous Anx A1 are identical. 33 kDa-Anx A1 has already been reported by Blackwell et al. (1980) and Vong et al. (2007). Moreover, phosphorylation on the Ser27 residue of the Anx A1

protein results in translocation of the molecule from the cytosol to the membrane and would yield an Anx A1 protein product of 33 kDa size (D'Acunto et al., 2014).

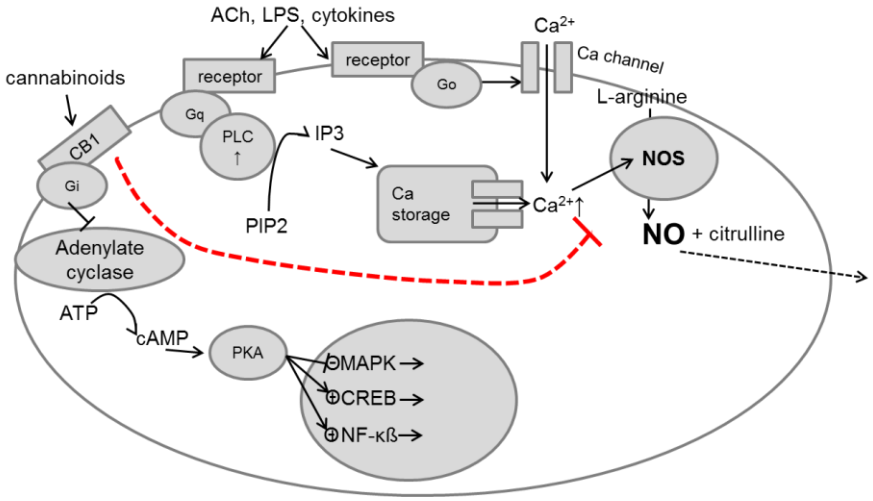


Fig. 79: Proposed mechanism of the influence of EC on NO in the fs or endocrine cell. It has been assumed that ECs act upon Gi-coupled $CB_1$ receptors to trigger an inhibition of the adenylate cyclase and subsequent depletion of its product cAMP that would have caused the PKA to activate the NF-κβ complex to induce NOS enzymes that would produce NO. On the other side, Go and Gq-coupled receptors would directly (through activation of N-/T-type voltage dependent $Ca^{2+}$ channels) or indirectly (through activating PLC to recruit more IP3 units to release $Ca^{2+}$ from the intracellular storages) lead to an increase of $Ca^{2+}$ in the cell. $Ca^{2+}$ interacts with NOS and thus activates the NO secretion. ACh acetylcholine; ATP adenosine triphosphate; cAMP cyclic adenosine monophosphate; IP3 inositol trisphosphate; LPS lipopolysaccharides; NF-κβ nuclear factor kappa-light-chain-enhancer of activated B cells; PIP2 phosphatidylinositol 4,5-bisphosphate; PKA protein kinase A; PLC phospholipase C.

## Regulation of hormonal release

Anx A1 is expressed in the pituitary gland, the olfactory bulb, and the hypothalamus (ME, PVN, Arc, aPV) (Smith et al., 1993). Anx A1 has been detected in the ependyma of the rat (Woods et al., 1990; Smith et al., 1993; McKanna and Zhang, 1997), of the human (Johnson et al., 1989; Dreier et al., 1998), in glial cells of the rat (McKanna, 1993; McKanna and Zhang, 1997), of the human (Johnson et al., 1989; Eberhard et al., 1994), in the human hippocampus (Eberhard et al., 1994), and the rat cerebellum (Young et al., 1999). The IHC studies demonstrated in this work show as well the expression of Anx A1 in the periaqueductal grey and along the third ventricle.

The reports about the location of Anx A1 where the fs cells contact endocrine cells, i. e. in their processes (Traverso et al., 1999; Chapman et al., 2002; John et al., 2008), were confirmed by ISH analysis of Anx A1 RNA in TtT/GF and Tpit/F1 cells. ISH analysis of Fpr-rs1 RNA demonstrated that both endocrine cell lines (C and L) express RNA for the Anx A1 receptor and can thus be regulated by Anx A1. The ISH analysis did not entirely exclude the possibility that Fpr-rs1 is expressed in Tpit/F1 as well, which would

promote an autocrine action of Anx A1. The Fpr-rs1 is a Gi pertussis toxin-insensitive receptor that activates the PLC and releases $Ca^{2+}$ from intracellular stores (Wenzel-Seifert et al., 1999). It causes a tyrosine kinase-mediated phosphorylation of PLA, PLD, and of members of the MAP kinase family (Gavins, 2010). According to the literature, full length Anx A1 and its N-terminal bioactive part activate all human Fprs and only Fpr1 and Fpr-rs1 in the mouse (Hayhoe et al., 2006; D'Acquisto et al., 2008; John et al., 2008). Fpr1 gene deletion does not lead to a reverse of Dex- and Anx A1-mediated ACTH inhibition (John et al., 2008). Therefore, my focus fell on Fpr-rs1 as target Anx A1 receptor. In the ISH analyses the Fpr-rs1 mRNA in murine PD tissue was significantly decreased during the subjective day (ZT16) as compared to the subjective night (ZT04), giving an indication on the timely regulation of the Anx A1 action. However, there was no significant change in the level of Anx A1 mRNA in the same regions and at the same time point.

**Effect of Anx A1 and NO on HPA**

The obtained results show that 2-AG had no effect, Anx A1 had stimulatory and NO inhibitory influence on ACTH. There is reported evidence that Anx A1 led to an increase of ACTH in rat pituitary tissue when administered alone (Taylor et al., 1993). When on the other side, pre-incubation with CRH took place, Anx A1 had an inhibitory effect on ACTH release (Taylor et al., 1993). AtT20/D16v cells are demonstrated to express nNOS (Qian et al., 1999), eNOS, and iNOS (Ohta et al., 1993). Since the C cell itself produces NO, that can be inhibited by 2-AG, the question about an exact mechanism emerges.

According to my experiments 2-AG had no influence on the C cell. The availability and concentration of 2-AG, CRH, GC, and probably Fpr-rs1, is timely (circadianly) regulated. ACTH is down-regulated under the influence of GC, that causes externalization of Anx A1 and thus potentiates fast exocytotic inhibition when combined with CRH (Chapman et al., 2002). The slow inhibition of ACTH by GC is mediated through CRH whose genetic expression in the hypothalamus is negatively influenced by GC (Smith and Vale, 2006). NO produced at basal level in the C cell, acts inhibitory on ACTH release. Considering that the amount of NO produced by fs cells exceeds 1.5 times the amount of NO produced by C cells, one cannot miss the link between the EC and Anx A1, that inhibits NO, that in turn inhibits ACTH. The overall

result is an activation of ACTH. Without CRH the antagonistic effect of Anx A1 is missing, resulting in a ACTH release. Moreover, the ISH analysis demonstrated that Fpr-rs1 was timely regulated. Subsequently, Anx A1 is prohibited from unfolding its action when its receptor is less expressed at certain times.

The mechanism of ACTH expression and release is shown in Fig. 80. Hypothalamic CRH binds its Gs-coupled CRH receptor to trigger an activation of the AC and a subsequent accumulation of its product cAMP that causes the PKA to activate CREB to bind on the promoter region of the POMC gene and initiate its expression. On the other side, the Gs α subunit activates $Ca^{2+}$ channels and thus increases $[Ca^{2+}]_i$ that is necessary for the exocytosis of ACTH. GC induce and support the mechanism of ACTH production and release. Cannabinoids were thought to act inhibitory upon the POMC expression via their Gi-coupled $CB_1$ receptor.

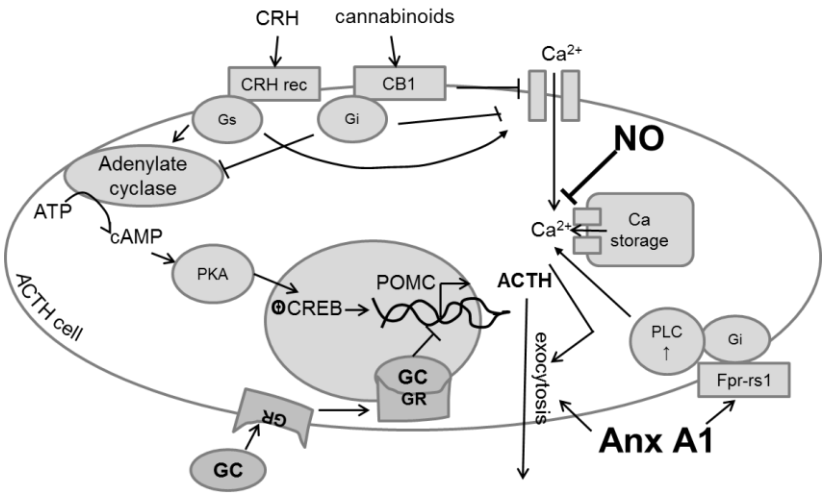


Fig. 80: Proposed mechanism of the influence of EC, Anx A1, and NO on POMC expression (and ACTH) in the C cell. Hypothalamic CRH binds its Gs-coupled CRH receptor to trigger an activation of the adenylate cyclase and subsequent accumulation of its product cAMP that causes the PKA to activate CREB to bind on the promoter region of the POMC gene and initiate its expression. On the other side, the Gs α subunit activates $Ca^{2+}$ channels and thus increases $Ca^{2+}$. $Ca^{2+}$ is necessary for the exocytosis of ACTH. GC induce and support the mechanism of ACTH production and release. ECs would act inhibitory upon the POMC expression via their Gi-coupled $CB_1$ receptor. 2-AG as a $CB_1$ agonist did not exert any change in ACTH. Anx A1 acted stimulatory on ACTH in the cell medium. NO negatively influenced ACTH possibly by interacting with $Ca^{2+}$ supplies. NO is known to negatively interact with exocytotic processes by utilizing $Ca^{2+}$ that is essential in externalizing the exocytotic vesicles. ATP adenosine triphosphate; cAMP cyclic adenosine monophosphate; CREB cyclic AMP-responding element-binding protein; CRH corticotropin; Fpr-rs1 formyl peptide receptor-related sequence 1; GC glucocorticoids; GR GC receptor; PKA protein kinase A; PLC phospholipase C.

In this study2-AG as a $CB_1$ agonist did not exert any change in ACTH. Anx A1 acted stimulatory on ACTH in the cell medium. NO negatively influenced ACTH possibly by interacting with the $Ca^{2+}$ supplies. NO is known to negatively interact with exocytotic

processes by utilize ng $Ca^{2+}$ that is essential for fusioning the exocytotic vesicles with the cellular membrane and thus release ACTH.

**Effect of Anx A1 and NO on PRL**

According to the results of this study, 2-AG did not produce any significant effect on PRL levels. Anx A1 had an inhibitory effect on PRL in the cell extract (but stimulatory in the cell medium). NO inhibited PRL in cell extract (and in the cell medium). John et al. suggest (2008) that the inhibition of hormone release from the endocrine cells by Anx A1 involves interactions with SNARE proteins, which are critical to exocytosis.

Reports about influence of ovariectomy on Anx A1 reveal the possible involvement of Anx A1 in reproduction. Ovariectomy leads to reduced Anx A1, which can be reversed by 17β-estradiol treatment. Moreover reduced Anx A1 at the pro-estrus coincides with an increase in endogenous 17β-estradiol (Christian et al., 1997). Furthermore, Anx A1 Ab or antisense oligonucleotides act inhibitory on PRL release from pituitary slices, indicating a stimulatory role of Anx A1 on PRL (Taylor et al., 1995; 2000). Additionally,estradiol, TRH, VIP, but also IL-6 and CINC that are produced by fs cells, induce rapid, non-genomic (Morris et al., 2002) and slow, genomic PRL release from L cells. GC are known to influence PRL release, but GH4C1 cells express intracellular ER α and no GR, meaning that GC cannot directly modify PRL release but indirectly via mediators (Tashjian, 1979). GC application *in vivo* leads to decrease in serum PRL (Euker et al., 1975; Fang and Shian, 1981). Adrenalectomized animals have increased PRL which is inversed by treatment with Dex (Watanobe, 1990). A study of co-cultures of TtT/GF cells and GH3 performed by Koike et al. demonstrated an increase in the resulting PRL (Koike et al., 1997). They proposed that IL-6 and CINC influence positively the basal PRL release. Hence, a stimulatory action of Anx A1 from the TtT/GF cells on the released PRL from the GH3 cells cannot be excluded.

However, many studies imply an inhibitory effect of Anx A1 on PRL. *In vitro* studies on GH3 cells showed that Dex suppresses PRL release and this action could be reversed by anti-Anx A1 polyclonal antiserum (Dannies and Tasjian, 1976; Perrone et al., 1980; Taylor et al., 1995; Taylor et al., 2000). Human recombinant Anx A1 mimics and anti-Anx A1 mAb reverses the Dex effect (Taylor et al., 1995; 2000). It has been further demonstrated that Anx A1 blocks the GC independent PRL release from the decidual

cells of the placenta (Wilber and Utiger, 1969; Handwerger et al., 1991; Pihoker et al., 1991).

Anx A1 is involved in the regulation of ACTH and PRL not only on the level of neighbouring cells. The protein is expressed in hypothalamic (Arc, PVN, aPV, OC, ME, VMH, V3) and pituitary gland structures that house descending neurons regulating the putative and circadian pattern of hormonal release. Anx A1 is abounding in ependymal cells, close to CRH/AVP neurons in the PVN (Theogaraj et al., 2005). The processes of tanycytes (a type of ependymal cells) from the ME accompany and enwrap neuroendocrine axons that course from hypothalamic nuclei to terminals in the ME. Large number of gap junctions have been found between adjacent ependymal cells and between adjacent tanycytes. The tanycytes endings are close to GnRH axon terminals and tend to induce GnRH axonal growth (Oota et al., 1974; Kozlowski and Coates, 1985; Silverman et al., 1991; Gibson et al., 2000). Moreover, tanycytes undergo morphological changes of their nucleus size and cell perikarya along the reproductive cycle and after ovariectomy (Kobayashi et al., 1972; Oksche et al., 1972). On the basis of anatomical proximity of Anx A1-positive areas to projections of neurons involved in the regulation of rhythms, feed behavior, and reproduction, one can deduce the effect Anx A1 can have on these functions.

According to the results obtained in this work NO inhibited PRL from the GH4C1 cells, which confirmed the reported negative effect of NO on PRL release from pituitary gland slices from male (Duvilanski et al. 1995) and female rats (Vankelecom et al., 1997). Moreover, NO is reported to interact with the intracellular $Ca^{2+}$ and thus prevent the release of PRL (Andric, 2003). Interesting, however, is the statement that fs cells influence the estradiol mitogenic function on L cells, leaving room for speculation about possible fs cell-produced mediators (Oomizu et al., 2004). Estradiol down-regulates the nNOS in rat anterior pituitary cells and GH3 tumors (Qian et al., 1999). GH4C1 cells are shown to express nNOS (Qian et al., 1998) and their precursor - GH3, eNOS, and iNOS (Qian et al., 1999). Thus, the stimulatory role of estradiol on PRL release can be supported by its influence on Anx A1 and NO.

The proposed mechanism of PRL expression and release is shown in Fig. 81. VIP binds to its Gs-coupled VPAC1 receptor to trigger an activation of the AC and subsequent accumulation of its product cAMP that causes the PKA to activate CREB to bind on the

promoter region of the PRL gene and initiate its expression. DA acts antagonistic on PRL expression and release via DA receptors to inhibit the AC and the voltage-dependent $Ca^{2+}$ channels. TRH binds its Gq-coupled TRH receptor to trigger an activation of the PLC and a subsequent accumulation of IP3 that causes the release of $Ca^{2+}$ from the intracellular storages. On the other side, the Gs α subunit activates $Ca^{2+}$ channels and thus increases $[Ca^{2+}]_i$ that is necessary for the exocytosis of PRL. E2 inibits PRL expression through binding on ER and repressing directly the PRL promoter. Cannabinoids are thought to act inhibitory upon the PRL expression via their Gi-coupled $CB_1$ receptor. According to the here presented results 2- AG did not exert an inhibitory action on PRL. Anx A1 acted inhibitory on PRL in the cell lysate, probably by activating its Fpr-rs1 receptor to stifle the exocytosis by depleting $[Ca^{2+}]_i$. NO negatively influenced PRL. NO is known to negatively interact with exocytotic processes by utilizing $Ca^{2+}$ that is essential for fusioning the exocytotic vesicles with the cellular membrane and thus release PRL.

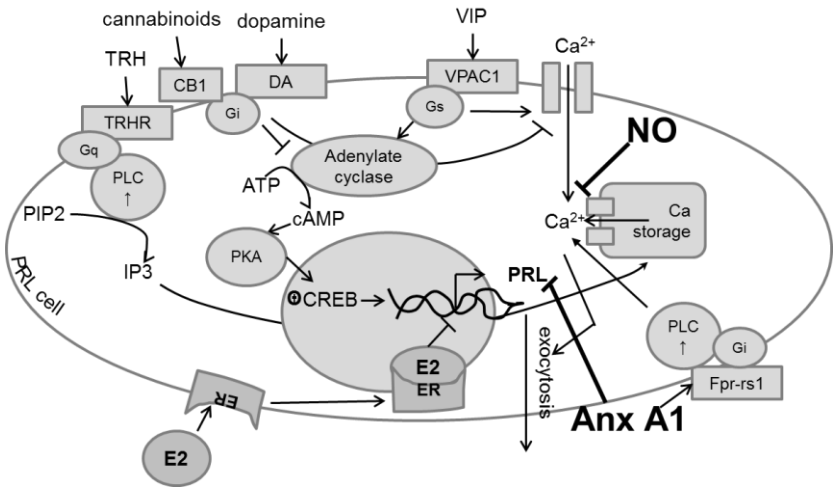


Fig. 81: Proposed mechanism of the influence of EC, Anx A1, and NO on PRL in the L cell. VIP binds its Gs-coupled VPAC1 receptor to trigger an activation of the adenylate cyclase and subsequent accumulation of its product cAMP that causes the PKA to activate CREB to bind on the promoter region of the PRL gene and initiate its expression. Dopamine acts antagonistic on PRL expression and release via DA receptors to inhibit the adenylate cyclase and the voltage dependent $Ca^{2+}$ channels. TRH binds its Gq-coupled TRH receptor to trigger an activation of the PLC and subsequent accumulation IP3 that causes the release of $Ca^{2+}$ from the intracellular storages. On the other side, the Gs α subunit activates $Ca^{2+}$ channels and thus increases $Ca^{2+}$ in the cell. $Ca^{2+}$ is necessary for the exocytosis of PRL. E2 inibits PRL expression through binding on ER and repressing directly the PRL promoter. ECs would act inhibitory upon the PRL expression via their Gi-coupled $CB_1$ receptor. 2-AG as a $CB_1$ agonist did not exert any change in PRL. Anx A1 acted inhibitory on the PRL in the cell lysate, presumingly by its Fpr-rs1 receptor to stifle the exocytosis by depleting $[Ca^{2+}]_i$. NO negatively influenced PRL possibly by interacting with $Ca^{2+}$ supplies. NO is known to negatively interact with exocytotic processes by utilizing $Ca^{2+}$ that is essential in externalizing the exocytotic vesicles. ATP adenosine triphosphate; cAMP cyclic adenosine monophosphate; $[Ca^{2+}]_I$ intracellular $Ca^{2+}$ concentration; CREB cyclic AMP-responding element-binding protein; DA dopamine receptor; E2 estradiol; ER E2 receptor; Fpr-rs1 formyl peptide receptor-related sequence 1; IP3 inositol trisphosphate; PIP2 phosphatidylinositol 4,5-bisphosphate; PKA protein kinase A; PLC phospholipase C; TRH thyrotropin; VIP vasoactive intestinal peptide; VPAC1 VIP/PACAP receptor type 1.

**Interactions between rhythmic and hormonal regulation**

The "master clock" SCN innervates either directly or indirectly through the medial preoptic area (POA) the PVN and the supraoptic nucleus (SON), thus dictating circadian rhythmicity in the HPA axis (Hofman, 1997; 2004). SCN lesions led to loss of corticosterone rhythm (Moore and Eichler, 1972). The amplitude of CRH and AVP releases increase in the early morning, which leads to an increase in the ACTH and subsequent GC release. This process is interrupted by light, feeding, and stress (Hiroshige and Wada-Okada, 1973; Geracioti et al., 1992). Humans, nonhuman primates, and rodents display circadian changes in their GC secretion (Weitzman et al., 1971; Moore and Eichler, 1972; Gallagher et al., 1973; Dubey et al., 1983; Van Cauter and Refetoff ,1985; Czeisler and Klerman, 1999). Already in 1983 Adler et al. gathered evidence that the corticoid secretion begins to rise before waking in nocturnal and diurnal species and peaks during the day in diurnal, and during the night in nocturnal species. This imlies that GC embody the function of a mediator for the activity period (Adler et al., 1983; Albers et al., 1985; Ottenweller et al., 1987). Márquez et al. and Armario confirmed these results by showing that the highest plasma levels of corticosterone in the rat occur shortly before darkness period (scotoperiod) (Márquez et al., 2005), and highest plasma cortisol levels occur shortly after awakening and are at their lowest in the evening (Armario, 2006). The adrenal gland itself also manifests rhythms in clock-gene expression, influencing the rhythmic responsiveness to pituitary-derived ACTH (Ungar and Halberg, 1962; Dunn et al., 1972; Buijs et al., 1997; Bittman et al., 2003; Kalsbeek et al., 2003; Oishi et al., 2003; Guo et al., 2006; Oster et al., 2006; Fahrenkrug et al., 2008). Kitchener et al. propose the interesting idea that binding of GR to correspondent GRE DNA segments is also circadianly dependent. This idea is based on the observation that at low GC levels (as during the day[12]), almost no GR-DNA binding took place, while at "night" high concentrations, significant GR-DNA-association occured (Kitchener et al., 2004).

The GC feedback inhibition of CRH and AVP release in the brain takes place through two types of GR: type I is activated by basal GC concentration, and type II is activated

[12] The experiments have been conducted in a rodent model.

by basal and elevated GC concentration. The PVN expresses high density of the GR type I, while the hippocampus expresses both types and GC infusion in those areas reduces HPA axis activity (Smith and Vale, 2006).

The Arc regulates blood glucose, insulin, and leptin, and is thus involved in the energy homeostasis (Sahu, 2004; Higuchi et al., 2005). It further regulates the reproduction, since it controls FSH, LH, GH, and PRL through the GnRH neurons that are inhibited by CRH (Gold and Chrousos, 2002). The HPA axis interferes further negatively with the reproductive function as it influences the estrous cycle (Rhodes et al., 2002; 2004), and CRH not only inhibits GnRH neurons, but also directly acts on gonadotroph cell in the pituitary gland (Westphal et al., 2009).

Like CRH, PRL acts suppressive on reproduction. It reduces GnRH secretion, suppresses LH and detriments reproduction by negatively regulating the reproductive behavior (Koike et al., 1984; Doherty et al., 1990; Tortonese et al., 2013). Regulation of OT neurons, fertility suppression, stress response and anxiety induced behavior suppression, stimulation of appetite, food intake, myelination in the CNS and neurogeneration in the olfactory bulb are some among the many features of PRL to be identified (Freeman et al., 2000; Grattan et al., 2008; Bole-Feysot et al., 2013). Moreover, reproductive dysfunction and infertility in both genders are often caused by hyperprolactinemia (Evans et al., 1982; Mah and Webster, 2002).

Some of the PRL available in the CNS is built in the periphery and transported via special carrier proteins to its target areas, the most important of which the hypothalamus (Walsh et al., 1987). Pi and Grattan detected PRL and PRL mRNA in the POA, PVN, aPV, and its highest expression was in the Arc. PRL receptor mRNA is found in SCN (Crumeyrolle-Arias et al., 1993; Roky et al., 1996). The highest level of PRL receptor mRNA was detected in the choroid plexus (Pi and Grattan, 1998; 1999).

In humans, PRL has a diurnal rhythm with the highest plasma concentration at night and the lowest concentration in the waking hours (Freeman et al., 2000). In rats, PRL follows a circadian pattern that is lost after SCN lesions (Bethea and Neill, 1979; Mai et al., 1994). Circandianly controlled PRL peaks occur additionally to the baseline along with the LH proestrus surge (when one/ some follicles in the ovary start growing) in rats and mice (Blake, 1976; Bethea and Neill, 1980). Moreover, estradiol induces PRL secretion according to a circadian rhythm (Palm et al., 2013). The GH4C1 cells used in

this study are also proven to be circadianic with PRL gene expression synchronizable by medium change (Guillaumond et al., 2011; Jean-Louis Franc oral communication, 2013). Intriguingly, Oishi et al. imply that fs cells proliferate the most during the estrus and the least during the diestrus in rat pituitary gland tissue (Oishi et al., 1993).

Lesions in the PVN and PN impair suckling-induced PRL (Kiss et al., 1986; Murai and Ben-Jonathan, 1987; Bodnár et al., 2004), meaning that a highly effective PRL releasing factor should have its origin in the PVN and should involve the PN. So far, there is a lot of controversy regarding TRH, TSH, AVP, OT and salsolinol as potential releasing factors for PRL (Samson et al., 1986; Greef et al., 1987; Johnston and Negro-Vilar, 1988; Rondeel et al., 1988; Thomas et al., 1988; Nagy et al., 1991; Tóth et al., 2001). Salsolinol is a DA derivative found in the PN and involved in stress- and suckling-induced PRL secretion, and thus a promising PRL releasing factor (Bodnár et al., 2004).

PRL secretion is inhibited by DA (Ben-Jonathan et al., 1977). There are three hypothalamic dopaminergic systems: the tuberoinfundibular (TIDA); the tuberohypophyseal (THDA) and the periventricular hypophyseal dopaminergic (PHDA) neural system (DeMaria et al., 1999), all under the control of SCN projections (Horvath, 1997). TIDA neurons project from the dorsomedial Arc to the external zone of the ME (Björklund et al., 1973). DA is transported to the anterior pituitary lobe, where it acts on type 2 DA receptors on L cells to inhibit PRL secretion (Mansour et al., 1990). THDA neurons project from the rostral Arc through the hypothalamo-pituitary axis to the PI and the PN (Fuxe, 1963). PHDA neurons project from the aPV to the PI (Goudreau et al., 1992). DA from the THDA and PHDA neurons is transported through the short vessels from the PN to the anterior lobe. Rhythmic PRL inhibition results from timed TIDA and PHDA neural activity, but not THDA (Sellix and Freeman, 2003; Sellix et al., 2004). Estrogens evoke TIDA activation (Neill et al., 1971) and VIP neurons project from the SCN to OT neurons. The timing of the PRL peak can be shifted by change in the light-dark cycle (Blake, 1976; Bethea and Neill, 1980). Kennett et al. applied VIP antisense oligonucleotides in ovariectomized estrogen treated rats, which resulted in a phase advance of the FOS (transcription factor activated by PRL) expression peak in periventricular OT neurons and of the PRL peak (Kennett et al., 2008).

Due to its role and function as “hormone of darkness”, melatonin is affecting and is being affected by circadian rhythms. It is further involved in timed events linked to

reproductivity (Berga et al., 1988; Brzezinski et al., 1988; Kadva et al., 2013). Kadva et al. found a relationship between increased nocturnal melatonin and hypothalamic amenorrhea, and the estrogen suppressing effect on melatonin in female subjects.

Melatonin acts in the hypothalamus to control the GnRH secretion, the pituitary gland to influence FSH and LH release and the gonads to affect responsiveness to gonadotropins. Long duration melatonin signals, corresponding to winter short day - long night conditions, suppress FSH and LH secretion from the anterior pituitary lobe (Badness et al., 1993). PRL secretion was inhibited during short days (SD) in sheep with disrupted hypothalamo-pituitary axis and melatonin PT implants (Lincoln and Clarke, 1997). Expression of clock genes in and outside the SCN is dependent on melatonin (Morgan et al., 1998; Messager et al., 1999; Messager et al., 2000). Melatonin suppressed *Per1* in PT of sheep and hamsters and *Cry1/2* were stimulated with a peak after dusk (Johnston et al., 2003). After entrainment to SD, *Cry1* still had a peak after dusk, but *Per1* lost its rhythmicity (Johnston et al., 2005).

Yasuo et al. demonstrated that the ECS localized to the PT of Syrian hamsters responds to photoperiodic changes (Yasuo et al., 2010) and transduces photoperiodic signals via multiple pathways and messenger molecules (Yasuo and Korf, 2011). They suggest that EC mediate the communication between the PT (where they are built) and the PD (where they unfold their action) in a photoperiod-, melatonin-, and forskolin –dependent way (Morgan, 2000; Yasuo and Korf, 2011). Genes and corresponding proteins of the enzymes for EC synthesis (NAPE-PLD, DAGL) and degradation (FAAH, MAGL) were detected in the PT (Yasuo et al., 2010). Expression of DAGL and levels of 2-AG were increased in the PT of Syrian hamsters, kept under long day (summer) conditions and PRL in the plasma was up-regulated (Yasuo and Korf, 2011). Yasuo et al. further detected $CB_1$ receptors in the PD and not in the PT with the assumption that the $CB_1$-positive cells represent fs cells. The idea introduced in their publications, is that the fs cells activate hormonal release in adjacent glandular cells (Yasuo et al., 2010; Yasuo and Korf, 2011). However, S-100-positive cells and Anx-A1-positive cells are also present in the PT, indicating that fs cells might not be restricted only to the PD.

**Further investigation and application**

Further investigation that will shed knowledge on the exact messenger cascade involving the $CB_1$ receptor in the ME, pituitary gland, and immortalized cells, is

needed. It can involve extensive analyses of $[Ca^{2+}]_i$ concentration, cAMP, cGMP, PKA, PLC, CREB, and MAPK proteins. Assays for phosphorylated Gi, Gs, Gq, and Go α subunits can complement the results. Precise definition of whether the $CB_1$ receptor is present as a dimer, and more precisely homo- or hetero-dimer is needed too, since that might be the case with fs cells ($CB_1$-adenosine) and L cells ($CB_1$-DA). A subsequent step can be the analysis of essential enzymes of ECS (NAPE-PLD, DAGL, FAAH, and MAGL) in the cell models. A technique for the detection of Anx A1 protein in the cell medium can be validated and a closer look on the posttranslational modification and location of Anx A1 protein, is necessary. Of equal importance is the development of specific anti-Fpr-rs1 antibodies, raised against the murine and or rat Fpr-rs1 protein.

After having achieved those aims, the next step can represent an investigation in an integrity model or a living organism, preferably mice or rats. One would find knock out models ($CB_1$, Anx A1, Fpr-rs1) useful and perform comparative analysis to illuminate the intricate links among the (photo)-neuroendocrine, EC, vascular, and immune systems.

The obtained data so far could be then applied on animal models of diseases, corresponding to conditions, such as sleep disorders, cancer, Parkinson, cerebrovascular disease, Addison/Cushing, hyper/hypoprolactinemy, and if applicable depressive disorders, to define new treatment targets and agents.

# Conclusion

The fs cells express $CB_1$ and there was reported data on the presence of $CB_1$ in the C and L cells (Yasuo et al., 2010). I confirmed that the $CB_1$ receptor is present in the TtT/GF and Tpit/F1, and in the AtT20/D16v and GH4C1 cells.

It was further known that the TtT/GF cells produce Anx A1 (Chapman et al., 2002). I have confirmed with the here presented data that Tpit/F1 cells produce Anx A1 as well. A novel concept was the link between ECS and Anx A1. I hereby show in this work for the first time that EC lead to an increase in Anx A1 in the fs cell models.

There were reported findings that "natural" C and L cells possess Anx A1 binding sites (Christian et al., 1997). I confirmed the presence of Fpr-rs1 receptors for Anx A1 on the AtT20/D16v and GH4C1 cells.

There are reports that fs (TtT/GF, Tpit/F1), C (AtT20/D16v), and L (GH4C1) cells synthetize NO (Ohta et al., 1993; Qian et al., 1998; Vankelecom et al., 1997). I confirmed with this work the presence of NO in the used TtT/GF, Tpit/F1, and AtT20/D16v cells.

According to the performed experiments, EC induced Anx A1 from the fs cell. Anx A1 acted stimulatory on ACTH in the C and inhibitory on PRL in the L cell. EC inhibited NO in the fs cell and NO inhibited ACTH and PRL release from the endocrine cells. Hence, I demonstrate that EC influence the ACTH release stimulatory by activating Anx A1 and inhibiting NO. Further, EC cause an inhibition of PRL by activating Anx A1, and stimulation by inhibiting NO. Thus the results manifest a clear regulatory link (possibly time-related) between the EC and ACTH and PRL control, involving the fs and the endocrine cells.

It is known that Anx A1 inhibits NO (Minghetti et al., 1999) and the AA cycle by blocking the PLA2. In addition, NO inhibits on its side the production of EC (Clancy et al., 2000). Furthermore, there is reported evidence that NO inhibits ACTH and PRL (Vankelecom et al., 1997). As for the influence Anx A1 has on ACTH and PRL, the data presented in the literature is even more controversial (Taylor et al., 1993; John et al., 2008).

The novel concept of this work is to connect the ECS to (timely) regulated hormone production through Anx A1 and NO and hence underline the involvement of $CB_1$ with future recognition of therapeutic targets and deeper insights in pathological conditions, such as Addison/Cushing, hyper/hypoprolactinemy, obesity, and sleep disorders.

The here reported findings are summarized graphically in the following scheme (Fig. 82).

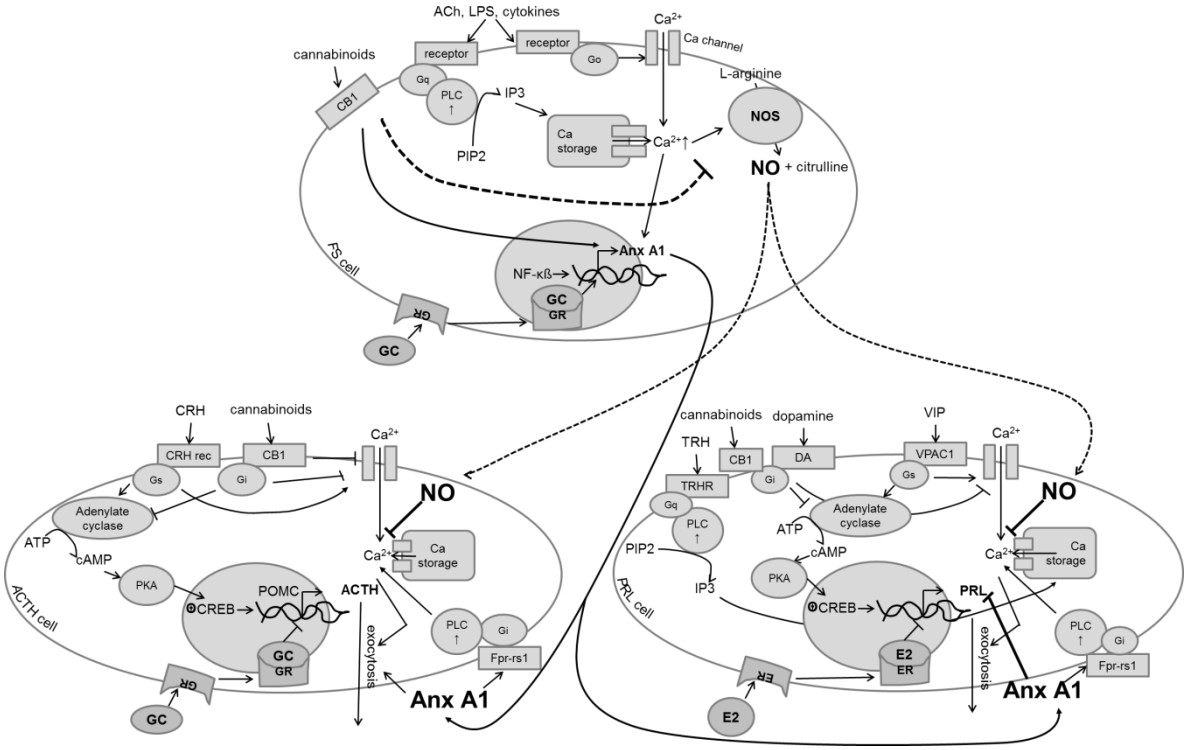


Fig. 82: Proposed mechanism of the influence of cannabinoids, Anx A1, and NO on hormonal release. The figure represents a summarized scheme from Fig. 78, Fig. 79, Fig. 80, and Fig. 81. $CB_1$ agonists led to Anx A1 increase and NO decrease. Anx A1 acted stimulatory on ACTH in the cell medium and inhibitory on the PRL in the cell lysate. NO negatively influenced both ACTH and PRL possibly by interacting with $Ca^{2+}$ supplies. 2-AG as a $CB_1$ agonist did not exert any change in ACTH and PRL. ACh acetylcholine; ATP adenosine triphosphate; cAMP cyclic adenosine monophosphate; CREB cyclic AMP-responding element-binding protein; CRH corticotropin; DA dopamine receptor; GC glucocorticoids; GR GC receptor; E2 estradiol; ER E2 receptor; Fpr-rs1 formyl peptide receptor-related sequence 1; IP3 inositol trisphosphate; PIP2 phosphatidylinositol 4,5-bisphosphate; PKA protein kinase A; PLC phospholipase C; TRH thyrotropin; VIP vasoactive intestinal peptide; VPAC1 VIP/PACAP receptor type 1.

# Bibliography


Adler M., Wong B., Sabol S., Busis N., Jackson M., and Weight F.. 1983. "Action Potentials and Membrane Ion Channels in Clonal Anterior Pituitary Cells." *Proceedings of the National Academy of Sciences* 80 (7): 2086–90.

Albers H., Yogev L., Todd R., and Goldman B.. 1985. "Adrenal Corticoids in Hamsters: Role in Circadian Timing." *American Journal of Physiology - Regulatory, Integrative and Comparative Physiology* 248 (4): R434–R438.

Alderton W., Cooper C., and Knowles R.. 2001. "Nitric Oxide Synthases: Structure, Function and Inhibition." *Biochemical Journal* 357 (Pt 3): 593–615.

Allaerts W. and Vankelecom H.. 2005. "History and Perspectives of Pituitary Folliculo-Stellate Cell Research." *European Journal of Endocrinology* 153 (1): 1–12.

Alldridge L., Hayley J., Plevin R., Hannon R., and Bryant C. 1999. "The Annexin Protein Lipocortin 1 Regulates the MAPK/ERK Pathway." *Journal of Biological Chemistry* 274 (53): 37620–28.

Altschul S., Gish W., Miller W., Myers E., and Lipman D.. 1990. "Basic Local Alignment Search Tool." *Journal of Molecular Biology* 215 (3): 403–10.

Alves V., Nonogaki S., Cury P., Wünsch-Filho V., de Carvalho M., Michaluart P., Moyses R., et al. 2008. "Annexin A1 Subcellular Expression in Laryngeal Squamous Cell Carcinoma." *Histopathology* 53 (6): 715–27.

Andric S. 2003. "Nitric Oxide Inhibits Prolactin Secretion in Pituitary Cells Downstream of Voltage-Gated Calcium Influx." *Endocrinology* 144 (7): 2912–21.

Antonicelli F., De Coupade C., Russo-Marie F., and Le Garrec Y.. 2001. "CREB Is Involved in Mouse Annexin A1 Regulation by cAMP and Glucocorticoids." *European Journal of Biochemistry* 268 (1): 62–69.

Archer S. 1993. "Measurement of Nitric Oxide in Biological Models." *The FASEB Journal* 7 (2): 349–60.

Arendt J., Bojkowski C., Folkard S., Franey C., Marks V., Minors D., Waterhouse J., Wever R., Wildgruber C., and Wright J.. 1985. "Some Effects of Melatonin and the Control of Its Secretion in Humans." In *Ciba Foundation Symposium 117 - Photoperiodism, Melatonin and the Pineal*, edited by David Evered Organizer and Sarah Clark, 266–83. John Wiley & Sons, Ltd.

Arendt J. and Skene D.. 2005. "Melatonin as a Chronobiotic." *Sleep Medicine Reviews* 9 (1): 25–39.

Arimura A., Bowers C., Schally A., Saito M., and Miller M.. 1969. "Effect of Corticotropin-Releasing Factor, Dexamethasone and Actinomycin D on the Release of ACTH from Rat Pituitaries *in Vivo* and *in Vitro*." *Endocrinology* 85 (2): 300–311.

Armario A.. 2006. "The Hypothalamic-Pituitary-Adrenal Axis: What Can It Tell Us About Stressors?" *CNS & Neurological Disorders - Drug Targets (Formerly Current Drug Targets* 5 (5): 485–501.

Badness T., Powers B., Hastings M., Bittman E., and Goldman B.. 1993. "The Timed Infusion Paradigm for Melatonin Delivery: What Has It Taught Us about the Melatonin Signal, Its Reception, and the Photoperiodic Control of Seasonal Responses?" *Journal of Pineal Research* 15 (4): 161–90.

Bailey J. 1991. "New Mechanisms for Effects of Anti-Inflammatory Glucocorticoids." *BioFactors (Oxford, England)* 3 (2): 97–102.

Bao L., Gerard N., Eddy R., Shows T., and Gerard C.. 1992. "Mapping of Genes for the Human C5a Receptor (C5AR), Human FMLP Receptor (FPR), and Two FMLP Receptor Homologue Orphan Receptors (FPRH1, FPRH2) to Chromosome 19." *Genomics* 13 (2): 437–40.

Bayatti N., Hermann H., Lutz B., and Behl C.. 2005. "Corticotropin-Releasing Hormone-Mediated Induction of Intracellular Signaling Pathways and Brain-Derived Neurotrophic Factor Expression Is Inhibited by the Activation of the Endocannabinoid System." *Endocrinology* 146 (3): 1205–13.

Beattie R., Goulding N.., Walker-Smith J., and MacDonald T.. 1995. “Lipocortin-1 Autoantibody Concentration in Children with Inflammatory Bowel Disease.” *Alimentary Pharmacology & Therapeutics* 9 (5): 541–45.

Ben-Jonathan N., Charles O., Weiner H., Mical R., and Porter J.. 1977. “Dopamine in Hypophysial Portal Plasma of the Rat During the Estrous Cycle and Throughout Pregnancy1.” *Endocrinology* 100 (2): 452–58.

Bensalem N., Ventura A., Vallée B., Lipecka J., Tondelier D., Davezac N., Dos Santos A., et al. 2005. “Down-Regulation of the Anti-Inflammatory Protein Annexin A1 in Cystic Fibrosis Knock-out Mice and Patients.” *Molecular & Cellular Proteomics: MCP* 4 (10): 1591–1601.

Berga S., Mortola J., and Yen S.. 1988. “Amplification of Nocturnal Melatonin Secretion in Women with Functional Hypothalamic Amenorrhea.” *The Journal of Clinical Endocrinology & Metabolism* 66 (1): 242–44.

Bethea C. and Neill J.. 1980. “Lesions of the Suprachiasmatic Nuclei Abolish the Cervically Stimulated Prolactin Surges in the Rat*.” *Endocrinology* 107 (1): 1–5.

Bethea C. and Neill J.. 1979. “Prolactin Secretion after Cervical Stimulation of Rats Maintained in Constant Dark or Constant Light*.” *Endocrinology* 104 (4): 870–76.

Bittman E., Doherty L., Huang L., and Paroskie A.. 2003. “Period Gene Expression in Mouse Endocrine Tissues.” *American Journal of Physiology - Regulatory, Integrative and Comparative Physiology* 285 (3): R561–R569.

Björklund A., Moore R., Nobin A., and Stenevi U.. 1973. “The Organization of Tubero-Hypophyseal and Reticulo-Infundibular Catecholamine Neuron Systems in the Rat Brain.” *Brain Research* 51 (March): 171–91.

Bjøro T., Englund K., Torjesen P., and Haug E.. 2009. “Inhibitors of the Arachidonic Acid Metabolism Attenuate the Thyroliberin (TRH) Stimulated Prolactin Production without Modifying the Production of Inositolphosphates in GH4C1 Pituitary Cells”. http://informahealthcare.com/doi/abs/10.3109/00365519309088397.

Blackwell G., Carnuccio R., Di Rosa M., Flower R. J., Parente L., and Persico P.. 1980. “Macrocortin: A Polypeptide Causing the Anti-Phospholipase Effect of Glucocorticoids.” *Nature* 287 (5778): 147–49.

Blake C. 1976. “Effects of Intravenous Infusion of Catecholamines on Rat Plasma Luteinizing Hormone and Prolactin Concentrations [1].” *Endocrinology* 98 (1): 99–104.

Blüm V. and Fiedler K.. 1965. “Hormonal Control of Reproductive Behavior in Some Cichlid Fish.” *General and Comparative Endocrinology* 5 (2): 186–96.

Bodnár I., Mravec B., Kubovcakova L., Tóth E., Fülöp F., Fekete M., Kvetnansky R., and Nagy G.. 2004. “Stress- as Well as Suckling-Induced Prolactin Release Is Blocked by a Structural Analogue of the Putative Hypophysiotrophic Prolactin-Releasing Factor, Salsolinol.” *Journal of Neuroendocrinology* 16 (3): 208–13.

Bole-Feysot C., Goffin V., Edery M., Binart N., and Kelly P.. 2013. “Prolactin (PRL) and Its Receptor: Actions, Signal Transduction Pathways and Phenotypes Observed in PRL Receptor Knockout Mice”. http://press.endocrine.org/doi/abs/10.1210/edrv.19.3.0334.

Boucher J., Moali C., and Tenu J.. 1999. “Nitric Oxide Biosynthesis, Nitric Oxide Synthase Inhibitors and Arginase Competition for L-Arginine Utilization.” *Cellular and Molecular Life Sciences* 55 (9): 1015.

Boulay F., Tardif M., Brouchon L., and Vignais P.. 1990. “The Human N-Formylpeptide Receptor. Characterization of Two cDNA Isolates and Evidence for a New Subfamily of G-Protein-Coupled Receptors.” *Biochemistry* 29 (50): 11123–33.

Bradford M. 1976. “A Rapid and Sensitive Method for the Quantitation of Microgram Quantities of Protein Utilizing the Principle of Protein-Dye Binding.” *Analytical Biochemistry* 72 (1–2): 248–54.

Brouet I. and Ohshima H.. 1995. “Curcumin, an Anti-Tumor Promoter and Anti-Inflammatory Agent, Inhibits Induction of Nitric Oxide Synthase in Activated Macrophages.” *Biochemical and Biophysical Research Communications* 206 (2): 533–40.

Browning J., Ward M., Wallner B., and Pepinsky R.. 1989. “Studies on the Structural Properties of Lipocortin-1 and the Regulation of Its Synthesis by Steroids.” *Progress in Clinical and Biological Research* 349 (December): 27–45.

Brzezinski A., Lynch H., Seibel M., Deng M., Nader T., and Wurtman R.. 1988. “The Circadian Rhythm of Plasma Melatonin During the Normal Menstrual Cycle and in Amenorrheic Women*.” *The Journal of Clinical Endocrinology & Metabolism* 66 (5): 891–95.

Buckingham J., John C., Solito E., Tierney T., Flower R. J., Christian H., and Morris J.. 2006. “Annexin 1, Glucocorticoids, and the Neuroendocrine–Immune Interface.” *Annals of the New York Academy of Sciences* 1088 (1): 396–409.

Buijs R., Wortel J., Van Heerikhuize J., and Kalsbeek A.. 1997. “Novel Environment Induced Inhibition of Corticosterone Secretion: Physiological Evidence for a Suprachiasmatic Nucleus Mediated Neuronal Hypothalamo-Adrenal Cortex Pathway.” *Brain Research* 758 (1–2): 229–36.

Burke J. and Dennis E.. 2008. “Phospholipase A2 Structure/function, Mechanism, and Signaling.” *The Journal of Lipid Research* 50 (Supplement): S237–S242.

Butler A. and Nicholson R.. 2003. *Life, Death and Nitric Oxide*. Royal Society of Chemistry.

Cao Y., Li Y., Edelweiss M., Arun B., Rosen D., Resetkova E., Wu Y., Liu J., Sahin A., and Albarracin C.. 2008. “Loss of Annexin A1 Expression in Breast Cancer Progression.” *Applied Immunohistochemistry & Molecular Morphology: AIMM / Official Publication of the Society for Applied Immunohistochemistry* 16 (6): 530–34.

Ceccatelli S., Hulting A. L., Zhang X.,. Gustafsson L, Villar M., and Hökfelt T.. 1993. “Nitric Oxide Synthase in the Rat Anterior Pituitary Gland and the Role of Nitric Oxide in Regulation of Luteinizing Hormone Secretion.” *Proceedings of the National Academy of Sciences* 90 (23): 11292–96.

Chang B., Hawes N., Hurd R., Davisson M., Nusinowitz S., and Heckenlively J.. 2002. “Retinal Degeneration Mutants in the Mouse.” *Vision Research* 42 (4): 517–25.

Chang J., Musser J., and McGregor H.. 1987. “Phospholipase A< Sub> 2</sub>: Function and Pharmacological Regulation.” *Biochemical Pharmacology* 36 (15): 2429–36.

Chapman L., Nishimura A., Buckingham J., Morris J., and Christian H.. 2002. “Externalization of Annexin I from A Folliculo-Stellate-Like Cell Line.” *Endocrinology* 143 (11): 4330–38.

Chapman L., Epton M., Buckingham J., Morris J., and Christian H.. 2003. “Evidence for a Role of the Adenosine 5′-Triphosphate-Binding Cassette Transporter A1 in the Externalization of Annexin I from Pituitary Folliculo-Stellate Cells.” *Endocrinology* 144 (3): 1062–73.

Childs G., Unabia G., Burke J., and Marchetti C.. 1987. “Secretion from Corticotropes after Avidin-Fluorescein Stains for Biotinylated Ligands (CRF or AVP).” *American Journal of Physiology - Endocrinology and Metabolism* 252 (3): E347–E356.

Christian H., Goulding N., Kahan M., Wang H., Morris J., Flower R. J., and Buckingham J.. 1996. “Detection of Lipocortin 1 (LC1) and LC1 Binding Sites in the Rat Aanterior Pituitary Gland by Fluorescent Aactivated Cell Analysis/Sorting (FACS).” *British Journal of Pharmacology* 119 (S1): 61P.

Christian H., Taylor A., Flower R. J., Morris J., and Buckingham J.. 1997. “Characterization and Localization of Lipocortin 1-Binding Sites on Rat Anterior Pituitary Cells by Fluorescence-Activated Cell Analysis/Sorting and Electron Microscopy.” *Endocrinology* 138 (12): 5341–51.

Chrousos and Gold. 1992. “The Concepts of Stress and Stress System Disorders: Overview of Physical and Behavioral Homeostasis.” *JAMA* 267 (9): 1244–52.

Cirino G., Flower R. J., Browning J., Sinclair L., and. Pepinsky R. 1987. “Recombinant Human Lipocortin 1 Inhibits Thromboxane Release from Guinea-Pig Isolated Perfused Lung.” *Nature* 328 (6127): 270–72.

Clancy R., Varenika B., Huang W., Ballou L., Attur M., Amin A., and Abramson S.. 2000. “Nitric Oxide Synthase/COX Cross-Talk: Nitric Oxide Activates COX-1 But Inhibits COX-2-Derived Prostaglandin Production.” *The Journal of Immunology* 165 (3): 1582–87.

Cocchia D. and Miami N.. 1980. “Immunocytochemical Localization of the Brain-Specific S-100 Protein in the Pituitary Gland of Adult Rat.” *Journal of Neurocytology* 9 (6): 771–82.

Cone R. and Mountjoy K.. 1993. “Molecular Genetics of the ACTH and Melanocyte-Stimulating Hormone Receptors.” *Trends in Endocrinology & Metabolism* 4 (7): 242–47.

Croxtall J. and Flower R. J.. 1992. “Lipocortin 1 Mediates Dexamethasone-Induced Growth Arrest of the A549 Lung Adenocarcinoma Cell Line.” *Proceedings of the National Academy of Sciences* 89 (8): 3571–75.

Croxtall J., Choudhury Q., Newman S., and Flower R. J.. 1996. “Lipocortin 1 and the Control of cPLA2 Activity in A549 Cells: Glucocorticoids Block EGF Stimulation of cPLA2 Phosphorylation.” *Biochemical Pharmacology* 52 (2): 351–56.

Crumeyrolle-Arias M., Latouche J., Jammes H., Djiane J., Kelly P., Reymond M., and Haour F.. 1993. “Prolactin Receptors in the Rat Hypothalamus: Autoradiographic Localization and Characterization.” *Neuroendocrinology* 57 (3): 457–66.

Crumpton M. and Dedman J.. 1990. “Protein Terminology Tangle.” *Nature* 345 (6272): 212–212.

Czeisler C. and Klerman E.. 1999. “Circadian and Sleep-Dependent Regulation of Hormone Release in Humans.” *Recent Progress in Hormone Research* 54: 97–130; discussion 130–132.

D’Acquisto F., Paschalidis N., Raza K., Buckley C., Flower R. J., and Perretti M.. 2008. “Glucocorticoid Treatment Inhibits Annexin-1 Expression in Rheumatoid Arthritis CD4+ T Cells.” *Rheumatology (Oxford, England)* 47 (5): 636–39.

D’Acquisto F., Merghani A., Lecona E., Rosignoli G., Raza K., Buckley C. D., Flower R. J., and Perretti M.. 2007. “Annexin-1 Modulates T-Cell Activation and Differentiation.” *Blood* 109 (3): 1095–1102.

D’Acunto C. W., Fontanella B., Rodriquez M., Taddei M., Parente L., and Petrella A.. 2010. “Histone Deacetylase Inhibitor FR235222 Sensitizes Human Prostate Adenocarcinoma Cells to Apoptosis through up-Regulation of Annexin A1.” *Cancer Letters* 295 (1): 85–91.

D’Acunto C. W., Gbelcova H., Festa M., and Ruml T.. 2014. “The Complex Understanding of Annexin A1 Phosphorylation.” *Cellular Signalling* 26 (1): 173–78.

Dasen J. S. and Rosenfeld M. G.. 2001. “Signaling and Transcriptional Mechanisms in Pituitary Development.” *Annual Review of Neuroscience* 24 (1): 327–55.

Dawson T. and Dawson V.. 1995. “REVIEW : Nitric Oxide: Actions and Pathological Roles.” *The Neuroscientist* 1 (1): 7 –18.

Dayanithi G. and Antoni F.. 1989. “Rapid as Well as Delayed Inhibitory Effects of Glucocorticoid Hormones on Pituitary Adrenocorticotropic Hormone Release Are Mediated by Type II Glucocorticoid Receptors and Require Newly Synthesized Messenger Ribonucleic Acid as Well as Protein*.” *Endocrinology* 125 (1): 308–13.

De Jesús M., Sallés J., Meana J., and Callado L.. 2006. “Characterization of CB1 Cannabinoid Receptor Immunoreactivity in Postmortem Human Brain Homogenates.” *Neuroscience 140* (2): 635–43.

De Maria J., Lerant A., and Freeman M.. 1999. “Prolactin Activates All Three Populations of Hypothalamic Neuroendocrine Dopaminergic Neurons in Ovariectomized Rats.” *Brain Research* 837 (1–2): 236–41.

Den Ouden D. and Meinders A.. 2005. “Vasopressin: Physiology and Clinical Use in Patients with Vasodilatory Shock: A Review.” *The Netherlands Journal of Medicine* 63 (1): 4–13.

Devnath S. and Inoue K.. 2008. “An Insight to Pituitary Folliculo-Stellate Cells.” *Journal of Neuroendocrinology* 20 (6): 687–91.

Di Rosa M., Flower R. J., Hirata F., Parente L., and Russo-Marie F.. 1984. “Anti-Phospholipase Proteins.” *Prostaglandins* 28 (4): 441–42.

Doherty P., Wu D., and Matt K.. 1990. “Hyperprolactinemia Preferentially Inhibits Erectile Function in Adrenalectomized Male Rats.” *Life Sciences* 47 (2): 141–48.

Dreier R., Schmid K., Gerke V., and Riehemann K.. 1998. “Differential Expression of Annexins I, II and IV in Human Tissues: An Immunohistochemical Study.” *Histochemistry and Cell Biology* 110 (2): 137–48.

Dubey A., Puri C., Puri V., and Kumar A.. 1983. “Day and Night Levels of Hormones in Male Rhesus Monkeys Kept under Controlled or Constant Environmental Light.” *Experientia* 39 (2): 207–9.

Dubois R. 1896. “Étude Sur Le Mécanisme de La Thermogenèse et Du Sommeil Chez Les Mammifères: Physiologie Comparée de La Marmotte.”

Dunlap J.. 1999. “Molecular Bases for Circadian Clocks.” *Cell*.

Dunn J., Scheving L., and Millet P.. 1972. “Circadian Variation in Stress-Evoked Increases in Plasma Corticosterone.” *American Journal of Physiology -- Legacy Content* 223 (2): 402–6.

Duvilanski B., Zambruno C., Seilicovich A., Pisera D., Lasaga M., Diaz M., Belova N.,. Rettori V., and McCann S.. 1995. “Role of Nitric Oxide in Control of Prolactin Release by the Adenohypophysis.” *Proceedings of the National Academy of Sciences* 92 (1): 170–74.

Dvornyk V., Vinogradova O., and Nevo E.. 2003. “Origin and Evolution of Circadian Clock Genes in Prokaryotes.” *Proceedings of the National Academy of Sciences of the United States of America* 100 (5): 2495–2500.

Eberhard D., Brown M., and Vandenberg S.. 1994. “Alterations of Annexin Expression in Pathological Neuronal and Glial Reactions. Immunohistochemical Localization of Annexins I, II (p36 and p11 Subunits), IV, and VI in the Human Hippocampus.” *The American Journal of Pathology* 145 (3): 640–49.

Elliott J. 1976. “Circadian Rhythms and Photoperiodic Time Measurement in Mammals.” *Federation Proceedings* 35 (12): 2339–46.

Euker J., Meites J., and Riegle G.. 1975. “Effects of Acute Stress on Serum LH and Prolactin in Intact, Castrate and Dexamethasone-Treated Male Rats*.” *Endocrinology* 96 (1): 85–92.

Evans W., Cronin M., and Thorner M.. 1982. “Hypogonadism in Hyperprolactinemia-Proposed Mechanisms.” *Frontiers in Neuroendocrinology* 7: 77–122.

Fahrenkrug J., Hannibal J., and Georg B.. 2008. “Diurnal Rhythmicity of the Canonical Clock Genes Per1, Per2 and Bmal1 in the Rat Adrenal Gland Is Unaltered after Hypophysectomy.” *Journal of Neuroendocrinology* 20 (3): 323–29.

Falini B., Tiacci E., Liso A., Basso K., Sabattini E., Pacini R., Foa R., Pulsoni A., Dalla Favera R., and Pileri S.. 2004. “Simple Diagnostic Assay for Hairy Cell Leukaemia by Immunocytochemical Detection of Annexin A1 (ANXA1).” *Lancet* 363 (9424): 1869–70.

Fang V. and Shian L.-R.. 1981. “Adrenal Influence on Pituitary Secretion of Thyrotropin and Prolactin in Rats.” *Endocrinology* 108 (4): 1545–51.

Faria P., Aparecida A., Nascimento R., João W., Mota A., José S., Francisco A., Domingos A., Maria S., and Ricardo L.. 2010. “Expression of Annexin A1 mRNA in Peripheral Blood from Oral Squamous Cell Carcinoma Patients.” *Oral Oncology* 46 (1): 25–30.

Ferlazzo V., D’Agostino P., Milano S., Caruso R., Feo S., Cillari E., and Parente L.. 2003. “Anti-Inflammatory Effects of Annexin-1: Stimulation of IL-10 Release and Inhibition of Nitric Oxide Synthesis.” *International Immunopharmacology* 3 (10–11): 1363–69.

Fletcher W., Anderson N., and Everett J.. 1975. “Intercellular Communication in the Rat Anterior Pituitary Gland: An in Vivo and in Vitro Study.” *The Journal of Cell Biology* 67 (2): 469 –476.

Flower R. J. and Blackwell G.. 1979. “Anti-Inflammatory Steroids Induce Biosynthesis of a Phospholipase A2 Inhibitor Which Prevents Prostaglandin Generation.” *Nature* 278 (5703): 456–59.

Fox S., Hoefer M., Bartke A., and Smith S.. 1987. “Suppression of Pulsatile LH Secretion, Pituitary GnRH Receptor Content and Pituitary Responsiveness to GnRH by Hyperprolactinemia in the Male Rat.” *Neuroendocrinology* 46 (4): 350–59.

Freeman M., Kanyicska B., Lerant A., and Nagy G.. 2000. “Prolactin: Structure, Function, and Regulation of Secretion.” *Physiological Reviews* 80 (4): 1523–1631.

Furth J., Gadsden E., and Upton A.. 1953. “ACTH Secreting Transplantable Pituitary Tumors” 84: 253–54.

Fuxe K.. 1963. “Cellular Localization of Monoamines in the Median Eminence and the Infundibular Stem of Some Mammals.” *Zeitschrift Für Zellforschung Und Mikroskopische Anatomie* 61 (5): 710–24.

Gallagher T., Yoshida K., Roffwarg H., Fukushima D., Weitzman E., and Hellman L.. 1973. “ACTH and Cortisol Secretory Patterns in Man.” *The Journal of Clinical Endocrinology & Metabolism* 36 (6): 1058–68.

Gao J.-L., Chen H., Filie J., Kozak C., and Murphy P.. 1998. “Differential Expansion of the N-Formylpeptide Receptor Gene Cluster in Human and Mouse.” *Genomics* 51 (2): 270–76.

Gavins F. 2010. “Are Formyl Peptide Receptors Novel Targets for Therapeutic Intervention in Ischaemia–reperfusion Injury?” *Trends in Pharmacological Sciences* 31 (6): 266–76.

Gavins F. and Hickey M.. 2012. “Annexin A1 and the Regulation of Innate and Adaptive Immunity.” *Frontiers in Immunology* 3 (November).

Geracioti T., Orth D., Ekhator N., Blumenkopf B., and Loosen P.. 1992. “Serial Cerebrospinal Fluid Corticotropin-Releasing Hormone Concentrations in Healthy and Depressed Humans.” *The Journal of Clinical Endocrinology & Metabolism* 74 (6): 1325–30.

Gerke V. and Moss S.. 2002. “Annexins: From Structure to Function.” *Physiological Reviews* 82 (2): 331–71.

Gibson M., Ingraham L., and Dobrjansky A.. 2000. “Soluble Factors Guide Gonadotropin-Releasing Hormone Axonal Targeting to the Median Eminence [1].” *Endocrinology* 141 (9): 3065–71.

Gilbert R. and Herschman H.. 1993. “‘Macrophage’ Nitric Oxide Synthase Is a Glucocorticoid-Inhibitable Primary Response Gene in 3T3 Cells.” *Journal of Cellular Physiology* 157 (1): 128–32.

Gimpl G. and Fahrenholz F.. 2001. “The Oxytocin Receptor System: Structure, Function, and Regulation.” *Physiological Reviews* 81 (2): 629–83.

Gloddek J., Pagotto U., Paez Pereda M., Arzt E., Stalla G., and Renner U.. 1999. “Pituitary Adenylate Cyclase-Activating Polypeptide, Interleukin-6 and Glucocorticoids Regulate the Release of Vascular Endothelial Growth Factor in Pituitary Folliculostellate Cells.” *Journal of Endocrinology* 160 (3): 483–90.

Gold P. and Chrousos G.. 2002. “Organization of the Stress System and Its Dysregulation in Melancholic and Atypical Depression: High vs Low CRH/NE States.” 7 (3): 254. 22p.

Goudreau J., Lindley S., Lookingland K., and Moore K.. 1992. “Evidence That Hypothalamic Periventricular Dopamine Neurons Innervate the Intermediate Lobe of the Rat Pituitary.” *Neuroendocrinology* 56 (1): 100–105.

Goulding N. and Guyre P.. 1992. “Regulation of Inflammation by Lipocortin 1.” *Immunology Today* 13 (8): 295–97.

Goulding N., Godolphin J., Sharland P., Maddison P., Sampson M., Peers S., and Flower. R. J. 1990. “Anti-Inflammatory Lipocortin 1 Production by Peripheral Blood Leucocytes in Response to Hydrocortisone.” *The Lancet*, Originally published as Volume 1, Issue 8703, 335 (8703): 1416–18.

Goulding N., Jefferiss C., An L., Rigby W., and Guyre P.. 1992. “Specific Binding of Lipocortin-1 (annexin I) to Monocytes and Neutrophils Is Decreases in Rheumatoid Arthritis.” *Arthritis and Rheumatism* 35 (11): 1395–97.

Grattan D., Steyn F., Kokay I., Anderson G., and Bunn S.. 2008. “Pregnancy-Induced Adaptation in the Neuroendocrine Control of Prolactin Secretion.” *Journal of Neuroendocrinology* 20 (4): 497–507.

Greef W. De, Voogt J., Visser T., Lamberts S., and Van Der Schoot P.. 1987. “Control of Prolactin Release Induced by Suckling.” *Endocrinology* 121 (1): 316–22.

Green E.. 1966. *Biology of the Laboratory Mouse*. Blakiston Division, McGraw-Hill.

Green J. and Harris G.. 1947.“The Neurovascular Link between the Neurohypophysis and Adenohypophysis.” *J. Endocr*.

Griess P. 1879. “Griess Reagent: A Solution of Sulphanilic Acid and A-Naphthylamine in Acetic Acid Which Gives a Pink Colour on Reaction with the Solution Obtained after Decomposition of Nitrosyl Complexes.” *Chem. Ber* 12: 427.

GuéRineau N., Corcuff J.-B., Tabarin A., and Mollard P.. 1991. “Spontaneous and Corticotropin-Releasing Factor-Induced Cytosolic Calcium Transients in Corticotrophs*.” *Endocrinology* 129 (1): 409–20.

Guerrera I., Quetier I., Fetouchi R., Moreau F., Vauloup-Fellous C., Lekbaby B., Rousselot C., et al. 2014. “Regulation of Interleukin-6 in Head and Neck Squamous Cell Carcinoma Is Related to Papillomavirus Infection.” *Journal of Proteome Research* 13 (2): 1002–11.

Guillaumond F., Boyer B., Becquet D., Guillen S., Kuhn L., Garin J., Belghazi M., Bosler O., Franc J.-L., and François-Bellan A.-M.. 2011. “Chromatin Remodeling as a Mechanism for Circadian Prolactin Transcription: Rhythmic NONO and SFPQ Recruitment to HLTF.” *The FASEB Journal* 25 (8): 2740–56.

Gumbiner B. and Kelly R.. 1982. “Two Distinct Intracellular Pathways Transport Secretory and Membrane Glycoproteins to the Surface of Pituitary Tumor Cells.” *Cell* 28 (1): 51–59.

Guo H., McKinley Brewer J., Lehman M., and Bittman E.. 2006. “Suprachiasmatic Regulation of Circadian Rhythms of Gene Expression in Hamster Peripheral Organs: Effects of Transplanting the Pacemaker.” *The Journal of Neuroscience* 26 (24): 6406–12.

Gwinner E.. 2010. “Artspezifische Muster Der Zugunruhe Bei Laubsängern Und Ihre Mögliche Bedeutung Für Die Beendigung Des Zuges Im Winterquartier.” *Zeitschrift Für Tierpsychologie* 25 (7): 843–53.

Gyr K., Beglinger C., Kohler E., Trautzl U., Keller U., and Bloom S.. 1987. “Circulating Somatostatin. Physiological Regulator of Pancreatic Function?” *Journal of Clinical Investigation* 79 (6): 1595–1600.

Halmi N. and Gude W.. 1954. “The Morphogenesis of Pituitary Tumors Induced by Radiothyroidectomy in the Mouse and the Effects of Their Transplantation on the Pituitary Body of the Host.” *The American Journal of Pathology* 30 (3): 403–19.

Handwerger S., Markoff E., and Richards R.. 1991. “3. Regulation of the Synthesis and Release of Decidual Prolactin by Placental and Autocrine/paracrine Factors.” *Placenta* 12 (2): 121–30.

Hazlerigg D., Andersson H., Johnston J., and Lincoln G.. 2004. “Molecular Characterization of the Long-Day Response in the Soay Sheep, a Seasonal Mammal.” *Current Biology* 14 (4): 334–39.

Herman J. and Seroogy K.. 2006. “Hypothalamic-Pituitary-Adrenal Axis, Glucocorticoids, and Neurologic Disease.” *Neurologic Clinics* 24 (3): 461–81.

Higuchi H., Hasegawa A., and Yamaguchi T.. 2005. “Transcriptional Regulation of Neuronal Genes and Its Effect on Neural Functions: Transcriptional Regulation of Neuropeptide Y Gene by Leptin and Its Effect on Feeding.” *Journal of Pharmacological Sciences* 98 (3): 225–31.

Hirata F. 1982. “Lipomodulin: A Possible Mediator of the Action of Glucocorticoids.” *Advances in Prostaglandin, Thromboxane, and Leukotriene Research* 11 (December): 73–78.

Hirata F., Schiffmann E., Venkatasubramanian K., Salomon D., and Axelrod J.. 1980. “A Phospholipase A2 Inhibitory Protein in Rabbit Neutrophils Induced by Glucocorticoids.” *Proceedings of the National Academy of Sciences* 77 (5): 2533–36.

Hiroshige T. and Wada-Okada S.. 1973. “Diurnal Changes of Hypothalamic Content of Corticotropin-Releasing Activity in Female Rats at Various Stages of the Estrous Cycle.” *Neuroendocrinology* 12 (4-5): 316–19.

Ho B., Stadnicka A., Prather P., Buckley A., Current L., Bosnjak Z., and Kwok W.-M.. 2000. “Cannabinoid CB1 Receptor-Mediated Inhibition of Prolactin Release and Signaling Mechanisms in GH $_4$ C $_1$ Cells $^1$.” *Endocrinology* 141 (5): 1675–85.

Ho B. and Zhao J.. 1996. “Determination of the Cannabinoid Receptors in Mouse × Rat Hybridoma NG108-15 Cells and Rat GH4C 1 Cells.” *Neuroscience Letters* 212 (2): 123–26.

Hofman, Michel A. 1997. “Lifespan Changes in the Human Hypothalamus.” *Experimental Gerontology* 32 (4–5): 559–75.

Hofman M. 2004. “The Brain’s Calendar: Neural Mechanisms of Seasonal Timing.” *Biological Reviews* 79 (1): 61–77.

Horlick K., Cheng I., Wong W., Wakeland E., and Nick H.. 1991. “Mouse Lipocortin I Gene Structure and Chromosomal Assignment: Gene Duplication and the Origins of a Gene Family.” *Genomics* 10 (2): 365–74.

Horvath T. 1997. “Suprachiasmatic Efferents Avoid Phenestrated Capillaries but Innervate Neuroendocrine Cells, Including Those Producing Dopamine [1].” *Endocrinology* 138 (3): 1312–20.

Howles C. 2000. “Role of LH and FSH in Ovarian Function.” *Molecular and Cellular Endocrinology* 161 (1–2): 25–30.

Howlett A. 2005. “Cannabinoid Receptor Signaling.” In *Cannabinoids*, edited by Prof. R. Pertwee, 53–79. Handbook of Experimental Pharmacology 168. Springer Berlin Heidelberg. http://link.springer.com/chapter/10.1007/3-540-26573-2_2.

Inokuchi J., Lau A., Tyson D., and Ornstein D.. 2009. “Loss of Annexin A1 Disrupts Normal Prostate Glandular Structure by Inducing Autocrine IL-6 Signaling.” *Carcinogenesis* 30 (7): 1082–88.

Inoue K., Matsumoto H., Koyama C., Shibata K., Nakazato Y., and Ito A.. 1992. “Establishment of a Folliculo-Stellate-like Cell Line from a Murine Thyrotropic Pituitary Tumor.” *Endocrinology* 131 (6): 3110–16.

Inoue K., Couch E., Takano K., and Ogawa S.. 1999. “The Structure and Function of Folliculo-Stellate Cells in the Anterior Pituitary Gland.” *Archives of Histology and Cytology* 62 (3): 205–18.

Ito A., Naito M., Kawashima K., and Watanabe H. 1984. “Establishment of transplantable thyrotropic pituitary tumor in radiothyroidectomized BdF, mice.” In *Proceedings 25th A-bomb Disease Study Group*. Nagasaki.

Jacobson L.. 2005. “Hypothalamic–pituitary–adrenocortical Axis Regulation.” *Endocrinology and Metabolism Clinics of North America* 34 (2): 271–92.

John C., Gavins F., Buss N., Cover P., and Buckingham J.. 2008. “Annexin A1 and the Formyl Peptide Receptor Family: Neuroendocrine and Metabolic Aspects.” *Current Opinion in Pharmacology* 8 (6): 765–76.

Johnson C., Golden S., and Kondo T.. 1998. “Adaptive Significance of Circadian Programs in Cyanobacteria.” *Trends in Microbiology*.

Johnson M., Kamso-Pratt J., Whetsell W., and Pepinsky R.. 1989. “Lipocortin-1 Immunoreactivity in the Normal Human Central Nervous System and Lesions with Astrocytosis.” *American Journal of Clinical Pathology* 92 (4): 424–29.

Johnston C. and Negro-Vilar A.. 1988. “Role of Oxytocin on Prolactin Secretion during Proestrus and in Different Physiological or Pharmacological Paradigms.” *Endocrinology* 122 (1): 341–50.

Johnston J., Cagampang F., J. Stirland A., Carr A.-J., White M., Davis J., and Loudon A.. 2003. “Evidence for an Endogenous per1- and ICER-Independent Seasonal Timer in the Hamster Pituitary Gland.” *The FASEB Journal* 17 (8): 810–15.

Johnston J., Ebling F., and Hazlerigg D.. 2005. “Photoperiod Regulates Multiple Gene Expression in the Suprachiasmatic Nuclei and Pars Tuberalis of the Siberian Hamster (Phodopus Sungorus).” *European Journal of Neuroscience* 21 (11): 2967–74.

Jones M. and Gillham B.. 1988. “Factors Involved in the Regulation of Adrenocorticotropic Hormone/beta-Lipotropic Hormone.” *Physiological Reviews* 68 (3): 743–818.

Kadva A., Djahanbakhch O., Monson J., Di W., and Silman R.. 2013. “Elevated Nocturnal Melatonin Is a Consequence of Gonadotropin-Releasing Hormone Deficiency in Women with Hypothalamic Amenorrhea”. http://press.endocrine.org/doi/abs/10.1210/jcem.83.10.5155.

Kalsbeek A., Ruiter M., La Fleur S., Van Heijningen C., and Buijs R.. 2003. “The Diurnal Modulation of Hormonal Responses in the Rat Varies with Different Stimuli.” *Journal of Neuroendocrinology* 15 (12): 1144–55.

Keller-Wood M. and Dallman M.. 1984. “Corticosteroid Inhibition of ACTH Secretion*.” *Endocrine Reviews* 5 (1): 1–24.

Kennett J., Poletini M., and Freeman M.. 2008. “Vasoactive Intestinal Polypeptide Modulates the Estradiol-Induced Prolactin Surge by Entraining Oxytocin Neuronal Activity.” *Brain Research* 1196 (February): 65–73.

Kishi T. and Elmquist J.. 2005. “Body Weight Is Regulated by the Brain: A Link between Feeding and Emotion.” *Molecular Psychiatry* 10 (2): 132–46.

Kiss J., Kanyicska B., and Nagy G.. 1986. “The Hypothalamic Paraventricular Nucleus Has a Pivotal Role in Regulation of Prolactin Release in Lactating Rats.” *Endocrinology* 119 (2): 870–73.

Kitchener P., Di Blasi F., Borrelli E., and Piazza P.. 2004. “Differences between Brain Structures in Nuclear Translocation and DNA Binding of the Glucocorticoid Receptor during Stress and the Circadian Cycle.” *European Journal of Neuroscience* 19 (7): 1837–46.

Knott C., Stern G., and Wilkin G.. 2000. “Inflammatory Regulators in Parkinson’s Disease: iNOS, Lipocortin-1, and Cyclooxygenases-1 and -2.” *Molecular and Cellular Neurosciences* 16 (6): 724–39.

Kobayashi H., Wada M., Uemura H., and Ueck M.. 1972. “Uptake of Peroxidase from the Third Ventricle by Ependymal Cells of the Median Eminence.” *Zeitschrift Für Zellforschung Und Mikroskopische Anatomie* 127 (4): 545–51.

Koike K., Aono T., Miyake A., Tasaka K., Chatani F., and Kurachi K.. 1984. “Effect of Pituitary Transplants on the LH-RH Concentrations in the Medial Basal Hypothalamus and Hypophyseal Portal Blood.” *Brain Research* 301 (2): 253–58.

Koike K., Zhang Z., Sakamoto Y., Kanda Y., Murakami K., Miyake A., and Inoue M.. 1997. “The Pituitary Folliculo-Stellate Cell Line TtT/GF Augments Basal and Trhinduced Prolactin Secretion by GH3 Cell.” *Life Sciences* 61 (25): 2491–97.

Kolesnick R., Musacchio I., Thaw C., and Gershengorn M.. 1984. “Arachidonic Acid Mobilizes Calcium and Stimulates Prolactin Secretion from GH3 Cells.” *American Journal of Physiology - Endocrinology and Metabolism* 246 (5): E458–E462.

Korf H.-W. and Stehle J.. 2002. “The Circadian System: Circuits-Cells-Clock Genes.” *Cell and Tissue Research* 309 (1): 1–2.

Korf H.-W. and von Gall C.. 2013. “Circadian Physiology.” In *Neuroscience in the 21st Century*, edited by Donald W. Pfaff, 1813–45. Springer New York. http://link.springer.com/referenceworkentry/10.1007/978-1-4614-1997-6_65.

Korf H.-W. and von Gall C.. 2013. *Neuroscience in the 21st Century*. Edited by Donald W. Pfaff. New York, NY: Springer New York.

Kozlowski G. and Coates P.. 1985. “Ependymoneuronal Specializations between LHRH Fibers and Cells of the Cerebroventricular System.” *Cell and Tissue Research* 242 (2): 301–11.

Lampiao F., Strijdom H., and Du Plessis S.. 2006. “Direct Nitric Oxide Measurement in Human Spermatozoa: Flow Cytometric Analysis Using the Fluorescent Probe, Diaminofluorescein.” *International Journal of Andrology* 29 (5): 564–67.

Lehrman D. and Brody P.. 1961. “Does Prolactin Induce Incubation Behaviour in the Ring Dove?” *Journal of Endocrinology* 22 (3): 269–75.

Lerant A., Herman M., and Freeman M.. 1996. “Dopaminergic Neurons of Periventricular and Arcuate Nuclei of Pseudopregnant Rats: Semicircadian Rhythm in Fos-Related Antigens Immunoreactivities and in Dopamine Concentration.” *Endocrinology* 137 (9): 3621–28.

Li C.-F., Shen K.-H., Huang L.-C., Huang H.-Y., Wang Y.-H., and Wu T.-F.. 2010. “Annexin-I Overexpression Is Associated with Tumour Progression and Independently Predicts Inferior Disease-Specific and Metastasis-Free Survival in Urinary Bladder Urothelial Carcinoma.” *Pathology* 42 (1): 43–49.

Lincoln G. and Clarke I.. 1997. “Refractoriness to a Static Melatonin Signal Develops in the Pituitary Gland for the Control of Prolactin Secretion in the Ram.” *Biology of Reproduction* 57 (2): 460–67.

Lincoln G., Clarke I., Hut R., and Hazlerigg D.. 2006. “Characterizing a Mammalian Circannual Pacemaker.” *Science* 314 (5807): 1941–44.

Liu C. and Hermann T.. 1978. “Characterization of Ionomycin as a Calcium Ionophore.” *Journal of Biological Chemistry* 253 (17): 5892–94.

Mah P. and Webster J.. 2002. “Hyperprolactinemia: Etiology, Diagnosis, and Management.” *Seminars in Reproductive Medicine* 20 (4): 365–74.

Mai L.-M., Shieh K.-R., and Pan J.-T.. 1994. “Circadian Changes of Serum Prolactin Levels and Tuberoinfundibular Dopaminergic Neuron Activities in Ovariectomized Rats Treated with or without Estrogen: The Role of the Suprachiasmatic Nuclei.” *Neuroendocrinology* 60 (5): 520–26.

Mansour A., Meador-Woodruff J., Bunzow J., Civelli O., Akil H., and Watson S.. 1990. “Localization of Dopamine D2 Receptor mRNA and D1 and D2 Receptor Binding in the Rat Brain and Pituitary: An in Situ Hybridization- Receptor Autoradiographic Analysis.” *The Journal of Neuroscience* 10 (8): 2587–2600.

Marchetti C., Childs G., and Brown A.. 1987. “Membrane Currents of Identified Isolated Rat Corticotropes and Gonadotropes.” *American Journal of Physiology - Endocrinology and Metabolism* 252 (3): E340–E346.

Márquez C., Nadal R., and Armario A.. 2005. “Responsiveness of the Hypothalamic–pituitary–adrenal Axis to Different Novel Environments Is a Consistent Individual Trait in Adult Male Outbred Rats.” *Psychoneuroendocrinology* 30 (2): 179–87.

Martin E., Nathan C., and Xie Q.. 1994. “Role of Interferon Regulatory Factor 1 in Induction of Nitric Oxide Synthase.” *The Journal of Experimental Medicine* 180 (3): 977–84.

Marzo V. Di, Bifulco M., and De Petrocellis L.. 2004. “The Endocannabinoid System and Its Therapeutic Exploitation.” *Nature Reviews Drug Discovery* 3 (9): 771–84.

Mastorakos G. and Pavlatou M.. 2005. “Exercise as a Stress Model and the Interplay Between the Hypothalamus-pituitary-adrenal and the Hypothalamus-pituitary-thyroid Axes.” *Hormone and Metabolic Research* 37 (9): 577–84.

McEwen B. 2000. “Allostasis, Allostatic Load, and the Aging Nervous System: Role of Excitatory Amino Acids and Excitotoxicity.” *Neurochemical Research* 25 (9-10): 1219–31.

McKanna J. 1993. “Lipocortin 1 Immunoreactivity Identifies Microglia in Adult Rat Brain.” *Journal of Neuroscience Research* 36 (4): 491–500.

McKanna J. and Zhang M.-Z.. 1997. “Immunohistochemical Localization of Lipocortin 1 in Rat Brain Is Sensitive to pH, Freezing, and Dehydration.” *Journal of Histochemistry & Cytochemistry* 45 (4): 527–38.

Meda P., Pepper M., Traub O., Willecke K., Gros D., Beyer E., Nicholson B., Paul D., and Orci L.. 1993. “Differential Expression of Gap Junction Connexins in Endocrine and Exocrine Glands.” *Endocrinology* 133 (5): 2371–78.

Messager S., Hazlerigg D., Mercer J., and Morgan P.. 2000. “Photoperiod Differentially Regulates the Expression of Per1 and ICER in the Pars Tuberalis and the Suprachiasmatic Nucleus of the Siberian Hamster.” *European Journal of Neuroscience* 12 (8): 2865–70.

Messager S., Ross A., Barrett P., and Morgan P.. 1999. “Decoding Photoperiodic Time through Per1 and ICER Gene Amplitude.” *Proceedings of the National Academy of Sciences* 96 (17): 9938–43.

Migeotte I., Communi D., and Parmentier M.. 2006. “Formyl Peptide Receptors: A Promiscuous Subfamily of G Protein-Coupled Receptors Controlling Immune Responses.” *Cytokine & Growth Factor Reviews* 17 (6): 501–19.

Minghetti L., Nicolini A., Polazzi E., Greco A., Perretti M., Parente L., and Levi G.. 1999. “Down-Regulation of Microglial Cyclo-Oxygenase-2 and Inducible Nitric Oxide Synthase Expression by Lipocortin 1.” *British Journal of Pharmacology* 126 (6): 1307–14.

Mitchner N., Garlick C., and Ben-Jonathan N.. 1998. “Cellular Distribution and Gene Regulation of Estrogen Receptorsα and B in the Rat Pituitary Gland [1].” *Endocrinology* 139 (9): 3976–83.

Mitsuishi H., Kato T., Chen M., L.-Y., Yako H., Higuchi M., Yoshida S., Kanno N., Ueharu H., and Kato Y.. 2013. “Characterization of a Pituitary-Tumor-Derived Cell Line, TtT/GF, That Expresses Hoechst Efflux ABC Transporter Subfamily G2 and Stem Cell Antigen 1.” *Cell and Tissue Research* 354 (2): 563–72.

Moncada S. and Higgs A.. 1993. “The L-Arginine-Nitric Oxide Pathway.” *New England Journal of Medicine* 329 (27): 2002–12.

Moore R. and Eichler V.. 1972. “Loss of a Circadian Adrenal Corticosterone Rhythm Following Suprachiasmatic Lesions in the Rat.” *Brain Research* 42 (1): 201–6.

Morgan P. 2000. “The Pars Tuberalis: The Missing Link in the Photoperiodic Regulation of Prolactin Secretion?” *Journal of Neuroendocrinology* 12 (4): 287–95.

Morgan P., Ross A., Graham S., Adam C., Messager S., and Barrett P.. 1998. “RAPID COMMUNICATION oPer1 Is an Early Response Gene Under Photoperiodic Regulation in the Ovine Pars Tuberalis.” *Journal of Neuroendocrinology* 10 (5): 319–23.

Mori M., Gotoh T., Nagasaki A., Takiguchi M., and Sonoki T.. 1998. “Regulation of the Urea Cycle Enzyme Genes in Nitric Oxide Synthesis.” *Journal of Inherited Metabolic Disease* 21 (1): 59–71.

Morris J., Christian H., Chapman L., Epton M., Buckingham J., Ozawa H., Nishi M., and Kawata M.. 2002. “Steroid Effects on Secretion from Subsets of Lactotrophs: Role of Folliculo-Stellate Cells and Annexin 1.” *Archives Of Physiology And Biochemistry* 110 (1-2): 54–61.

Morris J., and Christian H.. 2011. “Folliculo-Stellate Cells: Paracrine Communicators in the Anterior Pituitary.” *System* 1: 3.

Mountjoy K., Robbins L., Mortrud M., and Cone R.. 1992. “The Cloning of a Family of Genes That Encode the Melanocortin Receptors.” *Science* 257 (5074): 1248–51.

Munck, Allan. 2005. “Glucocorticoid Receptors and Physiology: A Personal History.” *Steroids* 70 (4): 335–44.

Munck A., Guyre P., and Holbrook N.. 1984. “Physiological Functions of Glucocorticoids in Stress and Their Relation to Pharmacological Actions*.” *Endocrine Reviews* 5 (1): 25–44.

Murai I. and Ben-Jonathan N.. 1987. “Posterior Pituitary Lobectomy Abolishes the Suckling-Induced Rise in Prolactin (PRL): Evidence for a PRLReleasing Factor in the Posterior Pituitary*.” *Endocrinology* 121 (1): 205–11.

Murphy L., Muñoz R., Adrian B., and Villanúa M.. 1998. “Function of Cannabinoid Receptors in the Neuroendocrine Regulation of Hormone Secretion.” *Neurobiology of Disease* 5 (6): 432–46.

Nagano T.. 1999. “Practical Methods for Detection of Nitric Oxide.” *Luminescence* 14 (6): 283–90.

Nagy G., Görcs T., and Halász B.. 1991. “Attenuation of the Suckling-Induced Prolactin Release and the High Afternoon Oscillations of Plasma Prolactin Secretion of Lactating Rats by Antiserum to Vasopressin.” *Neuroendocrinology* 54 (6): 566–70.

Nan Y., Yang S., Tian Y., Zhang W., Zhou B., Bu L., and Huo S.. 2009. “Analysis of the Expression Protein Profiles of Lung Squamous Carcinoma Cell Using Shot-Gun Proteomics Strategy.” *Medical Oncology (Northwood, London, England)* 26 (2): 215–21.

Neill J., Freeman M., and Tillson S.. 1971. “Control of the Proestrus Surge of Prolactin and Luteinizing Hormone Secretion by Estrogens in the Rat12.” *Endocrinology* 89 (6): 1448–53.

Newman S., Flower R. J., and Croxtall J.. 1994. “Dexamethasone Suppression of IL-1β-Induced Cyclooxygenase 2 Expression Is Not Mediated by Lipocortin-1 in A549 Cells.” *Biochemical and Biophysical Research Communications* 202 (2): 931–39.

Ohta K., Hirata Y., Imai T., and Marumo F.. 1993. “Interleukin-1β Induces Nitric Oxide Production by a Mouse Pituitary Tumour Cell Line (AtT20/D16).” *Journal of Endocrinology* 138 (3): 429–35.

Oishi K., Miyazaki K., Kadota K., Kikuno R., Nagase T., Atsumi G.-I., Ohkura N., et al. 2003. “Genome-Wide Expression Analysis of Mouse Liver Reveals CLOCK-Regulated Circadian Output Genes.” *Journal of Biological Chemistry* 278 (42): 41519–27.

Oishi Y., Okuda M., Takahashi H., Fujii T., and Morii S.. 1993. “Cellular Proliferation in the Anterior Pituitary Gland of Normal Adult Rats: Influences of Sex, Estrous Cycle, and Circadian Change.” *The Anatomical Record* 235 (1): 111–20.

Okamura H., Yamaguchi S., and Yagita K.. 2002. “Molecular Machinery of the Circadian Clock in Mammals.” *Cell and Tissue Research* 309 (1): 47–56.

Oksche A., Zimmermann P., and Oehmke H.. 1972. “Morphometric Studies of Tubero-Eminential Systems Controlling Reproductive Functions.” *Brain-Endocrine Interaction. Median Eminence: Structure and Function, Karger, Basel*, 142–53.

Oláh M., Milloh H., and Wenger T.. 2008. “The Role of Endocannabinoids in the Regulation of Luteinizing Hormone and Prolactin Release: Differences between the Effects of AEA and 2AG.” *Molecular and Cellular Endocrinology*, Supplement Issue: Basic and Pharmacological Aspects of Cannabinoid Activity in Nervous and Reproductive Systems, 286 (1–2, Supplement 1): S36–S40.

Oomizu S., Chaturvedi K., and Sarkar D.. 2004. “Folliculostellate Cells Determine the Susceptibility of Lactotropes to Estradiol’s Mitogenic Action.” *Endocrinology* 145 (3): 1473–80.

Oota Y., Kobayashi H., Nishioka R., and Bern H.. 1974. “Relationship Between Neurosecretory Axon and Ependymal Terminals on Capillary Walls in the Median Eminence of Several Vertebrates.” *Neuroendocrinology* 16 (2): 127–36.

Oster H., Damerow S., Kiessling S., Jakubcakova V., Abraham D., Tian J., Hoffmann M., and Eichele G.. 2006. “The Circadian Rhythm of Glucocorticoids Is Regulated by a Gating Mechanism Residing in the Adrenal Cortical Clock.” *Cell Metabolism* 4 (2): 163–73.

Ottenweller J., Tapp W., Pitman D., and Natelson B.. 1987. “Adrenal, Thyroid, and Testicular Hormone Rhythms in Male Golden Hamsters on Long and Short Days.” *American Journal of Physiology - Regulatory, Integrative and Comparative Physiology* 253 (2): R321–R328.

Pagotto U., Marsicano G., Fezza F., Theodoropoulou M., Grübler Y., Stalla J., Arzberger T., et al. 2001. “Normal Human Pituitary Gland and Pituitary Adenomas Express Cannabinoid Receptor Type 1 and Synthesize Endogenous Cannabinoids: First Evidence for a Direct Role of Cannabinoids on Hormone Modulation at the Human Pituitary Level [1].” *The Journal of Clinical Endocrinology & Metabolism* 86 (6): 2687–96.

Palacios M., Knowles R., Palmer M., and Moncada S.. 1989. “Nitric Oxide from L-Arginine Stimulates the Soluble Guanylate Cyclase in Adrenal Glands.” *Biochemical and Biophysical Research Communications* 165 (2): 802–9.

Paliege A., Kahl T., S. Schnermann S., and Bachmann S.. 2011. “Annexin A1 Inhibits Macula Densa Cyclooxygenase 2 and Nitric Oxide Synthase 1 Expression”, no. 25.

Palm I., van der Beek E., Swarts H., van der Vliet J., Wiegant V., Buijs R., and Kalsbeek A.. 2013. “Control of the Estradiol-Induced Prolactin Surge by the Suprachiasmatic Nucleus”. http://press.endocrine.org/doi/abs/10.1210/endo.142.6.8219.

Paschalidis N., Iqbal A., Maione F., Wood E., Perretti M., Flower R. J., and D’Acquisto F.. 2009. “Modulation of Experimental Autoimmune Encephalomyelitis by Endogenous Annexin A1.” *Journal of Neuroinflammation* 6: 33.

Pengelley E. and Fisher K.. 1957. “Onset and Cessation of Hibernation under Constant Temperature and Light in the Golden-Mantled Ground Squirrel (Citellus Lateralis).” *Nature* 180 (4598): 1371–72.

Perretti M. and Flower R. J.. 1993. “Modulation of IL-1-Induced Neutrophil Migration by Dexamethasone and Lipocortin 1.” *The Journal of Immunology* 150 (3): 992–99.

Perretti M. and Ahluwalia A.. 2000. “The Microcirculation and Inflammation: Site of Action for Glucocorticoids.” *Microcirculation* 7 (3): 147–61.

Perretti M. and Dalli J.. 2009. “Exploiting the Annexin A1 Pathway for the Development of Novel Anti-Inflammatory Therapeutics.” *British Journal of Pharmacology* 158 (4): 936–46.

Pertwee R. 2006. “The Pharmacology of Cannabinoid Receptors and Their Ligands: An Overview.” *International Journal of Obesity* 30 (S1): S13–S18.

Pertwee R. 2005. “Inverse Agonism and Neutral Antagonism at Cannabinoid CB1 Receptors.” *Life Sciences* 76 (12): 1307–24.

Philip J., Flower R. J., and Buckingham J.. 1998. “Blockade of the Classical Pathway of Protein Secretion Does Not Affect the Cellular Exportation of Lipocortin 1.” *Regulatory Peptides* 73 (2): 133–39.

Philipps C., Rose-John S., Rincke G., Fürstenberger G., and Marks F.. 1989. “cDNA-Cloning, Sequencing and Expression in Glucocorticoid-Stimulated Quiescent Swiss 3T3 Fibroblasts of Mouse Lipocortin I.” *Biochemical and Biophysical Research Communications* 159 (1): 155–62.

Phillips M. and Tashjian A.. 1982. “Characterization of an Early Inhibitory Effect of Glucocorticoids on Stimulated Adrenocorticotropin and Endorphin Release from a Clonal Strain of Mouse Pituitary Cells*.” *Endocrinology* 110 (3): 892–900.

Pi X. and Grattan D.. 1998. “Differential Expression of the Two Forms of Prolactin Receptor mRNA within Microdissected Hypothalamic Nuclei of the Rat.” *Molecular Brain Research* 59 (1): 1–12.

Pi X. and Grattan D.. 1999. “Expression of Prolactin Receptor mRNA Is Increased in the Preoptic Area of Lactating Rats.” *Endocrine* 11 (1): 91–98.

Pickering B., Andersen R., Lohmar P., Birk Y., and Li C.. 1963. “Adrenocorticotropin XXVII. On the Presence of Pig-Tyre Adrenocorticotropin in Sheep Pituitaries, and a Simple Method for the Isolation of As-Adrenocorticotropin.” *Biochimica et Biophysica Acta* 74: 763–73.

Pihoker C., Feeney R., Su J.-L., and Handwerger S.. 1991. “Lipocortin-I Inhibits the Synthesis and Release of Prolactin from Human Decidual Cells: Evidence for Autocrine/Paracrine Regulation by Lipocortin-I*.” *Endocrinology* 128 (2): 1123–28.

Piomelli D. 2003. “The Molecular Logic of Endocannabinoid Signalling.” *Nature Reviews Neuroscience* 4 (11): 873–84.

Popa G. 1930. “A Portal Circulation from the Pituitary to the Hypothalamic Region.” *Journal of Anatomy* 65 (Pt 1): 88–91.

Portanova R. and Sayers G.. 1974. “Corticosterone Suppression of ACTH Secretion: Actinomycin D Sensitive and Insensitive Components of the Response.” *Biochemical and Biophysical Research Communications* 56 (4): 928–33.

Probst-Cousin S., Kowolik D., Kuchelmeister K., Kayser C., Neundörfer B., and Heuss D.. 2002. “Expression of Annexin-1 in Multiple Sclerosis Plaques.” *Neuropathology and Applied Neurobiology* 28 (4): 292–300.

Qian X., Jin L., and Lloyd R.. 1998. “Percoll Density Gradient-Enriched Populations of Rat Pituitary Cells: Interleukin 6 Secretion, Proliferative Activity, and Nitric Oxide Synthase Expression.” *Endocrine Pathology* 9 (4): 339–46.

Qian X., Jin L., and Lloyd R.. 1999. “Estrogen Downregulates Neuronal Nitric Oxide Synthase in Rat Anterior Pituitary Cells and GH3 Tumors.” *Endocrine* 11 (2): 123–30.

Rees D., Palmer R., Schulz R., Hodson H., and Moncada S.. 1990. “Characterization of Three Inhibitors of Endothelial Nitric Oxide Synthase in Vitro and in Vivo.” *British Journal of Pharmacology* 101 (3): 746–52.

Reese J. and Katzenellenbogen B.. 1992. “Examination of the DNA-Binding Ability of Estrogen Receptor in Whole Cells: Implications for Hormone-Independent Transactivation and the Actions of Antiestrogens.” *Molecular and Cellular Biology* 12 (10): 4531–38.

Reppert S. and Weaver D.. 2002. “Coordination of Circadian Timing in Mammals.” *Nature* 418 (6901): 935–41.

Rhodes M.,Balestreire E., Czambel K., and Rubin R.. 2002. “Estrous Cycle Influences on Sexual Diergism of HPA Axis Responses to Cholinergic Stimulation in Rats.” *Brain Research Bulletin* 59 (3): 217–25.

Rhodes M., Kennell J., Belz E., Czambel K., and Rubin R.. 2004. “Rat Estrous Cycle Influences the Sexual Diergism of HPA Axis Stimulation by Nicotine.” *Brain Research Bulletin* 64 (3): 205–13.

Riddle O., Bates R., and Dykshorn S.. 1933. “The Preparation, Identification and Assay of Prolactin—a Hormone of the Anterior Pituitary.” *American Journal of Physiology -- Legacy Content* 105 (1): 191–216.

Rinehart J. and Farquhar M.. 1953. “Electron Microscopic Studies of the Anterior Pituitary Gland.” *Journal of Histochemistry & Cytochemistry* 1 (2): 93–113.

Rodrigues-Lisoni, Flavia Cristina, Sonia Oliani, Julia Buckingham, Egle Solito, and Eloiza Helena Tajara. 2006. “Annexin A1: From Gene Organization to Physiology.” *Calcium Binding Proteins* 1 (2): 72–76.

Roky R., Paut-Pagano L., Goffiri V., Kitahama K., Valatx J.-L., Kelly P., and Jouvet M.. 1996. “Distribution of Prolactin Receptors in the Rat Forebrain.” *Neuroendocrinology* 63 (5): 422–29.

Rondeel J., De Greef W., Visser T., and Voogt J.. 1988. “Effect of Suckling on the in Vivo Release of Thyrotropin-Releasing Hormone, Dopamine and Adrenaline in the Lactating Rat.” *Neuroendocrinology* 48 (1): 93–96.

Rosengarth A., Gerke V., and Luecke H.. 2001. “X-Ray Structure of Full-Length Annexin 1 and Implications for Membrane Aggregation.” *Journal of Molecular Biology* 306 (3): 489–98.

Rosengarth A., Rösgen J., Hinz H.-J., and Gerke V.. 2001. “Folding Energetics of Ligand Binding Proteins II. Cooperative Binding of Ca2+ to Annexin I.” *Journal of Molecular Biology* 306 (4): 825–35.

Rowan W.. 1926. “On Photoperiodism, Reproductive Periodicity, and the Animal Migrations of Birds and Certain Fishes.”

Russo-Marie F. and Duval D.. 1982. “Dexamethasone-Induced Inhibition of Prostaglandin Production Does Not Result from a Direct Action on Phospholipase Activities but Is Mediated through a Steroid-Inducible Factor.” *Biochimica et Biophysica Acta (BBA) - Lipids and Lipid Metabolism* 712 (1): 177–85.

Sahu, Abhiram. 2004. “Minireview: A Hypothalamic Role in Energy Balance with Special Emphasis on Leptin.” *Endocrinology* 145 (6): 2613–20.

Samson W., Lumpkin M., and McCann S.. 1986. “Evidence for a Physiological Role for Oxytocin in the Control of Prolactin Secretion*.” *Endocrinology* 119 (2): 554–60.

Schiffmann E., Corcoran B., and Wahl S.. 1975. “N-Formylmethionyl Peptides as Chemoattractants for Leucocytes.” *Proceedings of the National Academy of Sciences* 72 (3): 1059–62.

Schiffmann E., Showell H., Corcoran B., Ward P., Smith E., and Becker E.. 1975. “The Isolation and Partial Characterization of Neutrophil Chemotactic Factors from Escherichia Coli.” *The Journal of Immunology* 114 (6): 1831–37.

Schlaepfer D. and Haigler H.. 1987. “Characterization of Ca2+-Dependent Phospholipid Binding and Phosphorylation of Lipocortin I.” *Journal of Biological Chemistry* 262 (14): 6931–37.

Schlatter L. and Dokas L.. 1989. “Receptor Specificity of a Glucocorticoid- and Stress-Induced Hippocampal Protein.” *The Journal of Neuroscience* 9 (4): 1134–40.

Schmidt H.. 1994. “NO, Endogener Botenstoff Und Zellgift.” *Medizinische Monatsschrift Fur Pharmazeuten* 17 (6): 168–86.

Schwendemann J., Sehringer B., Noethling C., Zahradnik H., and Schaefer W.. 2008. “Nitric Oxide Detection by DAF (diaminofluorescein) Fluorescence in Human Myometrial Tissue.” *Gynecological Endocrinology* 24 (6): 306–11.

Scorticati C., Mohn C., De Laurentiis A., Vissio P., Solari J., Seilicovich A., McCann S., and Rettori V.. 2003. “The Effect of Anandamide on Prolactin Secretion Is Modulated by Estrogen.” *Proceedings of the National Academy of Sciences* 100 (4): 2134–39.

Sellix M., Egli M., Henderson R., and Freeman M.. 2004. “Ovarian Steroid Hormones Modulate Circadian Rhythms of Neuroendocrine Dopaminergic Neuronal Activity.” *Brain Research* 1005 (1–2): 164–81.

Sellix M. and Freeman M.. 2003. “Circadian Rhythms of Neuroendocrine Dopaminergic Neuronal Activity in Ovariectomized Rats.” *Neuroendocrinology* 77 (1): 59–70.

Sena A., Grishina I., Thai A., Goulart L., Macal M., Fenton A., Li J., et al. 2013. “Dysregulation of Anti-Inflammatory Annexin A1 Expression in Progressive Crohns Disease.” *PloS One* 8 (10).

Shibuki K.. 1990. “An Electrochemical Microprobe for Detecting Nitric Oxide Release in Brain Tissue.” *Neuroscience Research* 9 (1): 69–76.

Shire D., Carillon C., Kaghad M., Calandra B., Rinaldi-Carmona M., Le Fur G., Caput D., and Ferrara P.. 1995. “An Amino-Terminal Variant of the Central Cannabinoid Receptor Resulting from Alternative Splicing.” *Journal of Biological Chemistry* 270 (8): 3726–31.

Silistino-Souza R., Rodrigues-Lisoni F., Cury P., Maniglia J., Raposo L., Tajara E., Christian H., and Oliani S.. 2007. “Annexin 1: Differential Expression in Tumor and Mast Cells in Human Larynx Cancer.” *International Journal of Cancer. Journal International Du Cancer* 120 (12): 2582–89.

Silverman R., Gibson M., and Silverman A.-J.. 1991. “Relationship of Glia to GnRH Axonal Outgrowth from Third Ventricular Grafts in Hpg Hosts.” *Experimental Neurology* 114 (3): 259–74.

Simpson M., Evans H., and Li C.. 1943. “Bioassay of Adrenocorticotropic Hormone.” *Endocrinology* 33 (5): 261–68.

Smith M. and Vale W.. 2006. “The Role of the Hypothalamic-Pituitary-Adrenal Axis in Neuroendocrine Responses to Stress” 8 (4): 383.

Smith T., Flower R. J., and Buckingham J.. 1993. “Lipocortins 1, 2 and 5 in the Central Nervous System and Pituitary Gland of the Rat: Selective Induction by Dexamethasone of Lipocortin 1 in the Anterior Pituitary Gland.” *Molecular Neuropharmacology* 3: 45–55.

Solito E., Christian H., Festa M., Mulla A., Tierney T., Flower R. J., and Buckingham J.. 2006. “Post-Translational Modification Plays an Essential Role in the Translocation of Annexin A1 from the Cytoplasm to the Cell Surface.” *The FASEB Journal* 20 (9): 1498–1500.

Solito E., McArthur S., Christian H., Gavins F., Buckingham J., and Gillies G.. 2008. “Annexin A1 in the Brain – Undiscovered Roles?” *Trends in Pharmacological Sciences* 29 (3): 135–42.

Solito E., Mulla A., Morris J., Christian H., Flower R. J., and Buckingham J.. 2003. “Dexamethasone Induces Rapid Serine-Phosphorylation and Membrane Translocation of Annexin 1 in a Human Folliculostellate Cell Line Via a Novel Nongenomic Mechanism Involving the Glucocorticoid Receptor, Protein Kinase C, Phosphatidylinositol 3-Kinase, and Mitogen-Activated Protein Kinase.” *Endocrinology* 144 (4): 1164–74.

Song C. and Howlett A.. 1995 “Rat Brain Cannabinoid Receptors Are N-Linked Glycosylated Proteins.” *Life Sciences 56* (23–24) : 1983–89.

Stevens T., Smith S., and Rampton D.. 1993. “Antibodies to Human Recombinant Lipocortin-I in Inflammatory Bowel Disease.” *Clinical Science (London, England: 1979)* 84 (4): 381–86.

Sun G., Chuang D., Zong Y., Jiang J., Lee J., Gu Z., and Simonyi A.. 2014. “Role of Cytosolic Phospholipase A2 in Oxidative and Inflammatory Signaling Pathways in Different Cell Types in the Central Nervous System.” *Molecular Neurobiology*, 1–9. Accessed April 3.

Sun J., Zhang X., Broderick M., and Fein H.. 2003. “Measurement of Nitric Oxide Production in Biological Systems by Using Griess Reaction Assay.” *Sensors* 3 (8): 276–84.

Svec F. and Rudis M.. 1981. “Glucocorticoids Regulate the Glucocorticoid Receptor in the AtT-20 Cell.” *Journal of Biological Chemistry* 256 (12): 5984–87.

Takahashi J. 2004. “Finding New Clock Components: Past and Future.” *Journal of Biological Rhythms* 19 (5): 339–47.

Tashjian A., Yasumura Y., Levine L., Sato G., and Parker M.. 1968. “Establishment of Clonal Strains of Rat Pituitary Tumor Cells That Secrete Growth Hormone,” *Endocrinology* 82 (2): 342–52.

Tashjian A.. 1979. “[46] Clonal Strains of Hormone-Producing Pituitary Cells.” In *Methods in Enzymology*, edited by William B. Jakoby and Ira H. Pastan, Volume 58:527–35. Cell Culture. Academic Press.

Taylor A., Christian H., Morris J., Flower R. J., and Buckingham J.. 1997. “An Antisense Oligodeoxynucleotide to Lipocortin 1 Reverses the Inhibitory Actions of Dexamethasone on the Release of Adrenocorticotropin from Rat Pituitary Tissue in Vitro.” *Endocrinology* 138 (7): 2909–18.

Taylor A., Flower R. J., and Buckingham J.. 1995. “Dexamethasone Inhibits the Release of TSH from the Rat Anterior Pituitary Gland in Vitro by Mechanisms Dependent on de Novo Protein Synthesis and Lipocortin 1.” *Journal of Endocrinology* 147 (3): 533–44.

Taylor A., Philip J., John C., Cover P., Morris J., Flower R. J., and Buckingham J.. 2000. “Annexin 1 (Lipocortin 1) Mediates the Glucocorticoid Inhibition of Cyclic Adenosine 3′,5′-Monophosphate-Stimulated Prolactin Secretion [1].” *Endocrinology* 141 (6): 2209–19.

Taylor A., Cowell A.-M., Flower R. J., and Buckingham J.. 1993. “Lipocortin 1 Mediates an Early Inhibitory Action of Glucocorticoids on the Secretion of ACTH by the Rat Anterior Pituitary Gland in Vitro.” *Neuroendocrinology* 58 (4): 430–39.

Taylor A., Cowell A.-M., Flower R. J., and Buckingham J.. 1995. “Dexamethasone Suppresses the Release of Prolactin from the Rat Anterior Pituitary Gland by Lipocortin 1 Dependent and Independent Mechanisms.” *Neuroendocrinology* 62 (5): 530–42.

Taylor A., Loxley H., Flower R. J., and Buckingham J.. 1995. “Immunoneutralization of Lipocortin 1 Reverses the Acute Inhibitory Effects of Dexamethasone on the Hypothalamo-Pituitary-Adrenocortical Responses to Cytokines in the Rat in Vitro and in Vivo.” *Neuroendocrinology* 62 (1): 19–31.

Tazawa R., Xu X., Wu K., and Wang L.. 1994. “Characterization of the Genomic Structure, Chromosomal Location and Promoter of Human Prostaglandin H Synthase-2 Gene.” *Biochemical and Biophysical Research Communications* 203 (1): 190–99.

Theogaraj E., John C., Christian H., Morris J., Smith S., and Buckingham J.. 2005. “Perinatal Dexamethasone Treatment Causes Long-Term Changes in Brain Ependymal Cell Morphology and Annexin 1 Expression in the Rat.” *PA2Online* 2: 015P.

Thomas G., Cummins J., Yao B., Gordon K., and Clarke I.. 1988. “Release of Prolactin Is Independent of the Secretion of Thyrotrophin-Releasing Hormone into Hypophysial Portal Blood of Sheep.” *Journal of Endocrinology* 117 (1): 115–22.

Tierney T., Christian H., Morris J., Solito E., and Buckingham J.. 2003. “Evidence From Studies on Co-Cultures of TtT/GF and AtT20 Cells That Annexin 1 Acts as a Paracrine or Juxtacrine Mediator of the Early Inhibitory Effects of Glucocorticoids on ACTH Release.” *Journal of Neuroendocrinology* 15 (12): 1134–43.

Tortonese D., Brooks J., Ingleton P., and McNeilly A.. 2013. “Detection of Prolactin Receptor Gene Expression in the Sheep Pituitary Gland and Visualization of the Specific Translation of the Signal in Gonadotrophs”. http://press.endocrine.org/doi/abs/10.1210/endo.139.12.6365.

Tóth B., Homicskó K., Radnai B., Maruyama W., DeMaria J., Vecsernyés M., Fekete M., et al. 2001. “Salsolinol Is a Putative Endogenous Neuro-Intermediate Lobe Prolactin-Releasing Factor.” *Journal of Neuroendocrinology* 13 (12): 1042–50.

Towbin H., Staehelin T., and Gordon J.. 1979. “Electrophoretic Transfer of Proteins from Polyacrylamide Gels to Nitrocellulose Sheets: Procedure and Some Applications.” *Proceedings of the National Academy of Sciences* 76 (9): 4350–54.

Traverso V., Christian H., Morris J., and Buckingham J.. 1999. “Lipocortin 1 (Annexin 1): A Candidate Paracrine Agent Localized in Pituitary Folliculo-Stellate Cells [1].” *Endocrinology* 140 (9): 4311–19.

Tsao F., Meyer K., Chen X., Rosenthal N., and Hu J.. 1998. “Degradation of Annexin I in Bronchoalveolar Lavage Fluid from Patients with Cystic Fibrosis.” *American Journal of Respiratory Cell and Molecular Biology* 18 (1): 120–28.

Ungar F. and Halberg F.. 1962. “Circadian Rhythm in the in Vitro Response of Mouse Adrenal to Adrenocorticotropic Hormone.” *Science* 137 (3535): 1058–60.

Untergasser A., Cutcutache I., Koressaar T., Ye J., Faircloth B., Remm M., and Rozen S.. 2012. “Primer3--New Capabilities and Interfaces.” *Nucleic Acids Research* 40 (15): e115.

Vakalopoulou E., Schaack J., and Shenk T.. 1991. “A 32-Kilodalton Protein Binds to AU-Rich Domains in the 3’ Untranslated Regions of Rapidly Degraded mRNAs.” *Molecular and Cellular Biology* 11 (6): 3355–64.

Van Cauter E. and Refetoff S.. 1985. “Multifactorial Control of the 24-Hour Secretory Profiles of Pituitary Hormones.” *Journal of Endocrinological Investigation* 8 (4): 381–91.

Vankelecom H.. 2012. “Pituitary Stem Cells Drop Their Mask.” *Current Stem Cell Research & Therapy* 7 (1): 36–71.

Vankelecom H., Matthys P., and Denef C.. 1997. “Inducible Nitric Oxide Synthase in the Anterior Pituitary Gland: Induction by Interferon-Γ in a Subpopulation of Folliculostellate Cells and in an Unidentifiable Population of Non-Hormone-Secreting Cells.” *Journal of Histochemistry & Cytochemistry* 45 (6): 847 –857.

Vercelli C., Aisemberg J., Billi S., Wolfson M., and Franchi A.. 2009. “Endocannabinoid System and Nitric Oxide Are Involved in the Deleterious Effects of Lipopolysaccharide on Murine Decidua.” *Placenta* 30 (7): 579–84.

Vila-Porcile E.. 1972. “Le réseau des cellules folliculo-stellaires et les follicules de l’adénohypophyse du rat (Pars distalis).” *Zeitschrift für Zellforschung und Mikroskopische Anatomie* 129 (3): 328–69.

Von Gall C., Noton E., Lee C., and Weaver D.. 2003. “Light Does Not Degrade the Constitutively Expressed BMAL1 Protein in the Mouse Suprachiasmatic Nucleus.” *European Journal of Neuroscience* 18 (1): 125–33.

Vong L., D’Acquisto F., Pederzoli-Ribeil M., Lavagno L., Flower R. J., Witko-Sarsat V., and Perretti M.. 2007. “Annexin 1 Cleavage in Activated Neutrophils a Pivotal Role for Proteinase 3.” *Journal of Biological Chemistry* 282 (41): 29998–4.

Waksman Y., Olson J., Carlisle S., and Cabral G.. 1999. “The Central Cannabinoid Receptor (CB1) Mediates Inhibition of Nitric Oxide Production by Rat Microglial Cells.” *Journal of Pharmacology and Experimental Therapeutics* 288 (3): 1357–66.

Wallner B., Mattaliano R., Hession C., Cate R., Tizard R., Sinclair L., Foeller C., et al. 1986. “Cloning and Expression of Human Lipocortin, a Phospholipase A2 Inhibitor with Potential Anti-Inflammatory Activity.” *Nature* 320 (6057): 77–81.

Walsh R., Slaby F., and Posner B.. 1987. “A Receptor-Mediated Mechanism for the Transport of Prolactin from Blood to Cerebrospinal Fluid*.” *Endocrinology* 120 (5): 1846–50.

Wang L., Yang Y., Liu Y., Song H., Zhang L., and Li P.. 2008. “Decreased Expression of Annexin A1 during the Progression of Cervical Neoplasia.” *The Journal of International Medical Research* 36 (4): 665–72.

Wang L., Bi J., Yao C., Xu X., Li X., Wang S., Li Z., Zhang D., Wang M., and Chang G.. 2010. “Annexin A1 Expression and Its Prognostic Significance in Human Breast Cancer.” *Neoplasma* 57 (3): 253–59.

Wang W., Guan S., Sun S., Jin Y., Lee K.-H., Chen Y., and Wie J.. 2014. “Detection of Circulating Antibodies to Linear Peptide Antigens Derived from ANXA1 and DDX53 in Lung Cancer.” *Tumour Biology: The Journal of the International Society for Oncodevelopmental Biology and Medicine*

Ward S. and Raffa R.. 2011. “Rimonabant Redux and Strategies to Improve the Future Outlook of CB1 Receptor Neutral-Antagonist/Inverse-Agonist Therapies.” *Obesity* 19 (7): 1325–34.

Watanobe H.. 1990. “The Immunostaining for the Hypothalamic Vasoactive Intestinal Peptide, but Not for B-Endorphin, Dynorphin-A or Methionine-Enkephalin, Is Affected by the Glucocorticoid Milieu in the Rat: Correlation with the Prolactin Secretion.” *Regulatory Peptides* 28 (3): 301–11.

Weidenfeld J., Feldman S., and Mechoulam R.. 1994. “Effect of the Brain Constituent Anandamide, a Cannabinoid Receptor Agonist, on the Hypothalamo-Pituitary-Adrenal Axis in the Rat.” *Neuroendocrinology* 59 (2): 110–12.

Weitzman E., Fukushima D., Nogeire C., Roffwarg H., Gallagher T., and Hellman L.. 1971. “Twenty-Four Hour Pattern of the Episodic Secretion of Cortisol in Normal Subjects.” *The Journal of Clinical Endocrinology & Metabolism* 33 (1): 14–22.

Wennmalm Å., Lanne B., and Petersson A.-S.. 1990. “Detection of Endothelial-Derived Relaxing Factor in Human Plasma in the Basal State and Following Ischemia Using Electron Paramagnetic Resonance Spectrometry.” *Analytical Biochemistry* 187 (2): 359–63.

Wenzel-Seifert K., Arthur J., Liu H.-Y., and Seifert R.. 1999. “Quantitative Analysis of Formyl Peptide Receptor Coupling to Giα1, Giα2, and Giα3.” *Journal of Biological Chemistry* 274 (47): 33259–66.

Westphal N., Evans R., and Seasholtz A.. 2009. “Novel Expression of Type 1 Corticotropin-Releasing Hormone Receptor in Multiple Endocrine Cell Types in the Murine Anterior Pituitary.” *Endocrinology* 150 (1): 260–67.

Wilber J. and Utiger R.. 1969. “The Effect of Glucocorticoids on Thyrotropin Secretion.” *Journal of Clinical Investigation* 48 (11): 2096–2103.

Woods M., Shipston M., Mullens E., and Antoni F.. 1992. “Pituitary Corticotrope Tumor (AtT20) Cells as a Model System for the Study of Early Inhibition by Glucocorticoids.” *Endocrinology* 131 (6): 2873–80.

Woods M., Kiss J., Smith T., Buckingham J., Flower R. J., and Antoni F.. 1990. “Localization of Lipocortin-1 in Rat Hypothalamus and Pituitary Gland.” *Biochemical Society Transactions* 18 (6): 1236–37.

Wu C., Croxtall J., Perretti M., Bryant C., Thiemermann C., Flower R. J., and Vane J.. 1995. “Lipocortin 1 Mediates the Inhibition by Dexamethasone of the Induction by Endotoxin of Nitric Oxide Synthase in the Rat.” *Proceedings of the National Academy of Sciences* 92 (8): 3473–77.

Yamamura T., Yasuo S., Hirunagi K., Ebihara S., and Yoshimura T.. 2006. “T3 Implantation Mimics Photoperiodically Reduced Encasement of Nerve Terminals by Glial Processes in the Median Eminence of Japanese Quail.” *Cell and Tissue Research* 324 (1): 175–79.

Yasuo S., Koch M., Schmidt H., Ziebell S., Bojunga J., Geisslinger G., and Korf H.-W.. 2010. “An Endocannabinoid System Is Localized to the Hypophysial Pars Tuberalis of Syrian Hamsters and Responds to Photoperiodic Changes.” *Cell and Tissue Research* 340 (1): 127–36.

Yasuo S. and Korf H.-W.. 2011. “The Hypophysial Pars Tuberalis Transduces Photoperiodic Signals via Multiple Pathways and Messenger Molecules.” *General and Comparative Endocrinology* 172 (1): 15–22.

Yasuo S., Unfried C., Kettner M., Geisslinger G., and Korf H.-W.. 2010. “Localization of an Endocannabinoid System in the Hypophysial Pars Tuberalis and Pars Distalis of Man.” *Cell and Tissue Research* 342 (2): 273–81.

Young K., Hirst W., Solito E., and Wilkin G.. 1999. “De Novo Expression of Lipocortin-1 in Reactive Microglia and Astrocytes in Kainic Acid Lesioned Rat Cerebellum.” *Glia* 26 (4): 333–43.

Yu G., Wang J., Chen Y., Wang X., Pan J., Li Q., and Xie K.. 2008. “Tissue Microarray Analysis Reveals Strong Clinical Evidence for a Close Association between Loss of Annexin A1 Expression and Nodal Metastasis in Gastric Cancer.” *Clinical & Experimental Metastasis* 25 (7): 695–702.

Zafiriou O. and McFarland M.. 1980. “Determination of Trace Levels of Nitric Oxide in Aqueous Solution.” *Analytical Chemistry* 52 (11): 1662–67.

Zarrow M., Sawin P., Ross S., Denenberg V., Crary D., Wilson E., and Farooq A.. 1961. “Maternal Behaviour in the Rabbit: Evidence for an Endocrine Basis of Maternal-Nest Building and Additional Data on Maternal-Nest Building in the Dutch-Belted Race.” *Journal of Reproduction and Fertility* 2 (2): 152–62.

Zhang Z., Huang L., Zhao W., and Rigas B.. 2010. “Annexin 1 Induced by Anti-Inflammatory Drugs Binds to NF-κB and Inhibits Its Activation: Anticancer Effects In Vitro and In Vivo.” *Cancer Research* 70 (6): 2379–88.

Zhu D.-W., Liu Y., Yang X., Yang C.-Z., Ma J., Yang X., Qiao J.-K., et al. 2013. “Low Annexin A1 Expression Predicts Benefit from Induction Chemotherapy in Oral Cancer Patients with Moderate or Poor Pathologic Differentiation Grade.” *BMC Cancer* 13 (1): 301.

Zhu F., Wang Y., Zeng S., Fu X., Wang L., and Cao J.. 2009. “Involvement of Annexin A1 in Multidrug Resistance of K562/ADR Cells Identified by the Proteomic Study.” *Omics: A Journal of Integrative Biology* 13 (6): 467–76.

# Zusammenfassung

Einfluss der Endocannabinoide auf die Funktion der Hypophyse mit Berücksichtigung von follikulo-stellären, corticotrophen und lactotrophen Zellen

Die Hypophyse, die vom Hypothalamus gesteuert wird, hat als Hauptfunktion die Regulation der hormonellen Produktion im Körper. Die corticotrophen (C) und lactotrophen (L) Zellen, die sich in der Pars distalis (PD) der Hypophyse befinden, produzieren entsprechend Adrenokortikotropin (ACTH) und Prolaktin (PRL). Die Endocannabinoide (EC) sind für ihre Wirkung auf die Freisetzung von ACTH und PRL bekannt. Die EC führen bei der Ratte zu erhöhten ACTH-Spiegeln (Weidenfeld et al., 1994) und zu niedrigeren PRL-Spiegeln (Scorticati et al., 2003). Die EC und die Fettsäurenamidhydrolase (FAAH), ein EC-abbauendes Enzym, sind Bestandteile des sogennanten Endocannabinoid Systems (ECS), das Areale im Hypothalamus und in der Hypophyse umfasst. Die EC in der Hypophyse werden überwiegend in der Pars tuberalis (PT) gebildet. Die Annahme, dass EC auf die C und L Zellen der PD wirken, ist durch das Vorhandensein von Cannabinoid Rezeptoren Typ 1 ($CB_1$) belegt (Yasuo et al., 2010). Die follikulo-stellären (fs) Zellen, die sich in unmittelbarer Nähe zu den corticotrophen und lactotrophen Zellen befinden, stellen eine interessante Zellpopulation dar, deren Funktion sehr vielseitig und noch nicht vollständig geklärt ist (Allaerts and Vankelecom, 2005; Mitsuishi et al., 2013). Meine Annahme ist, dass die fs Zellen mit dem ECS auf einer Seite und mit den C und L Zellen auf anderer Seite interagieren.

Yasuo und Korf (2011) haben gezeigt, dass die EC die Kommunikation zwischen der PT und der PD vermitteln. Die EC werden durch NAPE-PLD und DAGL in der PT synthetisiert und durch FAAH und MAGL in der PD abgebaut. Der Nachweis der dazugehörigen $CB_1$ Rezeptoren in der PD (und nicht in der PT) unterstützt die veröffentlichten Aussagen. Yasuo et al. (2010) konnten belegen, dass die Spiegel von DAGL und 2-AG in der PT und von PRL im Plasma von Hamstern, die unter „Sommer“- Bedingungen gehalten wurden, erhöht waren.

Die Hypothese meiner Arbeit war ursprünglich, dass die EC zu einer Aktivierung der Produktion und Freisetzung von ACTH und PRL führen, die über die fs Zellen vermittelt wird. Es ist in der Literatur bekannt, dass die fs Zellen das Protein Annexin A1 (Anx A1) und das anorganische Molekül Stickstoffmonoxid (NO) bilden (Traverso et al., 1999; Devnath and Inoue, 2008). Ihre Funktion als Botenstoffe wurde untersucht. Es wurde angenommen, dass die EC die Ausschüttung von Anx A1 und NO hemmen, die ihrerseits hemmend auf die ACTH und PRL Synthese in den corticotrophen und lactotrophen Zellen der PD wirken, sodass diese gehemmte Hemmung (Disinhibition) zu einer vermehrten Freisetzung von ACTH und PRL führt.

Der Nachweis des $CB_1$ Rezeptors auf den hier verwendeten fs Zellmodellen (TtT/GF und Tpit/F1) war ein erstes essentielles Experiment. Auch musste experimentell geklärt werden, ob die untersuchten fs Zellen Anx A1 und NO produzieren. Daher wurden Nachweismethoden für Anx A1 und NO entwickelt und etabliert. Als nächstes sollten Stimulationen mit $CB_1$-Ago- und Antagonisten durchgeführt und Konzentrationen von Anx A1 und NO bestimmt werden. Weiterhin sollte geprüft werden, ob ein Rezeptor für Anx A1 an den C und L Zellen exprimiert wird. Hierzu musste eine Nachweismethode für den Anx A1 Rezeptor entwickelt werden, da es zur Zeit der Untersuchung keine passenden Antikörper auf dem Markt gab. Anschließend wurden Stimulationen mit EC, Anx A1 und NO bei den C und L Zellen durchgeführt und die Spiegel von ACTH und PRL bestimmt.

Immunocytochemie (ICC) mit DAB oder Fluoreszenz als Markierung wurde zunächst zum Nachweis des $CB_1$ Rezeptors verwendet. Die Ergebnisse wurden durch das Immunoblot Verfahren (IB; Western Blot) bestätigt.

Anx A1 wurde mittels Immunohistochemie (IHC), IB, Enzyme-linked Immunosorbent Assay (ELISA), *in situ* Hybridisierung (ISH) und Polymerase Ketten-Reaktion (PCR) bestimmt.

NO wurde durch die Griess Reaktion photometrisch und durch eine Ozon-Reaktion chemilumineszent bestimmt. Weiterhin erlaubte die Reaktion mit dem Fluorofor DAF-2AC eine direkte Detektion und Beobachtung der NO-positiven Zellen, sowohl an den immortalisierten Zelllinien, als auch am Gewebe mit konfokaler Mikroskopie. Weiterhin konnten DAF-2AC-markierte Zellen mit der FACS Methode selektiert und analysiert werden. Die Expression von NO-bildenden Enzymen nNOS, eNOS, iNOS wurde mittels quantitativer RT-PCR an den fs (TtT/GF und Tpit/F1), und C (AtT20/D16v) Zellen untersucht.

Der Anx A1 Rezeptor, Fpr-rs1, wurde mittels nicht-radioaktiver BCIP/NBT ISH an Gewebe- und Zellproben nachgewiesen.

Der Spiegel von ACTH der AtT20/D16v Zellen wurde mittels ELISA quantifiziert und die Expression des Prekursors von ACTH, Proopiomelanokortin (POMC) mittels PCR und ISH nachgewiesen. Die POMC ISH erfolgte sowohl radioaktiv mit [$^{32}$P]-ATP-markierten Sonden, als auch nicht-radioaktiv mit Digoxygenin-markierten Sonden.

PRL wurde an den GH4C1 Zellen mittels ELISA quantifiziert, mittels IB und PCR detektiert und am murinen Gewebe mittels IHC visualisiert.

$CB_1$, der in der Literatur als Gi/o Pertussis Toxin-sensitiver Rezeptor beschrieben ist, wurde mittels ICC und IB Methoden an den fs Zellen TtT/GF und Tpit/F1 nachgewiesen.

Die ICC und IB Methoden zeigten positive $CB_1$ Immunreaktionen an den C AtT20/D16v und den L GH4C1 Zellen. Weiterhin wurde FAAH in den TtT/GF und Tpit/F1 Zellen mittels ICC und PCR nachgewiesen.

Anx A1 wurde in den fs Zellen TtT/GF und Tpit/F1 mit IB, ELISA, PCR und ISH nachgewiesen. Die C AtT20/D16v Zellen und die L GH4C1 Zellen waren negativ in der IB und der PCR Analyse für Anx A1. Anx A1 wurde auch an murinem Gewebe mittels IHC und ISH festgestellt. Die IHC Analyse an Schnitten durch das Mausgehirn zeigte das Vorhandensein vom Anx A1 in der

Eminentia mediana, PT, Nucleus arcuatus, mediobasalen/ dorsolateralen Hypothalamus, im Bereich des dritten Ventrikels, im periaqueduktalen Grau, sowie in der PD. Parallele Anx A1- und PRL-Färbungen ließen erkennen, dass die zwei Proteine in der PD in unmittelbarer Nähe exprimiert sind. Die ISH Analyse wurde an Schnitten der Maus PD, die zu den Zeitpunkten ZT04 und ZT16 gewonnen wurden, durchgeführt und densidometrisch ausgewertet. Hierbei ergab sich keine Korrelation zwischen der Menge an Anx A1-mRNA und dem Zeitpunkt, an dem die Schnitte gewonnen wurden.

Anx A1 wird in verschiedenen molekularen Massen detektiert. Die verbreiteteste Form ist das Anx A1 Protein, das 37 kDa groß ist. Da das Anx A1 Protein sich im Cytoplasma, auf der Membran, aber auch im Interstitium befinden kann, wurde versucht, die membranäre von der cytoplasmatischen Form zu unterscheiden. Die Zellen wurden mit EDTA-haltigem Puffer nach Tierney gewaschen, die Waschfraktionen mit einer Vakuumzentrifuge aufkonzentriert und mittels IB analysiert. Das Anx A1 Protein der membranären Waschfraktionen hatte eine Größe von 33 kDa.

Der Anx A1 Rezeptor, Fpr-rs1, ein Gi Pertussis Toxin-insensitiver Rezeptor, wurde per ISH Reaktion an Maus PD Gewebe densitometrisch analysiert. Hierbei zeigte sich eine bestehende Korrelation zwischen der Menge an Anx A1 Rezeptor-mRNA und dem Zeitpunkt, an dem die Schnitte gewonnen wurden.

NO wurde an TtT/GF, Tpit/F1 und AtT20/D16v detektiert. Die Produktion von NO in GH4C1 ist in der Literatur bestätigt, (Qian et al., 1998). Stimulationen mit NOS Aktivatoren (Ionomycin und LPS) und NOS Inhibitoren (L-NAME und Curcumin) haben die Rolle der NOS Enzyme in der NO Bereitstellung bestätigt. Ein interessanter Befund war, dass das resultierende Anx A1 Protein nach Behandlung mit L-NAME oder Curcumin in der IB Analyse eine 33 kDa und eine 37 kDa Fraktion aufwies.

TtT/GF und Tpit/F1 Zellen wurden mit 2-AG, AEA, WIN 55,212-2 und Otenabant stimuliert und anschließend die Konzentrationen von Anx A1 und NO

bestimmt. Das Ergebnis zeigt, dass die EC zu einer Erhöhung von Anx A1 und einer Erniedrigung von NO führen.

Die C AtT20/D16v Zellen und die L GH4C1 Zellen wurden jeweils mit 2-AG, Anx A1 und NO stimuliert. Die Proben wurden anschließend mittels ELISA auf ACTH und PRL analysiert. 2-AG führte zu keiner signifikanten Änderung von ACTH und PRL. Anx A1 führte zur signifikanten Erhöhung von ACTH im Zellmedium von AtT20/D16v Zellen. Anx A1 hemmte die PRL Konzentration in Zelllysaten und stimulierte den PRL-Spiegel in den Zellmedien von GH4C1 Zellen. NO wirkte inhibierend auf die ACTH und PRL Produktion.

Die Tatsache, dass $CB_1$ auch von den C AtT20/D16v und den L GH4C1 Zellen exprimiert wird, sowie die Literaturhinweise, dass der $CB_1$ Rezeptor über Gi Untereinheiten eine inhibierende Wirkung entfaltet, ließen vermuten, dass die EC direkt und negativ die hormonelle Produktion der Zellen beeinflussen können. Allerdings hatte die direkte Stimulation mit 2-AG keinen signifikanten Einfluss auf die ACTH- und PRL-Spiegel. Darüber hinaus führte die Stimulation der fs Zellen zu einem Anstieg von Anx A1. Aufgrund der entstandenen Zweifel über den Rezeptortyp wurde die $[Ca^{2+}]_i$ Konzentration der TtT/GF und Tpit/F1 nach Stimulation mit 2-AG und AEA ermittelt. Die Auswertung zeigte, dass die TtT/GF Zellen keine $CB_1$-Gq Untereinheiten aufweisen, während bei den Tpit/F1 Zellen Gq Untereinheiten am beobachteten $Ca^{2+}$ -Anstieg beteiligt sein könnten. Darüber hinaus deuten Hinweise in der Literatur über Heterodimerenbildung mit Adenosin- oder Dopamin-Rezeptoren ($A_{2A}CB_1$, $CB_1D_2$), Rezeptordesensibilisierung und Rezeptorinternalisierung vom $CB_1$ auf eine komplexe Rezeptordynamik hin (Howlett, 2005; Pertwee, 2005; 2006). Ein weiteres Argument für das Vorhandensein von Heterodimerformen des $CB_1$ Rezeptors ist die Tatsache, dass Adenosin auch einen Einfluss auf Anx A1, NO, ACTH und PRL hat und Dopamin als PRL inhibierender Neurotransmitter fungiert. Die Menge an EC, die zur Stimulation der hormonproduzierenden Zellen eingesetzt wurde, lag umgerechnet 10fach höher als die entsprechende Bindungskonstante. Ein erhöhtes Angebot an Rezeptorligand (EC) kann zur

Internalisierung von Rezeptor-Ligand-Komplexen ($CB_1$-EC) von der Zellmembran in die Zelle oder zu einer Rezeptordesensibilisierung führen.

Das ermittelte Ergebnis bezüglich der ACTH Menge im Zellmedium nach 2-AG Stimulation deutet auf eine negative Tendenz und ist weder eine Bestätigung der angenommenen Hypothese, dass EC inhibierend auf ACTH wirken, noch eine Bestätigung der Hinweise in der Literatur auf erhöhten ACTH-Spiegel nach EC Stimulation (Weidenfeld et al., 1994; Pagotto et al., 2001).

2-AG zeigte auch keine signifikante Wirkung auf die PRL Menge in den L Zellen. Die Daten in der Literatur sind soweit kontrovers. Murphy et al. (1998), Ho et al. (2000) und Scorticati et al. (2003) haben die Beteiligung von $CB_1$ an der PRL Hemmung gezeigt. Auf der anderen Seite haben Kolesnick et al. (1984) gezeigt, dass AA die PRL-Freisetzung von GH3 Zellen stimuliert. Darüber hinaus haben Yasuo und Korf (2011) eine Korrelation zwischen erhöhtem PRL Plasmaspiegel und erhöhter Konzentration von 2-AG in der PT von Hamstern, die unter „Sommer“ Bedingungen gehalten wurden, gezeigt.

Die Bildung von NO in den fs TtT/GF Zellen und Tpit/F1 Zellen wurde von AEA gehemmt. Dass die hemmende Wirkung durch $CB_1$ vermittelt wird, wurde anschließend durch den Einsatz von WIN an den TtT/GF Zellen als synthetischer $CB_1$ Agonist bestätigt. Otenabant als $CB_1$ Antagonist bewirkte wie erwartet keine Änderung in der basalen NO Konzentration.

In der hier durchgeführten Experimenten führte Anx A1 zu einem Anstieg an ACTH im Zellmedium der AtT20/D16v Zellen. Veröffentlichungen der Gruppe von Taylor et al. (1993) bestätigen die hier aufgeführten Daten. Sie haben festgestellt, dass Anx A1, wenn allein appliziert, zum ACTH Anstieg führt.

In den von mir durchgeführten Experimenten hemmte Anx A1 in den GH4C1 Zellen die PRL Menge im Zelllysat, stimulierte sie aber im Zellmedium. Da die GC hemmend auf PRL wirken (Euker et al., 1975; Fang und Shian, 1981), lässt sich schließen, dass die GC Anx A1 induzieren, das wiederum PRL hemmen kann.

NO wirkte inhibierend auf ACTH und PRL. Der Wirkmechanismus schließt Interaktionen mit der $[Ca^{2+}]_i$ Konzentration ein, da $Ca^{2+}$ für die Vesikelfusion mit der Zellmembran und die anschließende Hormonfreisetzung unerlässlich ist. Venkelecom et al. (1997) haben gezeigt, dass NO die Freisetzung von PRL hemmt. Andric (2003) vermutet, dass die NO-Ca Interaktion für die hemmende Wirkung von NO verantwortlich ist.

Während die detektierte Anx A1 mRNA in murinen PD Proben keine signifikante Korrelation zu verschiedenen Zeitpunkten zeigte, war die Fpr-rs1 mRNA Menge am subjektiven Tag (ZT16) signifikant niedriger als in der subjektiven Nacht (ZT04). Die Schlussfolgerung ist, dass Anx A1, obwohl es nicht direkt zeitlich reguliert, eine zeitlich regulierte Wirkung durch seinen Rezeptor entfalten kann.

Die hier vorgestellte Arbeit bestätigt die Existenz einer Verbindung zwischen dem ECS und der hormonellen Regulation mit der Beteiligung einer rhythmischen Anpassung. Die EC haben eindeutig die Verfügbarkeit von Anx A1 in den fs Zellen um ca. 25% erhöht. Anx A1 stellt mehr als ein übiquitär vorhandenes, Zellmembran stützendes Element dar. Es fungiert als Botenprotein der fs Zellen und ist an der Regulation der umliegenden hormonproduzierenden Zellen und an der Inhibition von PLA2 und nachfolgenden inflammationsrelevanten Prozessen beteiligt. Extensive Experimente am gesamten Organismus sind notwendig um die hier vorgestellten Ergebnisse *in vivo* zu überprüfen.